Hypersensitivity Response to *Aspergillus fumigatus*: Immunopathogenesis of Allergic Airway Disease and Pulmonary Arterial Remodeling

by

Andrew Brent Shreiner

A dissertation submitted in partial fulfillment
of the requirements for the degree of
Doctor of Philosophy
(Immunology)
in The University of Michigan
2008

Doctoral Committee:

Professor Gary B. Huffnagle, Chair
Professor Dennis Keith Bishop
Professor David A. Fox
Professor Bruce C. Richardson
Professor Lloyd M. Stoolman
Associate Professor Cory M. Hogaboam

To My Parents

Acknowledgements

I would like to thank my advisor, Gary Huffnagle, for the opportunity to achieve this milestone in my professional development under his mentorship and in his laboratory. Gary, I greatly appreciate all the time, effort, and resources you expended on my behalf. I know I will especially take away the lessons you taught me on how to effectively communicate complex information and ideas whether in discussion or in writing. You were a great advisor because you are an excellent scientist and because you were genuinely concerned for my well-being. I hope to emulate your enthusiasm, positive approach, and compassion throughout my career. Ciao, for now.

I would like to thank all the members of the Huffnagle laboratory who supported me in my work and distracted me from it. Rod, Nicole, Katie, Tiffany, John, Ben, Gwo-Hsiao, Toby, Shikha, Mari, and Jami, it was fun, some of the time.

I would like to thank Cory Hogaboam, Eric White, and Paul Christensen for helpful discussions and collaborations. Cory, Eric, and Paul, I really appreciate all the time and insight you graciously shared with me in our many discussions. Also, I really appreciate the generous gift of your time and

resources in conducting experiments, mostly by my side, in your laboratories. I hope to emulate your collegiality and generosity throughout my career.

I would like to thank the many members of the following laboratories who supported me in my work: Galen Toews, Alfred Chang, Tom Moore, Michal Olszewski, John Kao, and Vince Young.

I would like to thank the following members of my dissertation committee who guided me through my work in excellent fashion: Keith Bishop, David Fox, Bruce Richardson, Lloyd Stoolman, and Cory Hogaboam. You all made meaningful contributions to my work and my development as a scientist. I respect and admire you all.

I would like to thank Ron Koenig and Keith Bishop for their tremendous support as directors of the Medical Scientist Training Program and the Graduate Program in Immunology, respectively. Ron and Keith, I greatly appreciate the concern for my success that you showed in guiding me through difficult times. It made all the difference for me. I hope to emulate your honesty and compassion throughout my career.

I would like to thank Penny Morris, Ellen Elkin, and Zarinah Aquil for their excellent assistance in managing a graduate school career. Penny, Ellen, and Zarinah, I truly appreciate all the time and work you contributed on my behalf. I appreciated all of your kind words and your interest in my family and me.

I would like to acknowledge the following funding from the NIH that supported me and my work: MSTP Training Grant and Immunology Training Grant.

I would like to thank my parents for all the love, guidance, and support I ever needed. Mom and Dad, I could never thank you enough for all that you've given to me. I truly believe you're the finest people I know. I could never hope to achieve more than to live up to your example. I love you both.

I would like to thank my sisters, Christina, Alicia, and Bridgette for their continued love and support. You're all a great source of happiness and pride for me. I love and admire you all.

I would like to thank my grandparents for all the love and support they have given to our family and me. You are all tremendous role models for me. I love you all.

I would like to thank my daughters, Lily and Maggie, for their unconditional love. You guys are the best. You're my favorite people in the world. Lily, I'm amazed at your compassion, thoughtfulness, gentleness, and wisdom. Maggie I'm amazed at your passion, zeal, hilarity, and potty mouth. This thing didn't come easy, but you showered me with love every day and made it so much easier. I love you both with all my heart and soul.

Lastly, and most importantly, I would like to thank my wife, Tammy. You've been there every day for me. You're love and support has made all the difference. You're a remarkable student, professional, wife, and mother. You're my greatest inspiration. I love you with all my heart and soul.
(Oh, and I dedicate all my future work to you, $$$)

Table of Contents

List of Figures

List of Appendices

List of Abbreviations

αSMA	α smooth muscle actin
AAD	allergic airway disease
AAMϕ	alternatively-activated macrophage
ABPA	allergic bronchopulmonary aspergillosis
AHR	airway hyperreactivity
APC	antigen-presenting cell
BAL	bronchoalveolar lavage
BALF	bronchoalveolar lavage fluid
BALT	bronchial-associated lymphoid tissue
CMIS	common mucosal immune system
DC	dendritic cell
ELISA	enzyme-linked immunosorbent assay
FACS	fluorescent-activated cell sorting
FSC	forward scatter
GMS	Gomori methenamine silver
H&E	hematoxylin & eosin
HDM	house dust mite
HP	hypersensitivity pneumonitis
ILF	isolated lymph follicles
LDLN	lung-draining lymph node
LN	lymph node
LV	left ventricle
M	microfold
Mϕ	macrophage
MACS	magnetic-activated cell sorting
MALT	mucosal-associated lymphoid tissue
NALT	nasal-associated lymphoid tissue
OVA	ovalbumin
PAH	pulmonary arterial hypertension
PAMP	pathogen-associated molecular pattern
PAS	periodic acid-Schiff
PBS	phosphate-buffered saline
PP	Peyer's patch
PRR	pattern-recognition receptor
RV	right ventricle
S	septum
SSC	side scatter
T_H	T helper

TLR	toll-like receptor
T_{Reg}	T regulatory

Chapter 1

Background

Overview

The United States population experienced an increase of 75% in the **prevalence of asthma** from 1980 to 1994[1]. Distant countries with similar lifestyles, such as the United Kingdom[2] and Australia[3], reported comparable increases in asthma prevalence during this period of time. Currently, in the United States, Canada, United Kingdom, Ireland, New Zealand and Australia, the prevalence of allergic airway disease among 13-14 year old children is among the highest in the world and ranges from 22-32%[4]. In response to these developments, the International Study of Asthma and Allergies in Childhood (ISAAC) was initiated with a stated goal to determine the prevalence of allergic disorders in children living throughout the world using standardized criteria, increasing comparative value. The Phase I survey of 450,000+ children in 56 countries revealed stark geographic differences in prevalences[5]. The pattern and magnitude of variation throughout the world suggest that environmental factors are critical to the development of allergies in childhood. Upon further evaluation of the ISAAC and the European Community Respiratory Health Survey (ECRHS) of asthma prevalence in adults, several trends became apparent including (1) an increase in allergy prevalence throughout the world, (2) a pattern of asthma prevalence where it is more common in Westernized

countries and less common in developing countries, and (3) an increase in prevalence as countries Westernize or as communities urbanize[6].

Allergic responses are a form of hypersensitivity response, where the term "**hypersensitivity**" refers to an adverse state of heightened immune reactivity to innocuous antigens. Allergic diseases are manifested by inappropriate immune responses to harmless foreign materials in those with a genetic predisposition. The magnitude of the hypersensitivity reaction is out of proportion to the posed threat, so these immune responses are unnecessarily injurious to the host. Hypersensitivity reactions occur in the pre-sensitized host upon re-exposure to the inciting antigen, and they are mediated by T cells and immunoglobulins of the adaptive immune system. Hypersensitivity responses that occur repeatedly can result in significant disease. Indeed, chronic inflammation can lead to severe morbidity and mortality.

In those with respiratory allergies, hypersensitivity to **fungal allergens** is common. At least 20-25% of those with asthma are skin-test positive for fungal allergens, commonly including *Aspergillus fumigatus*[7, 8]. Moreover, current evidence suggests an association between fungal sensitization and asthma severity[9]. Patients with severe asthma requiring multiple hospital visits were significantly more likely to be sensitized to fungal allergens than those with mild asthma[10]. The true impact of fungi on those with respiratory allergies is not well understood, because fungi are ubiquitous but hard to measure and exposure is universal but variable with respect to time and intensity.

$CD4^+$ T helper (T_H) cells are central regulators of the hypersensitivity reaction, because they serve an essential role in the coordination of the adaptive immune response. Separate, distinct subsets of $CD4^+$ T_H cells mediate a variety of distinct adaptive immune response "programs". Antigen, including allergen, exposure can initiate the afferent phase of the adaptive immune response that includes all subsequent events that lead to the formation of a poised antigen-specific response. The priming of $CD4^+$ T_H cells from naïve precursor $CD4^+$ T cells is a critical component of the afferent phase. $CD4^+$ T_H cells aid B cells in the production of antibodies that mediate components of the hypersensitivity reaction. Endowed with antigen-specific receptors, T cells and antibodies mediate the efferent phase of the adaptive immune response that encompasses all the immune activities directed at the antigen source. Pre-formed antibodies trigger the immediate hypersensitivity reaction. Meanwhile, primed T cells mediate delayed hypersensitivity responses, mainly through the secretion of immune signaling molecules, especially cytokines. The coordinated immune response against the innocuous antigen results in collateral damage to host tissue, manifesting as the symptoms of hypersensitivity disease.

Current Hypotheses for the Pathogenesis of Allergies

After comparing allergic, or atopic, disease prevalence between white and Aboriginal families in Saskatchewan, Gerrard and co-workers suggested in 1976 that atopic disease may be the price paid for freedom from infectious diseases[11]. The "**hygiene hypothesis**" for allergy gained widespread attention after

Strachan proposed in 1981 that a decrease in the episodes of early life infections due to increased cleanliness in the home and decreased sibship may underlie the increasing incidence of hay fever noted in the UK[12]. Prior to the identification of additional $CD4^+$ T cell subsets, the T_H1/T_H2 dichotomy was considered a cornerstone of adaptive immunity for decades after it's inception in the 1980s[13]. It was purported that $CD4^+$ T cells differentiated into either $CD4^+$ T_H1 or T_H2 cells, and each mediated unique immune responses. Accordingly, the T_H1/T_H2 dichotomy was incorporated into explanations for the alarming increase in the prevalence of allergic diseases, including atopic asthma, noted in the latter half of the 20th century in developed countries[1]. The "hygiene hypothesis" for allergies stated that a paucity of T_H1-promoting infections early in life disrupted the T_H1/T_H2 balance and resulted in an increased propensity for developing T_H2-mediated allergies[11, 12].

The depth of the collective understanding of **immune regulation** has been greatly increased during the intervening period through revelatory work on the biology of $CD4^+$ T regulatory cells (T_{Reg}) and certain dendritic cell (DC) subsets with regulatory function. Furthermore, the identification of pattern recognition receptors (PRRs) including the Toll-like receptor (TLR) family has further illuminated the expansive ability of cells of the immune system to interact with the microbial world in order to achieve an appropriate immune response. This type of information regarding immune regulation taken together with accumulated epidemiological evidence concerning the association between environmental factors and diseases of immune dysregulation, has lead to a

refashioning of the original “hygiene hypothesis”. A revised understanding of the hypothesis should encompass the idea that alterations in certain interactions with the microbial world in general, and not infections in particular, in Westernized countries has led to defects in the maintenance of immune regulation resulting in an increase in the incidence of allergic, and possibly autoimmune disease[14, 15].

Rook and Burnet suggest that nonpathogenic microbes which have shared human’s evolutionary past are recognized by the innate immune system and instruct the development of immunoregulatory responses that inhibit allergic disorders, autoimmune disease, and inflammatory bowel disease[16, 17]. Bjorksten contends that no major risk factors leading to the development of allergies have been identified, but rather that recent evidence indicates a deficit in the protective influence of interactions with the intestinal microbiota during infancy may be leading to the increase in allergic disease[18]. There is a significant amount of epidemiologic and clinical data supporting this **altered microbiota hypothesis**. These include correlations between allergic airway disease and (1) altered fecal microbiota, (2) antibiotic use early in life, and (3) dietary changes over the past two decades (reviewed in[19]).

Mucosal Immune System

The mucosal immune system monitors the epithelium of the respiratory, gastrointestinal, and genitourinary tracts, where vital interactions with the outside world are undertaken. The mucosal immune system is charged with guarding the epithelial surfaces to protect the host against infection, but inappropriate

inflammation can damage the epithelium and impair important physiologic functions. For this reason, tolerance and inflammation are tightly controlled by complex, multi-layered regulatory mechanisms along the mucosa. Many features of the mucosal immune system commensurate with this task have been identified, including unique epithelial cells and innate and adaptive immune cells. Similarities in the structure and function of different musoca-associated lymphoid tissues (MALT) have encouraged the concept of a common mucosal immune system (CMIS), but differences do exist. A shared property is the propensity to generate systemic tolerance to antigens encountered via the oral, nasal, and airway routes[20-23].

MALT is organized into unique inductive and effector sites[24, 25]. Inductive sites include specialized lymphoid follicles underlying the epithelium, such as nasopharynx-associated lymphoid tissue (NALT) and bronchial-associated lymphoid tissue (BALT) in the upper and lower airway, respectively, and Peyer's patches (PP) and isolated lymph follicles (ILF) in the gut, and downstream lymph nodes, including cervical and mediastinal lymph nodes (LN) draining the respiratory mucosa and mesenteric LN draining the intestinal mucosa. MALT effector sites include the epithelium and lamina propria.

The **lungs** are comprised of two functionally distinct compartments, the conducting airways and the lung parenchyma[26]. The conducting airways are lined with mucosal epithelium, containing ciliated and secretory cells that together mediate the mucociliary clearance of inhaled antigens. The lung parenchyma is composed of the thin-walled alveoli that are specialized for the

purpose of gas exchange between the inhaled air and underlying capillaries. The regulation of inflammation in the lung parenchyma is critical in order to protect the host and to permit gas exchange. In addition to antigen exclusion and mucociliary clearance, airway epithelial cells secrete a variety of soluble products that protect the tissue from both pathogens and inflammation.

In the lungs, **macrophages** are critical mediators of both host defense and immune homeostasis. Macrophages are found throughout the respiratory tree and are the major leukocyte subset found within the alveolar space. A primary role of alveolar macrophages is to phagocytose and sequester inhaled antigens, thereby preventing the development of an adaptive immune response[27]. TGFβ-dependent interactions with airway epithelial cells inhibit the inflammatory response of macrophages[28]. However, in response to certain stimuli, including those provided by microorganisms or cytokines, alveolar macrophages will disengage with the airway epithelial cells and acquire a pro-inflammatory phenotype in order to phagocytose and kill microorganisms and stimulate the innate immune response[29, 30]. **Neutrophils** are the first responders to arrive after the pro-inflammatory innate immune response has been initiated. Neutrophils aid in host defense through the phagocytosis of microorganisms and particularly, through the release of microbicidal products.

Antigens are acquired by LP-resident **dendritic cells** (DC) directly by sampling the lumen, or indirectly through the action of specialized Microfold (M) cells situated in the epithelium which transfer luminal antigens to DC in underlying lymphoid tissues including NALT and PP[31, 32]. Interactions between

antigen-loaded DC and $CD4^+$ T cells in the inductive sites determine the nature of the ensuing response. In particular, the activation state of the DC affects the outcome of tolerance or inflammation[33]. Evolutionarily conserved microbial products, termed pathogen-associated molecular patterns (PAMP), signal through PRR that are highly expressed by DC. Signals received through PRR, including TLR, are synthesized in complex fashion that depends on the variety and duration of the stimulation[34]. As an example, signaling through TLR9 on DC induced T_{Reg} activity in one study, and signaling through TLR4 or TLR9 on DC abolished T_{Reg}-mediated suppression in another[35, 36]. Therefore, interactions with microbial products can influence the propensity for DC to stimulate tolerance or inflammation.

$CD4^+$ T cells coordinate antigen-specific immune responses against inhaled or ingested antigens. It is widely accepted that priming of $CD4^+$ T cells requires contact with antigen presenting cells (APC), especially DC, that have acquired antigen, presented antigen in the context of MHCII, and expressed certain co-stimulatory receptors[37, 38]. APC acquire antigen at the site of introduction and migrate to draining lymph nodes to prime naïve $CD4^+$ T cells. Naïve $CD4^+$ T cells undergo multiple rounds of division and progress through multiple stages of differentiation along the pathway to becoming effector $CD4^+$ T_H cells[39].

$CD4^+$ T_H cells differentiate into one of several distinct subsets that in turn mediate a distinct adaptive immune response “program”. Each program has a genetic foundation in $CD4^+$ T_H cells. Master regulation by a specific transcription

factor promotes the acquisition of a particular T_H phenotype at the expense of the other phenotypes. Tbet (Tbx21) promotes T_H1 development, GATA3 promotes T_H2 development, and it seems RORγT may similarly promote T_H17 development[40-42]. Likewise, $CD4^+$ T_{Reg} cells that inhibit $CD4^+$ T_H activity to limit harmful inflammation are specified by the transcription factor Foxp3[43]. During $CD4^+$ T_H cell activation, the cytokine milieu present guides cellular differentiation along one of the particular pathways. IL-12 along with IFNγ promotes T_H1 cell development, IL-4 promotes T_H2 cell development, and the combination of TGFβ and IL-6 promotes T_H17 development[44-47]. The presence of TGFβ alone supports the differentiation of T_{Reg} cells.

Cytokine production represents a key effector function by which $CD4^+$ T_H cells coordinate adaptive immune responses[48]. By producing a distinct set of cytokines, each $CD4^+$ T_H cell subset coordinates a distinctive adaptive immune response program that likely developed evolutionarily to counter a particular pathogenic threat. T_H1 cells produce IFNγ, along with IL-2 and TNFα, and help protect against intracellular pathogens, but also mediate delayed-type-hypersensitivity. T_H2 cells produce IL-4, IL-5, and IL-13 and promote a response to parasite infection, but also mediate allergic responses. Recently identified T_H17 cells produce IL-17. T_H17 cells promote damage to self-tissue in autoimmune disease, but it is not yet clear what their role is in host defense. Likewise, $CD4^+$ T_{Reg} cells are recognized for the production of cytokines with anti-inflammatory activity, including IL-10 and TGFβ, and are able to limit $CD4^+$ T_H responses. The capacity of the immune system to prevent the development or

inhibit the activity of $CD4^+$ T_H cell responses against innocuous antigens is paramount to averting hypersensitivity disease.

Activated T and B cells travel through the lymphatics and eventually the thoracic duct where they enter the bloodstream and traffic to effector sites in the lamina propria (LP) and epithelium. It is suggested that lymphocytes return to the tissue in which they were activated, and PP express mucosal vascular addressin cell-adhesion molecule 1 (MADCAM1) whereas NALT express peripheral-node addressin[49]. However, lymphocyte migration to MLN relied on adhesion molecules that bind both mucosal and peripheral node addressins, indicating that MLN could serve an important role as a crossover point for cells activated in the GALT. Activated B cells undergo immunoglobulin class switch to IgA in PP and NALT and are chemotactically attracted to the epithelium where they differentiate further into antibody-secreting plasma cells[50, 51 52]. Likewise, "effector memory" $CD4^+$ and $CD8^+$ T cells and presumably, T_{Reg} also take up residence in the LP[53, 54].

Antigens encountered at mucosal sites preferentially lead to tolerance induction. As mentioned above, antigens delivered via oral, nasal, or airway routes can induce systemic unresponsiveness to the particular antigen. Oral tolerance has been rigorously investigated for its therapeutic potential in the setting of autoimmune diseases, where prevention or amelioration was seen in mouse models of rheumatoid arthritis, multiple sclerosis and type I diabetes[55-57]. Oral tolerance can also inhibit the cardinal features of allergic airway disease (AAD) in the well-studied OVA model[58]. In human adult volunteers, oral

tolerance was demonstrated after a prolonged feeding regimen with keyhole limpet hemocyanin resulted in T cell, but not B cell, systemic unresponsiveness[59].

The mechanisms mediating oral tolerance depend on the dose of antigen administered[60, 61]. High doses lead to anergy/deletion, but for this discussion the ability of low dose antigen to induce suppression is most interesting. The results of depletion, reconstitution, and adoptive transfer studies convincingly demonstrate that tolerance in this setting is mediated by $CD4^+$ T_{Reg}[62-65]. The mechanisms of T_{Reg}-mediated suppression are not entirely known, but it is clear that T_{Reg} require T cell receptor stimulation and that production of immunosuppressive cytokines, IL-10 and TGFβ, are critical mediators *in vivo*[66]. Thus, T_{Reg} require specific activation but can mediate nonspecific suppression in what is termed "bystander suppression." As mentioned previously, DC-T cell interactions control the immunological outcome, and expansion of the DC population with the *in vivo* administration of flt3 ligand can enhance the induction of oral tolerance[67]. Similarly, repeated antigen exposure in the airways leads to the development of dominant tolerance mediated by CD4+ T_{Reg}[68]. Depletion and adoptive transfer studies of lung DC, indicate that these cells are crucial to tolerance induction at this mucosal site as well[69, 70]. In humans, genetic deficiency in the FOXP3 gene that controls the transcriptional program for T_{Reg} commitment leads to a complex syndrome characterized by severe autoimmune and allergic manifestations[71-73]. Moreover, defects in the ability of T_{Reg} from

allergic patients to inhibit allergen-specific T_H2 responses support the functional role of these cells in maintaining tolerance[74-76].

Host Defense to *Aspergillus fumigatus*

Aspergillus fumigatus is a ubiquitous, airborne fungus that does not pose an infectious threat to immunocompetent individuals. *A. fumigatus* is a eukaryotic organism with a complex life cycle. Conidia are specialized bodies made expressly for the purpose of air-borne dissemination of the fungus. Conidia disseminate in a dormant, resting state, but they commence germination soon upon arrival in a warm, moist location, such as the lung[77]. While pulmonary infection with *A. fumigatus* is a major concern in the treatment of immunosuppressed patients, the innate immune system effectively protects immunocompetent individuals.

The innate immune system efficiently clears the lungs of inhaled *A. fumigatus* conidia. Macrophages and neutrophils cooperate to protect the host from *A. fumigatus* infection[78]. Alveolar macrophages clear resting conidia without promoting inflammation[79, 80]. Germination of conidia triggers a pro-inflammatory response in macrophages based on the recognition of fungal PAMP by host PRR[79, 80]. The release of pro-inflammatory mediators results in the recruitment of neutrophils that assist in eliminating the inhaled fungus[81, 82]. Pro-inflammatory cytokines including TNFα and IL-6 promote the innate host defense response[83, 84]. Innate inflammation may serve to promote an adaptive immune response.

Hypersensitivity to *Aspergillus fumigatus*

Due to the level of exposure and/or a genetic predisposition, inhaled *A. fumigatus* induces hypersensitivity responses in otherwise healthy individuals. *A. fumigatus* is implicated in three lower respiratory tract hypersensitivity diseases: atopic asthma, allergic bronchopulmonary aspergillosis (ABPA), and hypersensitivity pneumonitis (HP). $CD4^+$ T_H2 cells mediate atopic asthma and ABPA, and T_H1 $CD4^+$ T cells participate in HP. Interestingly, allergic asthma or HP may develop in different individuals exposed to *A. fumigatus* under very similar occupational circumstances, suggesting that the manifestation of either hypersensitivity disease may be determined primarily by the host response[85, 86].

Allergic asthma is a lung hypersensitivity disease characterized by reversible obstruction of the airways. An inappropriate inflammatory response to inhaled particles, the allergens, underlies the pathogenesis of allergic asthma. IgE, bound to the surface of mast cells, mediates the acute phase of the allergic response, and $CD4^+$ T_H2 cells mediate the late phase of the allergic response, including airway eosinophilia. Inflammation organizes along the conducting airways in the peribronchial and peribronchiolar regions. The inflammatory response leads to goblet cell metaplasia with mucous hypersecretion and remodeling of the peribronchial layers of smooth muscle and collagen. The cumulative immunopathological effect is to render the airways hyperreactive to inhaled stimuli. Upon re-exposure to the allergen, an “asthma attack” ensues. Sensitization to *Aspergillus* or other molds among populations of patients with severe asthma is 20-25%[7-9, 87].

Hypersensitivity pneumonitis is also termed 'extrinsic allergic alveolitis.' In patients with HP, prolonged or repeated exposure to high levels of certain organic dusts induces an inappropriate inflammatory response. It appears that particles of a certain size, those that they are able to reach the alveoli, may lead to HP. The list of causative agents includes microorganisms that do not cause disease in healthy individuals, including *A. fumigatus*[88-90]. Inflammation develops in the alveoli and in the interstitial space leading to thickening of the alveolar wall and eventually to interstitial fibrosis. HP is associated with a $CD4^+$ T_H1 response, and other features of the underlying inflammation include an influx of neutrophils in terminal airways, a low $CD4^+/CD8^+$ T cell ratio, and the presence of precipitating IgG antibodies[91]. Acute HP presents with fever, cough, and shortness of breath. HP can be difficult to diagnose and, if untreated, can be severe. The National Heart, Lung, and Blood Institute in collaboration with the Office of Rare Diseases of the National Institutes of Health recently called for an "improvement of animal models [for hypersensitivity pneumonitis] that are more relevant for human disease[92]."

Allergic bronchopulmonary aspergillosis is a severe hypersensitivity disease induced by colonization of the airway by *A. fumigatus*[93, 94]. Individuals with asthma or cystic fibrosis are most likely to develop ABPA, probably due to increased airway mucus. Persistence of *A. fumigatus* in the airway leads to an intense $CD4^+$ T_H2 response, high levels of IgE and IgG antibodies, and accumulation of eosinophils and neutrophils in the airway. In patients with

ABPA, the ongoing inflammation in the airway leads to severe asthma, bronchiectasis, and, potentially, fibrosis.

For patients with respiratory hypersensitivity diseases, the **chronicity** of the inflammation generally determines the severity of the morbidity and mortality. For those with asthma, chronic inflammation is associated with nonspecific bronchial hyperreactivity, and chronic inflammation promotes airway remodeling. Airway remodeling is associated with reversible airways obstruction[95]. Bronchial hyperreactivity and reversible airways obstruction promote an "asthma attack". The frequency, severity, and controllability of attacks combine to determine the morbidity and mortality of the disease. Recent data suggests that chronic inflammation in asthma patients is associated with abnormal remodeling of bronchial arteries and narrowing of arterial lumens[96]. Arterial remodeling is a component of the pathogenesis of pulmonary arterial hypertension (PAH), an idiopathic disease correlated with inflammation that can precipitate right sided-heart failure and death[97]. For those with HP, chronic inflammation can result in progressive, irreversible interstitial fibrosis, potentially leading to respiratory failure and death[91].

Investigations into the Allergic Response to *A. fumigatus*

Laboratory experiments demonstrate that exposure to *A. fumigatus* can result in multiple $CD4^+$ T_H subset responses. The initial response to inhaled conidia includes the release of pro-inflammatory and T_H1-promoting cytokines[81]. After a single exposure to viable conidia, $CD4^+$ T_H1 cells develop[98, 99]. It is

currently unknown whether $CD4^+$ T_H1 cells induced by the inhalation of *A. fumigatus* conidia can mediate a hypersensitivity disease like HP with repeated exposure. *A. fumigatus* hyphae or preparations of *A. fumigatus* antigens, containing hyphae and conidia present in the growing mycelium, are allergenic (i.e. T_H2-promoting)[99-102]. The majority of allergens identified for *A. fumigatus* are derived from products expressed during germination[9]. The ability of inhaled conidia to promote $CD4^+$ T_H2 cell development is less clear, but inhaled conidia stimulated a response from pre-formed $CD4^+$ T_H2 cells, present in mice previously sensitized to *A. fumigatus* antigens[103]. Mice do not develop asthma *per se*, but they can develop an allergic airway disease (AAD) with many of the immunological features identified in atopic asthma.

In a series of experiments, Kurup and colleagues explored the development and immune regulation of the allergic response to *A. fumigatus* in mice. Repeated intranasal exposure to *A. fumigatus* conidia, specifically 5×10^4 conidia each day on days 0-15 and 25-30, resulted in peribronchial and perivascular inflammation with macrophages, lymphocytes, and eosinophils[104]. However, in a direct comparison, *A .fumigatus* antigens were more allergenic than conidia[105]. The strength of the allergic response to inhaled *A. fumigatus* antigens was increased by several weeks of exposure, prior intraperitoneal sensitization, and attachment to inert particles[100, 106, 107]. Sensitization and respiratory challenge with *A. fumigatus* antigens resulted in IL-5-dependent bone marrow, peripheral blood, and lung eosinophila[108-112]. In this model, IgE production and the development of airway hyperreactivity were dependent on IL-

4, but the absence of IL-4 had little effect on pulmonary inflammation and eosinophilia[109, 113-115]. Neutralization experiments demonstrated that IFNγ normally limited the IgE and eosinophil responses to *A. fumigatus* exposure[108]. Interestingly, Kurup and colleagues reported fibromuscular thickening of bronchial vascular walls with chronic inflammation in this model of T_H2 AAD to *A. fumigatus*.

Laviolette and colleagues developed a murine model of AAD that developed after exposure to *A. fumigatus* antigens three times a week for three weeks[101]. Based on studies with the anti-inflammatory drug dexamethasone, data suggested that T cells promoted the allergic response to *A. fumigatus* characterized by lung eosinophil recruitment and increased IgE production[116, 117]. In this model, allergic inflammation was associated with increased production of IL-1, TNFα, IL-4, IL-5, GM-CSF, and ICAM-1 in the lungs[118-120].

Hogaboam et al. developed a model of chronic pulmonary inflammation involving the delivery of *A. fumigatus* conidia into the lungs of mice that were previously sensitized to *A. fumigatus* antigens via the intraperitoneal and intranasal routes[103]. Thirty days after the delivery of conidia, sustained features of AAD included airway hyperreactivity, airway lymphocytes, T_H2 cytokine levels, goblet cell metaplasia, and fibrosis. The primary contribution of the T_H2 immune response to the observed chronic allergic inflammation was demonstrated by disrupting IL-13 function and the signal transducer and activator of transcription 6 (Stat6) pathway[121-123]. The Hogaboam group used this model to extensively

characterize the role of various chemokine-signaling pathways in orchestrating the inflammatory response to *A. fumigatus*[124-134].

Noverr et al. demonstrated that microbiota disruption promoted the development of an allergic airway response to *A. fumigatus* conidia or ovalbumin challenge[135, 136]. In these studies, antibiotic-induced gastrointestinal (GI) microbiota disruption was accompanied by stable increases in GI enteric bacteria and *C. albicans*. There was no evidence of microbial growth in the lungs or inflammation in the GI tract in this model. The allergic parameters significantly elevated in the microbiota-disrupted mice included pulmonary eosinophilia, total serum IgE, lung leukocyte IL-5, IL-13, and IFNγ, and goblet cell metaplasia. The response did not develop in IL-13-deficient mice or mice that had been depleted of $CD4^+$ T cells. In addition, vigorous allergic airway responses were generated in both C57BL/6 and Balb/c mice following microbiota disruption and antigen challenge but not in antigen-challenged "normal microbiota" C57BL/6 and Balb/c mice.

Hypothesis

Repeated respiratory exposure to viable *A. fumigatus* conidia will result in a $CD4^+$ T cell-mediated hypersensitivity disease eventually leading to pulmonary pathophysiology.

Study Objectives

- To determine if repeated exposure to viable *A. fumigatus* conidia in previously unsensitized mice induces hypersensitivity.
- To determine the phenotype and function of $CD4^+$ T cells in the hypersensitivity response to *A. fumigatus*.
- To determine the pulmonary pathophysiological consequences of a chronic hypersensitivity response to *A. fumigatus*.
- To determine the immune mechanisms responsible for the hypersensitivity response to *A. fumigatus*.

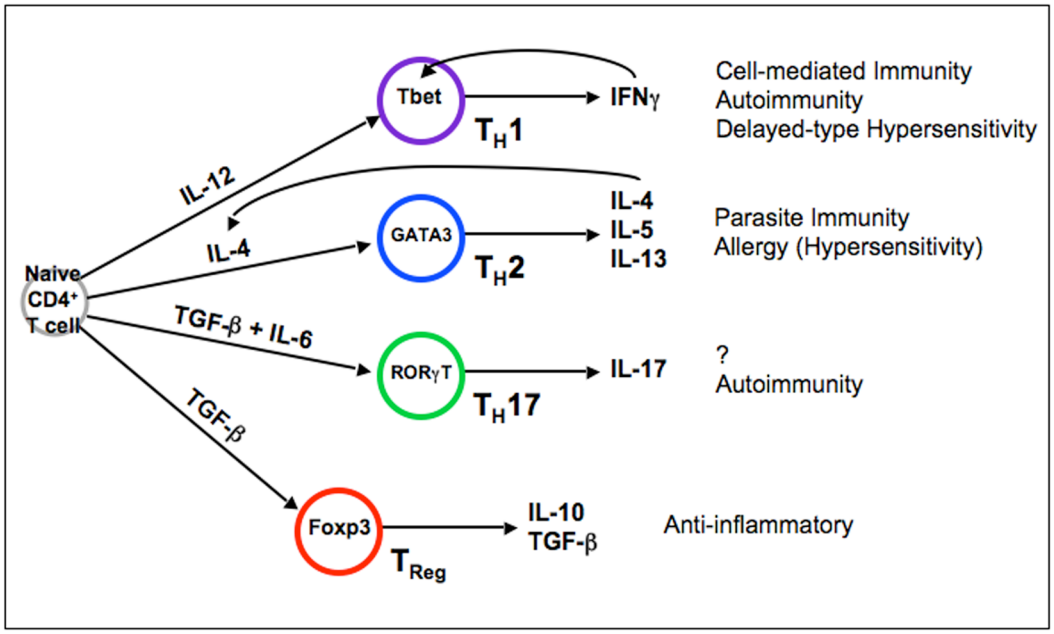

Figure 1-1. CD4$^+$ T cell subsets
For each subset, this diagram depicts the cytokines responsible for CD4$^+$ T cell differentiation, the transcription factors that regulate the CD4$^+$ T cell phenotype, and the cytokines that mediate the CD4$^+$ T cell effector functions. This diagram also depicts the type(s) of adaptive immune response(s) coordinated by each CD4$^+$ T cell subset.

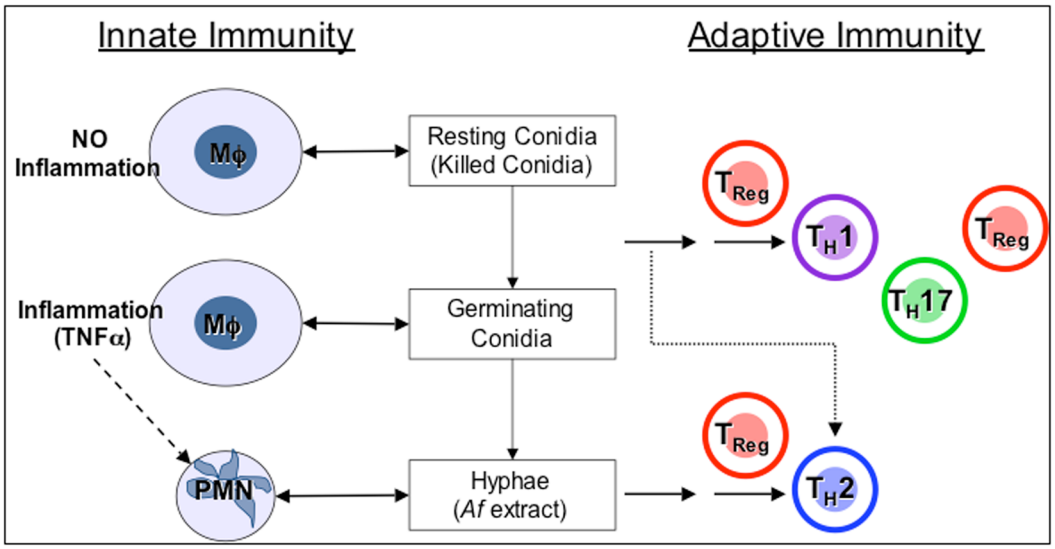

Figure 1-2. Innate and adaptive immune response to *Aspergillus fumigatus*
This diagram depicts the leukocytes that are involved in the response to various biological forms of *A. fumigatus* after inhalation. Macrophages (Mϕ) kill resting and germinating conidia and neutrophils (PMN) kill hyphae. Resting conidia do not induce a pro-inflammatory response from Mϕ, but germinating conidia do. The innate inflammatory response mediated by Mϕ includes the production of TNFα and the recruitment of PMN. Viable conidia are reported to prime $CD4^+$ T_H1 and T_H17 cells. Hyphae and fungal extract, composed of all forms but primarily hyphae, are reported to prime $CD4^+$ T_H2 cells. $CD4^+$ T_{Reg} cells respond to viable conidia and hyphae and inhibit $CD4^+$ T_H cell responses. Nonviable, resting conidia do not promote $CD4^+$ T cell responses.

References

1. Mannino, D. M. et al. Surveillance for asthma--United States, 1960-1995. MMWR CDC Surveill Summ 47, 1-27 (1998).
2. Upton, M. N. et al. Intergenerational 20 year trends in the prevalence of asthma and hay fever in adults: the Midspan family study surveys of parents and offspring. Bmj 321, 88-92 (2000).
3. Peat, J. K. et al. Changing prevalence of asthma in Australian children. Bmj 308, 1591-6 (1994).
4. Worldwide variations in the prevalence of asthma symptoms: the International Study of Asthma and Allergies in Childhood (ISAAC). Eur Respir J 12, 315-35 (1998).
5. Worldwide variation in prevalence of symptoms of asthma, allergic rhinoconjunctivitis, and atopic eczema: ISAAC. The International Study of Asthma and Allergies in Childhood (ISAAC) Steering Committee. Lancet 351, 1225-32 (1998).
6. Beasley, R., Crane, J., Lai, C. K. & Pearce, N. Prevalence and etiology of asthma. J Allergy Clin Immunol 105, S466-72 (2000).
7. Boulet, L. P. et al. Comparative degree and type of sensitization to common indoor and outdoor allergens in subjects with allergic rhinitis and/or asthma. Clin Exp Allergy 27, 52-9 (1997).
8. Mari, A., Schneider, P., Wally, V., Breitenbach, M. & Simon-Nobbe, B. Sensitization to fungi: epidemiology, comparative skin tests, and IgE reactivity of fungal extracts. Clin Exp Allergy 33, 1429-38 (2003).
9. Denning, D. W., O'Driscoll, B. R., Hogaboam, C. M., Bowyer, P. & Niven, R. M. The link between fungi and severe asthma: a summary of the evidence. Eur Respir J 27, 615-26 (2006).
10. O'Driscoll, B. R., Hopkinson, L. C. & Denning, D. W. Mold sensitization is common amongst patients with severe asthma requiring multiple hospital admissions. BMC Pulm Med 5, 4 (2005).
11. Gerrard, J. W., Geddes, C. A., Reggin, P. L., Gerrard, C. D. & Horne, S. Serum IgE levels in white and metis communities in Saskatchewan. Ann Allergy 37, 91-100 (1976).
12. Strachan, D. P. Hay fever, hygiene, and household size. Bmj 299, 1259-60 (1989).
13. Mosmann, T. R. & Coffman, R. L. TH1 and TH2 cells: different patterns of lymphokine secretion lead to different functional properties. Annu Rev Immunol 7, 145-73 (1989).
14. Wills-Karp, M., Santeliz, J. & Karp, C. L. The germless theory of allergic disease: revisiting the hygiene hypothesis. Nat Rev Immunol 1, 69-75 (2001).
15. Umetsu, D. T., McIntire, J. J., Akbari, O., Macaubas, C. & DeKruyff, R. H. Asthma: an epidemic of dysregulated immunity. Nat Immunol 3, 715-20 (2002).
16. Rook, G. A. & Brunet, L. R. Give us this day our daily germs. Biologist (London) 49, 145-9 (2002).

17. Rook, G. A. & Brunet, L. R. Old friends for breakfast. Clin Exp Allergy 35, 841-2 (2005).
18. Bjorksten, B. Effects of intestinal microflora and the environment on the development of asthma and allergy. Springer Semin Immunopathol 25, 257-70 (2004).
19. Noverr, M. C. & Huffnagle, G. B. Does the microbiota regulate immune responses outside the gut? Trends Microbiol (in press) (2004).
20. Chase, M. W. Inhibition of experimental drug allergy by prior feeding of the sensitizing agent. Proc Soc Exp Biol 61, 257-259 (1946).
21. Boyaka, P. N. et al. Therapeutic manipulation of the immune system: enhancement of innate and adaptive mucosal immunity. Curr Pharm Des 9, 1965-72 (2003).
22. Macaubas, C., DeKruyff, R. H. & Umetsu, D. T. Respiratory tolerance in the protection against asthma. Curr Drug Targets Inflamm Allergy 2, 175-86 (2003).
23. Mayer, L. & Shao, L. Therapeutic potential of oral tolerance. Nat Rev Immunol 4, 407-19 (2004).
24. Kiyono, H. & Fukuyama, S. NALT- versus Peyer's-patch-mediated mucosal immunity. Nat Rev Immunol 4, 699-710 (2004).
25. Eberl, G. Inducible lymphoid tissues in the adult gut: recapitulation of a fetal developmental pathway? Nat Rev Immunol 5, 413-20 (2005).
26. Holt, P. G., Strickland, D. H., Wikstrom, M. E. & Jahnsen, F. L. Regulation of immunological homeostasis in the respiratory tract. Nat Rev Immunol 8, 142-52 (2008).
27. MacLean, J. A. et al. Sequestration of inhaled particulate antigens by lung phagocytes. A mechanism for the effective inhibition of pulmonary cell-mediated immunity. Am J Pathol 148, 657-66 (1996).
28. Munger, J. S. et al. The integrin alpha v beta 6 binds and activates latent TGF beta 1: a mechanism for regulating pulmonary inflammation and fibrosis. Cell 96, 319-28 (1999).
29. Underhill, D. M. & Ozinsky, A. Phagocytosis of microbes: complexity in action. Annu Rev Immunol 20, 825-52 (2002).
30. Takabayshi, K. et al. Induction of a homeostatic circuit in lung tissue by microbial compounds. Immunity 24, 475-87 (2006).
31. Rescigno, M. et al. Dendritic cells express tight junction proteins and penetrate gut epithelial monolayers to sample bacteria. Nat Immunol 2, 361-7 (2001).
32. Kerneis, S., Bogdanova, A., Kraehenbuhl, J. P. & Pringault, E. Conversion by Peyer's patch lymphocytes of human enterocytes into M cells that transport bacteria. Science 277, 949-52 (1997).
33. Mowat, A. M. Dendritic cells and immune responses to orally administered antigens. Vaccine 23, 1797-9 (2005).
34. Reis e Sousa, C. Toll-like receptors and dendritic cells: for whom the bug tolls. Semin Immunol 16, 27-34 (2004).
35. Mellor, A. L. et al. Cutting edge: CpG oligonucleotides induce splenic CD19+ dendritic cells to acquire potent indoleamine 2,3-dioxygenase-

dependent T cell regulatory functions via IFN Type 1 signaling. J Immunol 175, 5601-5 (2005).
36. Pasare, C. & Medzhitov, R. Toll pathway-dependent blockade of CD4+CD25+ T cell-mediated suppression by dendritic cells. Science 299, 1033-6 (2003).
37. Croft, M., Duncan, D. D. & Swain, S. L. Response of naive antigen-specific CD4+ T cells in vitro: characteristics and antigen-presenting cell requirements. J Exp Med 176, 1431-7 (1992).
38. Dubey, C., Croft, M. & Swain, S. L. Costimulatory requirements of naive CD4+ T cells. ICAM-1 or B7-1 can costimulate naive CD4 T cell activation but both are required for optimum response. J Immunol 155, 45-57 (1995).
39. Swain, S. Lymphocyte effector functions - Lymphocyte heterogeneity - is it limitless? Curr Opin Immunol 15, 332-335 (2003).
40. Ivanov, II et al. The orphan nuclear receptor RORgammat directs the differentiation program of proinflammatory IL-17+ T helper cells. Cell 126, 1121-33 (2006).
41. Szabo, S. J. et al. A novel transcription factor, T-bet, directs Th1 lineage commitment. Cell 100, 655-69 (2000).
42. Zheng, W. & Flavell, R. A. The transcription factor GATA-3 is necessary and sufficient for Th2 cytokine gene expression in CD4 T cells. Cell 89, 587-96 (1997).
43. Fontenot, J. D., Gavin, M. A. & Rudensky, A. Y. Foxp3 programs the development and function of CD4+CD25+ regulatory T cells. Nat Immunol 4, 330-6 (2003).
44. Magram, J. et al. IL-12-deficient mice are defective in IFN gamma production and type 1 cytokine responses. Immunity 4, 471-81 (1996).
45. Gessner, A. & Rollinghoff, M. Biologic functions and signaling of the interleukin-4 receptor complexes. Immunobiology 201, 285-307 (2000).
46. Zhang, Y. et al. Interferon gamma stabilizes the T helper cell type 1 phenotype. J Exp Med 194, 165-72 (2001).
47. McGeachy, M. J. & Cua, D. J. Th17 cell differentiation: the long and winding road. Immunity 28, 445-53 (2008).
48. Steinman, L. A brief history of T(H)17, the first major revision in the T(H)1/T(H)2 hypothesis of T cell-mediated tissue damage. Nat Med 13, 139-45 (2007).
49. Csencsits, K. L., Jutila, M. A. & Pascual, D. W. Nasal-associated lymphoid tissue: phenotypic and functional evidence for the primary role of peripheral node addressin in naive lymphocyte adhesion to high endothelial venules in a mucosal site. J Immunol 163, 1382-9 (1999).
50. Spalding, D. M. & Griffin, J. A. Different pathways of differentiation of pre-B cell lines are induced by dendritic cells and T cells from different lymphoid tissues. Cell 44, 507-15 (1986).
51. Shikina, T. et al. IgA class switch occurs in the organized nasopharynx- and gut-associated lymphoid tissue, but not in the diffuse lamina propria of airways and gut. J Immunol 172, 6259-64 (2004).

52. Bowman, E. P. et al. The intestinal chemokine thymus-expressed chemokine (CCL25) attracts IgA antibody-secreting cells. J Exp Med 195, 269-75 (2002).
53. Masopust, D., Vezys, V., Marzo, A. L. & Lefrancois, L. Preferential localization of effector memory cells in nonlymphoid tissue. Science 291, 2413-7 (2001).
54. Reinhardt, R. L., Khoruts, A., Merica, R., Zell, T. & Jenkins, M. K. Visualizing the generation of memory CD4 T cells in the whole body. Nature 410, 101-5 (2001).
55. Higgins, P. J. & Weiner, H. L. Suppression of experimental autoimmune encephalomyelitis by oral administration of myelin basic protein and its fragments. J Immunol 140, 440-5 (1988).
56. Homann, D., Dyrberg, T., Petersen, J., Oldstone, M. B. & von Herrath, M. G. Insulin in oral immune "tolerance": a one-amino acid change in the B chain makes the difference. J Immunol 163, 1833-8 (1999).
57. Nagler-Anderson, C., Bober, L. A., Robinson, M. E., Siskind, G. W. & Thorbecke, G. J. Suppression of type II collagen-induced arthritis by intragastric administration of soluble type II collagen. Proc Natl Acad Sci U S A 83, 7443-6 (1986).
58. Russo, M. et al. Suppression of asthma-like responses in different mouse strains by oral tolerance. Am J Respir Cell Mol Biol 24, 518-26 (2001).
59. Husby, S., Mestecky, J., Moldoveanu, Z., Holland, S. & Elson, C. O. Oral tolerance in humans. T cell but not B cell tolerance after antigen feeding. J Immunol 152, 4663-70 (1994).
60. Friedman, A. & Weiner, H. L. Induction of anergy or active suppression following oral tolerance is determined by antigen dosage. Proc Natl Acad Sci U S A 91, 6688-92 (1994).
61. Mitchison, N. A. Induction of Immunological Paralysis in Two Zones of Dosage. Proc R Soc Lond B Biol Sci 161, 275-92 (1964).
62. Barone, K. S., Jain, S. L. & Michael, J. G. Effect of in vivo depletion of CD4+ and CD8+ cells on the induction and maintenance of oral tolerance. Cell Immunol 163, 19-29 (1995).
63. Garside, P., Steel, M., Liew, F. Y. & Mowat, A. M. CD4+ but not CD8+ T cells are required for the induction of oral tolerance. Int Immunol 7, 501-4 (1995).
64. Yoshida, H. et al. Induction of oral tolerance in splenocyte-reconstituted SCID mice. Clin Immunol Immunopathol 87, 282-91 (1998).
65. Zhang, X., Izikson, L., Liu, L. & Weiner, H. L. Activation of CD25(+)CD4(+) regulatory T cells by oral antigen administration. J Immunol 167, 4245-53 (2001).
66. von Boehmer, H. Mechanisms of suppression by suppressor T cells. Nat Immunol 6, 338-44 (2005).
67. Viney, J. L., Mowat, A. M., O'Malley, J. M., Williamson, E. & Fanger, N. A. Expanding dendritic cells in vivo enhances the induction of oral tolerance. J Immunol 160, 5815-25 (1998).

68. Hall, G., Houghton, C. G., Rahbek, J. U., Lamb, J. R. & Jarman, E. R. Suppression of allergen reactive Th2 mediated responses and pulmonary eosinophilia by intranasal administration of an immunodominant peptide is linked to IL-10 production. Vaccine 21, 549-61 (2003).
69. Akbari, O., DeKruyff, R. H. & Umetsu, D. T. Pulmonary dendritic cells producing IL-10 mediate tolerance induced by respiratory exposure to antigen. Nat Immunol 2, 725-31 (2001).
70. de Heer, H. J. et al. Essential role of lung plasmacytoid dendritic cells in preventing asthmatic reactions to harmless inhaled antigen. J Exp Med 200, 89-98 (2004).
71. Bennett, C. L. et al. The immune dysregulation, polyendocrinopathy, enteropathy, X-linked syndrome (IPEX) is caused by mutations of FOXP3. Nat Genet 27, 20-1 (2001).
72. Chatila, T. A. et al. JM2, encoding a fork head-related protein, is mutated in X-linked autoimmunity-allergic disregulation syndrome. J Clin Invest 106, R75-81 (2000).
73. Wildin, R. S. et al. X-linked neonatal diabetes mellitus, enteropathy and endocrinopathy syndrome is the human equivalent of mouse scurfy. Nat Genet 27, 18-20 (2001).
74. Bellinghausen, I., Klostermann, B., Knop, J. & Saloga, J. Human CD4+CD25+ T cells derived from the majority of atopic donors are able to suppress TH1 and TH2 cytokine production. J Allergy Clin Immunol 111, 862-8 (2003).
75. Grindebacke, H. et al. Defective suppression of Th2 cytokines by CD4CD25 regulatory T cells in birch allergics during birch pollen season. Clin Exp Allergy 34, 1364-72 (2004).
76. Ling, E. M. et al. Relation of CD4+CD25+ regulatory T-cell suppression of allergen-driven T-cell activation to atopic status and expression of allergic disease. Lancet 363, 608-15 (2004).
77. Latge, J. P. Aspergillus fumigatus and aspergillosis. Clin Microbiol Rev 12, 310-50 (1999).
78. Schaffner, A., Douglas, H. & Braude, A. Selective protection against conidia by mononuclear and against mycelia by polymorphonuclear phagocytes in resistance to Aspergillus. Observations on these two lines of defense in vivo and in vitro with human and mouse phagocytes. J Clin Invest 69, 617-31 (1982).
79. Hohl, T. M. et al. Aspergillus fumigatus triggers inflammatory responses by stage-specific beta-glucan display. PLoS Pathog 1, e30 (2005).
80. Steele, C. et al. The beta-glucan receptor dectin-1 recognizes specific morphologies of Aspergillus fumigatus. PLoS Pathog 1, e42 (2005).
81. Brieland, J. K. et al. Cytokine networking in lungs of immunocompetent mice in response to inhaled Aspergillus fumigatus. Infect Immun 69, 1554-60 (2001).
82. Bonnett, C. R., Cornish, E. J., Harmsen, A. G. & Burritt, J. B. Early neutrophil recruitment and aggregation in the murine lung inhibit

germination of Aspergillus fumigatus Conidia. Infect Immun 74, 6528-39 (2006).
83. Cenci, E. et al. Impaired antifungal effector activity but not inflammatory cell recruitment in interleukin-6-deficient mice with invasive pulmonary aspergillosis. J Infect Dis 184, 610-7 (2001).
84. Mehrad, B., Strieter, R. M. & Standiford, T. J. Role of TNF-alpha in pulmonary host defense in murine invasive aspergillosis. J Immunol 162, 1633-40 (1999).
85. Quirce, S., Hinojosa, M., Blanco, R., Cespon, C. & Yoldi, M. Aspergillus fumigatus is the causative agent of hypersensitivity pneumonitis caused by esparto dust. J Allergy Clin Immunol 102, 147-8 (1998).
86. Ruiz-Hornillos, F. J. et al. Occupational asthma due to esparto hypersensitivity in a building worker. Allergy Asthma Proc 28, 571-3 (2007).
87. Schwartz, H. J. & Greenberger, P. A. The prevalence of allergic bronchopulmonary aspergillosis in patients with asthma, determined by serologic and radiologic criteria in patients at risk. J Lab Clin Med 117, 138-42 (1991).
88. Aebischer, C. C., Frey, U. & Schoni, M. H. Hypersensitivity pneumonitis in a five-year-old boy: an unusual antigen source. Pediatr Pulmonol 33, 77-8 (2002).
89. Enriquez-Matas, A. et al. Hypersensitivity pneumonitis caused by domestic exposure to molds. J Investig Allergol Clin Immunol 17, 126-7 (2007).
90. Yoshida, K. et al. Hypersensitivity pneumonitis resulting from Aspergillus fumigatus in a greenhouse. Arch Environ Health 48, 260-2 (1993).
91. Patel, A. M., Ryu, J. H. & Reed, C. E. Hypersensitivity pneumonitis: current concepts and future questions. J Allergy Clin Immunol 108, 661-70 (2001).
92. Fink, J. N. et al. Needs and opportunities for research in hypersensitivity pneumonitis. Am J Respir Crit Care Med 171, 792-8 (2005).
93. Gibson, P. G. Allergic bronchopulmonary aspergillosis. Semin Respir Crit Care Med 27, 185-91 (2006).
94. Tillie-Leblond, I. & Tonnel, A. B. Allergic bronchopulmonary aspergillosis. Allergy 60, 1004-13 (2005).
95. Bousquet, J., Jeffery, P. K., Busse, W. W., Johnson, M. & Vignola, A. M. Asthma. From bronchoconstriction to airways inflammation and remodeling. Am J Respir Crit Care Med 161, 1720-45 (2000).
96. Green, F. H., Butt, J. C., James, A. L. & Carroll, N. G. Abnormalities of the bronchial arteries in asthma. Chest 130, 1025-33 (2006).
97. Chin, K. M. & Rubin, L. J. Pulmonary arterial hypertension. J Am Coll Cardiol 51, 1527-38 (2008).
98. Rivera, A. et al. Innate immune activation and CD4+ T cell priming during respiratory fungal infection. Immunity 25, 665-75 (2006).

99. Bozza, S. et al. Dendritic cells transport conidia and hyphae of Aspergillus fumigatus from the airways to the draining lymph nodes and initiate disparate Th responses to the fungus. J Immunol 168, 1362-71 (2002).
100. Kurup, V. P., Mauze, S., Choi, H., Seymour, B. W. & Coffman, R. L. A murine model of allergic bronchopulmonary aspergillosis with elevated eosinophils and IgE. J Immunol 148, 3783-8 (1992).
101. Wang, J. M., Denis, M., Fournier, M. & Laviolette, M. Experimental allergic bronchopulmonary aspergillosis in the mouse: immunological and histological features. Scand J Immunol 39, 19-26 (1994).
102. Kheradmand, F. et al. A protease-activated pathway underlying Th cell type 2 activation and allergic lung disease. J Immunol 169, 5904-11 (2002).
103. Hogaboam, C. M. et al. Chronic airway hyperreactivity, goblet cell hyperplasia, and peribronchial fibrosis during allergic airway disease induced by Aspergillus fumigatus. Am J Pathol 156, 723-32 (2000).
104. Murali, P. S., Bamrah, B. S., Choi, H., Fink, J. N. & Kurup, V. P. Hyperimmune serum modulates allergic response to spores in a murine model of allergic aspergillosis. J Leukoc Biol 55, 29-34 (1994).
105. Kurup, V. P. et al. Role of particulate antigens of Aspergillus in murine eosinophilia. Int Arch Allergy Immunol 112, 270-8 (1997).
106. Kurup, V. P., Choi, H., Resnick, A., Kalbfleisch, J. & Fink, J. N. Immunopathological response of C57BL/6 and C3H/HeN mice to Aspergillus fumigatus antigens. Int Arch Allergy Appl Immunol 91, 145-54 (1990).
107. Kurup, V. P., Seymour, B. W., Choi, H. & Coffman, R. L. Particulate Aspergillus fumigatus antigens elicit a TH2 response in BALB/c mice. J Allergy Clin Immunol 93, 1013-20 (1994).
108. Kurup, V. P., Choi, H., Murali, P. S. & Coffman, R. L. IgE and eosinophil regulation in a murine model of allergic aspergillosis. J Leukoc Biol 56, 593-8 (1994).
109. Kurup, V. P. et al. Anti-interleukin (IL)-4 and -IL-5 antibodies downregulate IgE and eosinophilia in mice exposed to Aspergillus antigens. Allergy 52, 1215-21 (1997).
110. Murali, P. S., Dai, G., Kumar, A., Fink, J. N. & Kurup, V. P. Aspergillus antigen-induced eosinophil differentiation in a murine model. Infect Immun 60, 1952-6 (1992).
111. Murali, P. S. et al. Aspergillus fumigatus antigen induced eosinophilia in mice is abrogated by anti-IL-5 antibody. J Leukoc Biol 53, 264-7 (1993).
112. Murali, P. S., Kurup, V. P., Guo, J. & Fink, J. N. Development of bone marrow eosinophilia in mice induced by Aspergillus fumigatus antigens. Clin Immunol Immunopathol 84, 216-20 (1997).
113. Kurup, V. P. et al. Immune responses to Aspergillus antigen in IL-4-/-mice and the effect of eosinophil ablation. Allergy 54, 420-7 (1999).
114. Kurup, V. P., Guo, J., Murali, P. S., Choi, H. & Fink, J. N. Immunopathologic responses to Aspergillus antigen in interleukin-4 knockout mice. J Lab Clin Med 130, 567-75 (1997).

115. Kurup, V. P. et al. Aspergillus fumigatus antigen exposure results in pulmonary airway resistance in wild-type but not in IL-4 knockout mice. Clin Immunol 90, 404-10 (1999).
116. Wang, J. M. et al. Dexamethasone and cyclosporin A modulation of cytokine expression and specific antibody synthesis in an allergic bronchopulmonary aspergillosis murine model. Eur J Clin Invest 26, 951-9 (1996).
117. Wang, J. M., Denis, M., Fournier, M. & Laviolette, M. Cyclosporin A increases the pulmonary eosinophilia induced by inhaled Aspergillus antigen in mice. Clin Exp Immunol 93, 323-30 (1993).
118. Chu, H. W., Wang, J. M., Boutet, M., Boulet, L. P. & Laviolette, M. Increased expression of intercellular adhesion molecule-1 (ICAM-1) in a murine model of pulmonary eosinophilia and high IgE level. Clin Exp Immunol 100, 319-24 (1995).
119. Chu, H. W., Wang, J. M., Boutet, M., Boulet, L. P. & Laviolette, M. Immunohistochemical detection of GM-CSF, IL-4 and IL-5 in a murine model of allergic bronchopulmonary aspergillosis. Clin Exp Allergy 26, 461-8 (1996).
120. Chu, H. W., Wang, J. M., Boutet, M. & Laviolette, M. Tumor necrosis factor-alpha and interleukin-1 alpha expression in a murine model of allergic bronchopulmonary aspergillosis. Lab Anim Sci 46, 42-7 (1996).
121. Blease, K. et al. IL-13 fusion cytotoxin ameliorates chronic fungal-induced allergic airway disease in mice. J Immunol 167, 6583-92 (2001).
122. Blease, K. et al. Therapeutic effect of IL-13 immunoneutralization during chronic experimental fungal asthma. J Immunol 166, 5219-24 (2001).
123. Blease, K. et al. Stat6-deficient mice develop airway hyperresponsiveness and peribronchial fibrosis during chronic fungal asthma. Am J Pathol 160, 481-90 (2002).
124. Blease, K., Kunkel, S. L. & Hogaboam, C. M. Acute inhibition of nitric oxide exacerbates airway hyperresponsiveness, eosinophilia and C-C chemokine generation in a murine model of fungal asthma. Inflamm Res 49, 297-304 (2000).
125. Blease, K. et al. Antifungal and airway remodeling roles for murine monocyte chemoattractant protein-1/CCL2 during pulmonary exposure to Asperigillus fumigatus conidia. J Immunol 166, 1832-42 (2001).
126. Blease, K. et al. Enhanced pulmonary allergic responses to Aspergillus in CCR2-/- mice. J Immunol 165, 2603-11 (2000).
127. Blease, K. et al. Airway remodeling is absent in CCR1-/- mice during chronic fungal allergic airway disease. J Immunol 165, 1564-72 (2000).
128. Buckland, K. F. et al. Remission of chronic fungal asthma in the absence of CCR8. J Allergy Clin Immunol 119, 997-1004 (2007).
129. Carpenter, K. J. et al. Therapeutic targeting of CCR1 attenuates established chronic fungal asthma in mice. Br J Pharmacol 145, 1160-72 (2005).

130. Hogaboam, C. M. et al. Immunomodulatory role of C10 chemokine in a murine model of allergic bronchopulmonary aspergillosis. J Immunol 162, 6071-9 (1999).
131. Schuh, J. M., Blease, K. & Hogaboam, C. M. The role of CC chemokine receptor 5 (CCR5) and RANTES/CCL5 during chronic fungal asthma in mice. Faseb J 16, 228-30 (2002).
132. Schuh, J. M., Blease, K. & Hogaboam, C. M. CXCR2 is necessary for the development and persistence of chronic fungal asthma in mice. J Immunol 168, 1447-56 (2002).
133. Schuh, J. M., Blease, K., Kunkel, S. L. & Hogaboam, C. M. Eotaxin/CCL11 is involved in acute, but not chronic, allergic airway responses to Aspergillus fumigatus. Am J Physiol Lung Cell Mol Physiol 283, L198-204 (2002).
134. Schuh, J. M. et al. Airway hyperresponsiveness, but not airway remodeling, is attenuated during chronic pulmonary allergic responses to Aspergillus in CCR4-/- mice. Faseb J 16, 1313-5 (2002).
135. Noverr, M. C., Noggle, R. M., Toews, G. B. & Huffnagle, G. B. Role of antibiotics and fungal microbiota in driving pulmonary allergic responses. Infect Immun 72, 4996-5003 (2004).
136. Noverr, M. C., Falkowski, N. R., McDonald, R. A. & Huffnagle, G. B. The development of allergic airway disease in mice following antibiotic therapy and fungal microbiota increase: role of host genetics, antigen and IL-13. Infect Immun 73, 30-8 (2005).

Chapter 2

Materials and Methods

Mice. IL-4$^{-/-}$ (B6.129P2-*Il4*^{tm1Cgn}/J), IL-10$^{-/-}$ (B6.129P2-*Il10*^{tm1Cgn}/J), IFN$\gamma^{-/-}$ (B6.129S7-*Ifng*^{tm1Ts}/J), and wild-type (C57BL/6J) mice were obtained from the Jackson Laboratories (Bar Harbor, ME). IL-5$^{-/-}$ mice on a C57BL/6 background were obtained from a breeding colony maintained at the University of Michigan. Mice were housed under pathogen-free conditions in enclosed filter-topped cages. Clean food and water were given *ad libitum*. The mice were handled and maintained using microisolator techniques, with daily veterinarian monitoring. All studies involving mice were approved by the University Committee on Use and Care of Animals at the University of Michigan

Aspergillus fumigatus. Strain ATCC 13073 was grown on Sabouraud dextrose agar (Difco) for 14 days. Conidia were harvested by washing plates with sterile phosphate-buffered saline (pH 7.4) with 0.1% Tween 80 (PBS-Tween), followed by filtration of the suspension through two layers of sterile gauze to remove hyphae. Conidia were washed in PBS-Tween, counted with a hemocytometer, diluted to 10^8 spores/ml in sterile PBS-Tween, and stored at 4°C for up to 4 months.

Respiratory Exposure Protocol. For each exposure, 2×10^6 conidia/mouse were administered to the nostrils of mice in a volume of 20μl. Repeat intranasal

exposures were administered every 7 days. Prior to intranasal inoculation, mice were anesthetized by intraperitoneal injection of a ketamine-xylazine solution (2.5 mg of ketamine (Fort Dodge Animal Health, Fort Dodge, IA)/mouse plus 0.1 g of xylazine (Lloyd Laboratories, Shenandoah, IA)/mouse).

Lung Histology. Lungs were fixed by inflation with 10% neutral buffered formalin. After paraffin embedding, 5-μm sections were cut and stained with hematoxylin and eosin, periodic acid-Schiff (to detect mucus), Masson's trichrome (to detect collagen), Verhoeff's-van Gieson's (to detect elastin), and Gomori's methenamine-silver (to dectect fungi).

Bronchoalveolar Lavage for Cell and Solute Recovery. Airway contents were recovered by instillation and retrieval of 1ml of sterile PBS through a tracheotomy tube. The first lavage was centrifuged and the cell-free fluid was immediately frozen down at -20°C. Cells collected with three total lavages were pooled. After erythrocyte lysis using NH_4Cl buffer (0.83% NH_4Cl, 0.1% $KHCO_3$, 0.037% Na_2 EDTA, pH 7.4), cells were washed, resuspended in complete medium (RPMI 1640, 10% fetal calf serum, 2 mmol/liter L-glutamine, 50 μmol/liter 2-mercaptoethanol, 100 U/ml penicillin, 100 μg/ml streptomycin sulfate), and enumerated under a light microscope in the presence of trypan blue using a hemocytometer.

Flow Cytometry for Cell Surface Molecules. Cells were washed and resuspended at a concentration of 10^7 cells/ml in FA buffer (Difco) + 0.1% NaN_3, Fc receptors were blocked by the addition of unlabeled anti-CD16/32 (Fc block; BD Pharmingen, San Diego, CA). After Fc receptor blocking, 0.5-1$\times 10^6$ cells were stained in a final volume of 100 µl in 12 x 75-mm^2 polystyrene tubes (Becton Dickinson, Franklin Lakes, NJ) for 30 minutes at 4°C. All antibodies used for flow cytometry were obtained from BD Pharmingen and used per the manufacturer's instructions. Cells were washed twice with FA buffer, resuspended in 100 µl, and an equal volume of 4% formalin was added to fix the cells. A minimum of 20,000 events were acquired on a FACScaliber flow cytometer (BD Pharmingen) using Cell-Quest software (BD Pharmingen). Acquired data was analyzed with FlowJo software (Tree Star, Standford, CA).

Flow Cytometric Leukocyte Differential Analysis. Cells of the main leukocyte subsets, macrophages, neutrophils, lymphocytes, and eosinophils, were distinguished by virtue of unique combinations of FSC and SSC profiles and CD11c and Gr1 surface expression, as described in detail in Appendix 1. During the development of the method BAL leukocytes were enriched via fluorescence-activated cell sorting (FACS). FACS analysis was performed on a FACSVantage SE Cell Sorter (BD Immunocytometry systems, San Jose, CA).

Blood Collection and Serum Separation. Blood was collected from the tail vein of live mice or by retro-orbital vein bleed at the time of harvest. Serum was

collected after centrifugation for 1min at 6000rpm in Microtainer tubes (BD Pharmingen).

Enzyme-Linked Immunosorbent Assay. Cytokines in BALF and IgE in serum were measured by sandwich ELISA using the manufacturer's instructions supplied with the specific kits (BD Pharmingen and R&D Systems).

Airway Resistance. Bronchial hyperresponsiveness was measured in a Buxco™ plethysmograph (Buxco, Troy, NY, U.S.A.) as previously described[1]. Each mouse was anesthetized with sodium pentobarbital (Butler Co., Columbus OH; 0.4mg/g of body weight), intubated via the trachea, and ventilated with a Harvard pump ventilator (Harvard Apparatus, Reno, NV). Ventilation parameters were set as follows: tidal volume = 0.25ml, respirations = 120/min, and positive end-expiratory pressure = 3 cm H_2O. Transpulmonary pressure (i.e. tracheal pressure – mouse chamber pressure) and inspiratory volume or flow were continuously monitored by computer. Using Buxco software, airway resistance was calculated by the division of transpulmonary pressure by the change in inspiratory volume and continuously displayed online. Values for airway resistance on the Buxco apparatus were recorded at baseline and after direct airway exposure to 1 mg and 1.6 mg of nebulized methacholine. These methacholine doses were chosen based on the results of previous experiments that revealed changes in bronchial hyperresponsiveness in treated versus control mice.

Spleen and Lymph Node Cell Preparation. Spleens and lung-draining lymph nodes (LDLN) were excised and cells dispersed with the plunger of a 3-ml syringe. After erythrocytes were lysed with NH_4Cl buffer, cells were washed and resuspended in complete media.

Flow Cytometry for Intracellular Molecules. Prior to intracellular cytokine staining, cells were stimulated *in vitro* for 5 hours with PMA (50ng/ml) and ionomycin (1μg/ml) in the presence of brefeldin A (BD Pharmingen) to promote the intracellular accumulation of cytokines. After stimulation, cells were washed twice prior to surface molecule staining. After surface molecule staining, intracellular molecules were stained using the BD Cytofix/Cytoperm kit according to the manufacturer's instructions (BD Pharmingen).

$CD4^+$ Cell Depletion. Mice were treated intraperitoneal injections with 300 μg of anti-CD4 monoclonal antibody (MAb) GK1.5 on the day prior to the first exposure to conidia and boosted with 100 μg of MAb every 7 days. Antibody was prepared from ascites by dilution in PBS and filtering through a 0.45-μm syringe filter. The efficiency of T-cell depletion was assessed by flow cytometric analysis using anti-CD4 Ab RM 4-4, which binds to a region of CD4 distinct from GK1.5. Depletion was >99% for $CD4^+$ T cells in the lungs as well as spleen. Anti-CD4 antibody (GK1.5) prevents the development of an anti-rat Ig response because an anti-rat Ig response requires $CD4^+$ T-cell help. Thus, PBS diluent was used for control

mice instead of isotype-matched rat Ig that would lead to a mouse anti-rat Ig response, potentially resulting in Ab-antigen complexes and immune deviation or inflammation.

Lung Digest for Whole Lung Leukocyte Enrichment. Lungs from each mouse were excised, washed in PBS, minced, and digested enzymatically for 30 minutes in 15 ml/lung of digestion buffer (RPMI, 5% fetal calf serum, 1 mg/ml collagenase (Boehringer Mannheim Biochemical, Chicago, IL), and 30 μg/ml DNase (Sigma Chemical Co., St. Louis, MO)). After erythrocyte lysis using NH_4Cl buffer, cells were washed, resuspended in complete media, and centrifuged for 30 minutes at 2000 x *g* in presence of 20% Percoll (Sigma) to separate leukocytes from cell debris and epithelial cells. Total lung leukocyte numbers were assessed in the presence of trypan blue using a hemocytometer.

$CD4^+$ T Cell Enrichment. $CD4^+$ T cells were enriched from splenocyte populations and from combined lung and LDLN populations via magnetic-activated cell sorting (MACS). For MACS, cell suspensions were stained with CD4 (L3T4) Microbeads (Miltenyi Biotec, Auburn, CA) and enriched via positive selection on a MidiMACS separator (Miltenyi Biotec). Enriched populations were >90% pure as assessed by flow cytometry.

CFSE Staining. After enrichment, and before adoptive transfer, $CD4^+$ T cells were labeled with the Vybrant CFDA SE (CFSE) Cell Tracer Kit (Molecular

Probes, Eugene, OR) according to the manufacturer's instructions. CFSE is fluorescent dye that is retained within cells and divided between daughter cells with each division.

Adoptive Transfer. Enriched, CFSE-labeled $CD4^+$ T cells were suspended in PBS at $0.8\text{-}1\times10^7$/ml and 1ml of cell suspension was adoptively transferred to naïve recipient mice via lateral tail vein injection.

Immunohistochemistry. Immunohistochemistry was performed as previously described[2]. Lungs were inflated and fixed in 10% buffered formalin overnight, embedded in paraffin, and sectioned. Following de-paraffinization and rehydration, sections were blocked and then stained with or anti-α-smooth muscle actin (SMA) antibody (clone 1A4, DAKO, Carpinteria, CA). Color development for α-SMA staining was achieved with DAB (Vector Labs, Burlingame, CA). Sections were then counterstained with hematoxylin and mounted.

Morphological Leukocyte Differential Analysis. Macrophages, neutrophils, lymphocytes, and eosinophils were visually counted by standard morphological criteria in Wright-Giemsa-stained samples of lung cell suspensions cytospun onto glass slides (Shandon Cytospin, Pittsburgh, PA). For Wright-Giemsa staining, the slides were fixed for 2 min with a one-step, methanol-based Wright-Giemsa stain (Harleco; EM Diagnostics, Gibbstown, NJ) followed by steps 2 and 3 of the

Diff-Quik whole-blood stain kit (Diff-Quik, Baxter Scientific, Miami, FL). A total of 200 to 300 cells were counted from randomly chosen high-power microscope fields for each sample.

Right Ventricular Systolic Pressure. Mice were anesthetized by intraperitoneal injections with ketamine and xylazine. A 19-gauge metal tracheostomy tube, fitted with an adaptor to attach to a mechanical ventilator, was inserted into the trachea and secured with a nylon suture. Mice were placed on a mechanical ventilator (settings: respiratory rate 150 breaths/minute, volume limits engaged (max 2.0ml), and minimum 30% of the breath cycle for exhalation) as part of the Pulmonary Maneuvers System (Buxco Electronics). A midline thoracotomy was performed and the chest wall was retracted exposing the heart. A 26 gauge needle attached to pressure tubing connected to a Cobe pressure transducer (Cobe Cardiovascular, Arvada, CO) was inserted into the right ventricle. After RV pressure was recorded, a blood sample was obtained by ventricular puncture with a heparinized syringe. The mouse was then euthanized for organ harvest. The RVSP and heart rate were obtained by analyzing tracings using the Left Ventricular Pressure Analyzer as part of Biosystem XA software (Buxco, Electronics). RVSP for six consecutive beats were averaged to obtain the mean RVSP for each mouse. RVSP measurements were excluded if the heart rate dropped below 300 beats per minute based on published investigations into cardiac function[3]. The total time of mechanical ventilation required for these measurements was less than 5 minutes.

Morphometric Analysis of Pulmonary Arteries. Excised lungs were inflated via the trachea with 1 cc of 10% buffered formalin. The trachea was ligated and the lungs were immersed in 10% buffered formalin for 24 hours. The left lung from each mouse was removed, imbedded in alginate, and sectioned into 3mm slices along the long axis. A coin flip determined whether odd or even sections were chosen for analysis. After embedding the chosen slices in paraffin, five-micron sections were cut, fixed to glass slides, and stained with hematoxylin and eosin. Morphometry was performed using an Olympus BX40 microscope fitted with a DP71 digital camera (Olympus, Melville, NY) and a XYZ microscope stage (Prior Scientific, Rockland, MA) controlled by a Dell computer running Visopharm v 2.14 software (Visopharm, Denmark). Slides were coded and analyzed by the reader in a blinded fashion. Using a 4x low power objective, the entire area of lung from each tissue section was outlined and included in the sampling area. Under 40x magnification, a computer assisted sampling protocol chose a random starting field from the selected area and subsequent fields were determined by using a fixed step in the x and y position. Thus, a random sampling of the entire tissue section was examined allowing for objective measurements. All muscular pulmonary arteries appearing in the selected fields were assessed. For each artery, diameter (in both the long and short axis), total area, and luminal area were measured and recorded. A value of % lumen was obtained by dividing the luminal area by the total area x100%. Vessels were excluded from analysis if the length/width measurements were >2.5 to exclude tangentially sliced arteries.

Vessels were excluded from analysis if the total area was >20,000μm^2 to exclude large pulmonary arteries. Data for each artery measured was pooled within each experimental group from 2-4 separate experiments.

Right Ventricular Mass. The great vessels and atria were removed from the ventricles and septum for each mouse. The right ventricular (RV) free wall was dissected away from the septum (S) and attached left ventricle (LV). The masses of the RV free wall and the S+LV were measured. The right ventricle mass was calculated by RV/(RV+(S+LV)).

Blood Hemoglobin. A blood sample was obtained by ventricular puncture with a heparinized syringe, placed on ice, and hemoglobin content was determined within 30 min at the hematology lab at the Veterans' Affairs Hospital (Ann Arbor, MI).

Statistical Analyses. All values are reported as mean ± standard error of the mean unless otherwise noted. Mean values were pooled from 2-4 independent experiments unless otherwise noted. Differences between two groups were evaluated with a two-tailed Student's *t* test, and all differences between three or more groups were evaluated with a one-way ANOVA with Bonferroni's multiple comparison post-test. $p<0.05$ were considered statistically significant.

References

1. Hogaboam, C. M. et al. Chronic airway hyperreactivity, goblet cell hyperplasia, and peribronchial fibrosis during allergic airway disease induced by Aspergillus fumigatus. Am J Pathol 156, 723-32 (2000).
2. White, E. S. et al. Negative regulation of myofibroblast differentiation by PTEN (Phosphatase and Tensin Homolog Deleted on chromosome 10). Am J Respir Crit Care Med 173, 112-21 (2006).
3. Hart, C. Y., Burnett, J. C., Jr. & Redfield, M. M. Effects of avertin versus xylazine-ketamine anesthesia on cardiac function in normal mice. Am J Physiol Heart Circ Physiol 281, H1938-45 (2001).

Chapter 3

Hypersensitivity Response to *Aspergillus fumigatus*: Development of Allergic Airway Disease

INTRODUCTION

Rationale

Upon re-exposure, an unnecessary and over-exuberant adaptive immune response to *Aspergillus fumigatus* can result in the development of hypersensitivity diseases, including allergic asthma and hypersensitivity pneumonitis (HP)[1]. Hypersensitivity responses to *A. fumigatus* likely result from the inhalation of conidia, because conidia are specialized structures made specifically for the air-borne dissemination of the fungus[2]. Atopic asthma is mediated by a T_H2 immune response, and HP is characterized by a T_H1 immune response. As is the case with humans, inhalation of *A. fumigatus* by mice reportedly can lead to T_H1 and/or T_H2 immune responses[3, 4]. However, the response to repeated inhalation of viable *A. fumigatus* conidia has not been well studied. A common weakness of murine studies of hypersensitivity disease is the necessity for systemic immunization with antigen to prime the hypersensitivity response.

Hypothesis

Pulmonary hypersensitivity disease will result from repeated inhalation of viable *A. fumigatus* conidia, a natural aeroallergen in its native form.

Objectives

1. To determine the strength and character of the local immune response after each of multiple, weekly inhalations of viable *A. fumigatus* conidia.
2. To determine the extent of histopathological alterations in the lung following repeated inhalation of conidia.
3. To determine the extent of pathophysiological alterations in pulmonary function following repeated inhalation of conidia.

RESULTS

To determine if repeated exposure to viable conidia led to the development of a hypersensitivity response to *Aspergillus fumigatus*, a kinetic study was performed. Based on the results of a preliminary examination (see Appendix 2, Figure A2-1), a "minimum inflammatory dose" of 2×10^6 viable conidia was instilled intranasally into C57BL/6 mice every 7 days, and mice were evaluated 24 hours after each exposure. The study was focused on the evaluation of characteristic features of the clinical hypersensitivity diseases, atopic asthma and HP, that may be caused by *A. fumigatus*.

To demonstrate that the fungus did not escape innate immune clearance in the lung, histological samples of lung tissue were stained with gomori methenamine silver (GMS) 24 hours after each exposure (Figure 3-1). GMS stains fungal material black. Few, sporadic conidia were identified in each lung sample, and most were found inside phagocytes. Rare conidial or hyphal germinations were observed, but not overt growth of the fungus as seen in the anti-Gr1-treated neutropenic mice. Mice examined after three exposures did not have more GMS-stained fungi than mice harvested after one exposure, suggesting that *A. fumigatus* growth and persistence were prevented.

Histological sections of lung tissue were stained with H&E to examine cellular inflammation (Figure 3-2). Cells accumulated adjacent to the airways distally to the level of the terminal bronchioles. Inflammation was considerably more pronounced after three exposures than after one. The alveoli were relatively clear of inflammatory infiltrate. This pattern of inflammation is more

consistent with atopic asthma, an allergic airway disease (AAD), than with HP, an alveolitis.

In order to quantify the cellular infiltrate, cells were recovered from the airway by bronchoalveolar lavage (BAL) and counted under a light microscope (Figure 3-3). A single exposure to conidia induced a slight increase in the total number of cells present 24h later. A similar magnitude of cells was measured after the second exposure. However, the total number of cells recovered from the airway increased significantly, by several-fold, after the third exposure, 15 days after the initial exposure.

In order to characterize the cellular infiltrate, leukocyte differential analyses were performed on cells recovered from the airway using flow cytometry according to the method described in Appendix 1 (Figure 3-4). The total number of macrophages was relatively constant throughout the period of exposure and similar in number to unexposed mice. Neutrophils are a critical component of the innate host defense to *A. fumigatus*. Neutrophils constituted the majority of the cells recruited after a single exposure, and similar numbers of neutrophils were present after each subsequent exposure. Eosinophils predominated in the airway after three exposures, coinciding with the surge in total cell number. Airway eosinophilia is a cardinal feature of asthma. Lymphocytes increased significantly after three exposures, as well. The significant increase in lymphocytes and eosinophils coupled with an absence of fungal accumulation was evidence of a hypersensitivity response manifesting as an AAD.

To analyze the quality and intensity of the response to inhaled conidia, cytokines were measured in the bronchoalveolar lavage fluid (BALF), collected 24h after exposure, by ELISA (Figure 3-5). A single exposure to conidia led to an increase in TNFα. As TNFα is a component of the innate inflammatory response, this observation was consistent with the early recruitment of neutrophils to the airway. The level of IL-5, a prototypical T_H2 cytokine, increased significantly after three challenges. IL-5 is critical for the recruitment of eosinophils, so the detection of IL-5 was consistent with the influx of eosinophils previously observed. Not surprisingly, the level of detectable IL-4 followed the trend for IL-5, but the low amount of IL-4 was just above the level of detection (see Appendix 2, Figure A2-2). The level of IFNγ was low-to-undetectable after each exposure (see Appendix 2, Figure A2-2). The early detection of TNFα was consistent with a role in the innate immune response. The production of IL-5 after several exposures was further evidence of a mounting T_H2 response.

The secretion of IgE was measured serially in mice after each exposure to *A. fumigatus* (Figure 3-6). A small sample of blood was collected from the tail vein, and the total IgE level in the serum was measured by ELISA. After four exposures, mice that inhaled conidia had significantly higher levels of total IgE in the serum than mice that inhaled vehicle only. T_H2 $CD4^+$ T cells instruct B cells to produce IgE, and increased IgE is a hallmark of an allergic reaction. Increased IgE is not associated with HP.

Lung histopathology was examined with periodic acid-Schiff (PAS) stain to identify mucus (Figure 3-7). Mucus hyperproduction was apparent in the upper

airways of mice exposed to conidia multiple times, but not in naïve mice. Goblet cell metaplasia and mucus hypersecretion contribute to airway obstruction in asthma[5].

While mice do not develop a breathing disorder similar to asthma, increased airway resistance is often demonstrated by methacholine challenge[6]. In spite of the presence of multiple features of AAD, mice repeatedly exposed to conidia did not exhibit a significant increase in airway resistance compared to untreated control mice (Figure 3-8).

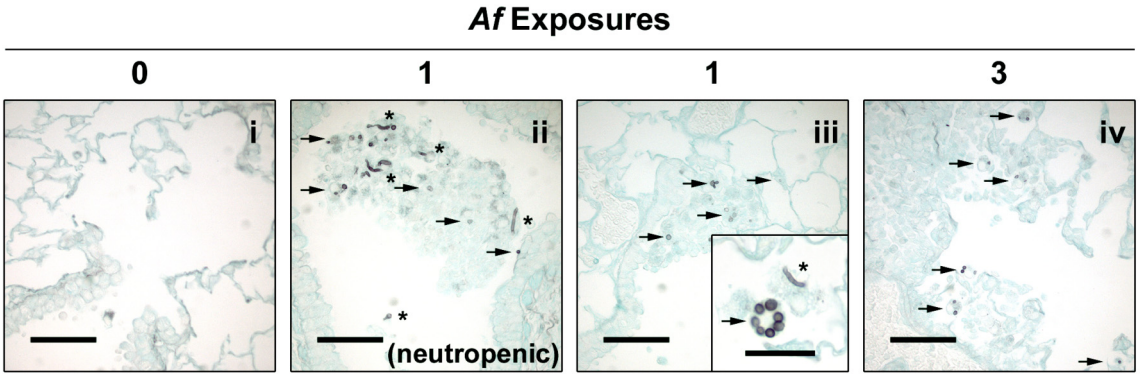

Figure 3-1. *Aspergillus fumigatus* does not escape host protection in the lungs of mice after repeated, weekly inhalation of viable conidia.
Histological sections of lung tissue were stained with Gomori Methenamine Silver in order to detect fungal material, which is stained black. Representative photomicrographs are shown. An unexposed lung sample is included as a negative control (i). A lung sample from a mouse treated with anti-Gr1 to deplete neutrophils is included as a positive control for *A. fumigatus* infection (ii). Additional lung samples demonstrate the fungal burden that was present 24h after one exposure (iii) and 24h after the third weekly exposure (iv). Rare germlings were found in immunocompetent mice (iii – inset). Arrows point to phagocytosed conidia, and asterisks identify hyphal germinations. Black bars are 50μm in length (Black bar in inset is 20μm in length).

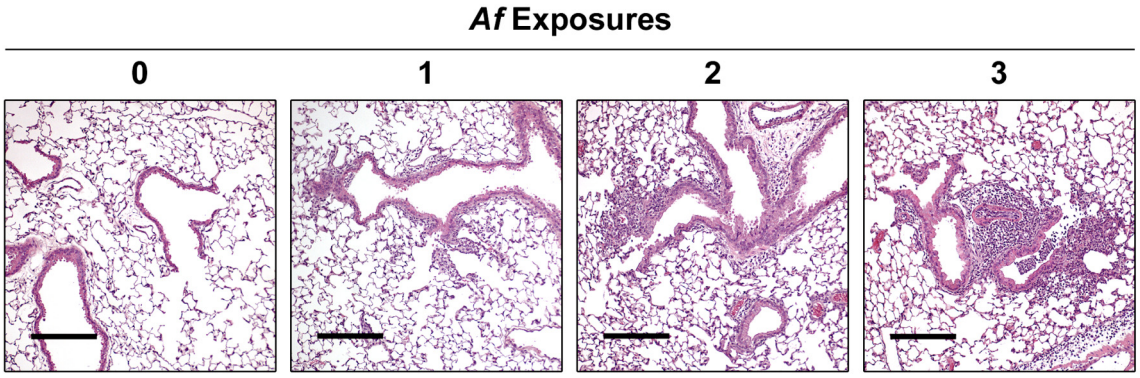

Figure 3-2. Cellular inflammation organizes along the airways distally to the bronchioles.
Histological sections of lung tissues were stained with H&E. Representative photomicrographs include terminal bronchioles. Images depict the extent of cellular inflammation present in an untreated sample (0), 24h after the first exposure (1), and 24h after the second and third weekly exposures (2 and 3, respectively). Black bars are 200μm in length.

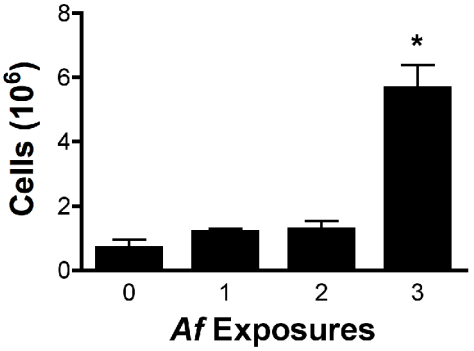

Figure 3-3. A significant increase in airway cellular inflammation occurs after several, weekly exposures.
Cells were recovered from the airway by bronchoalveolar lavage and enumerated under a light microscope with a hemacytometer. These data were collected from three independent experiments for each group, containing three or mice per group per experiment. The mean value for each group in each experiment was compiled. The graph illustrates the mean (+ SEM) number of total cells present in the airways 24h after 0, 1, 2 or 3 weekly exposures. *$p < 0.001$ compared to all other groups.

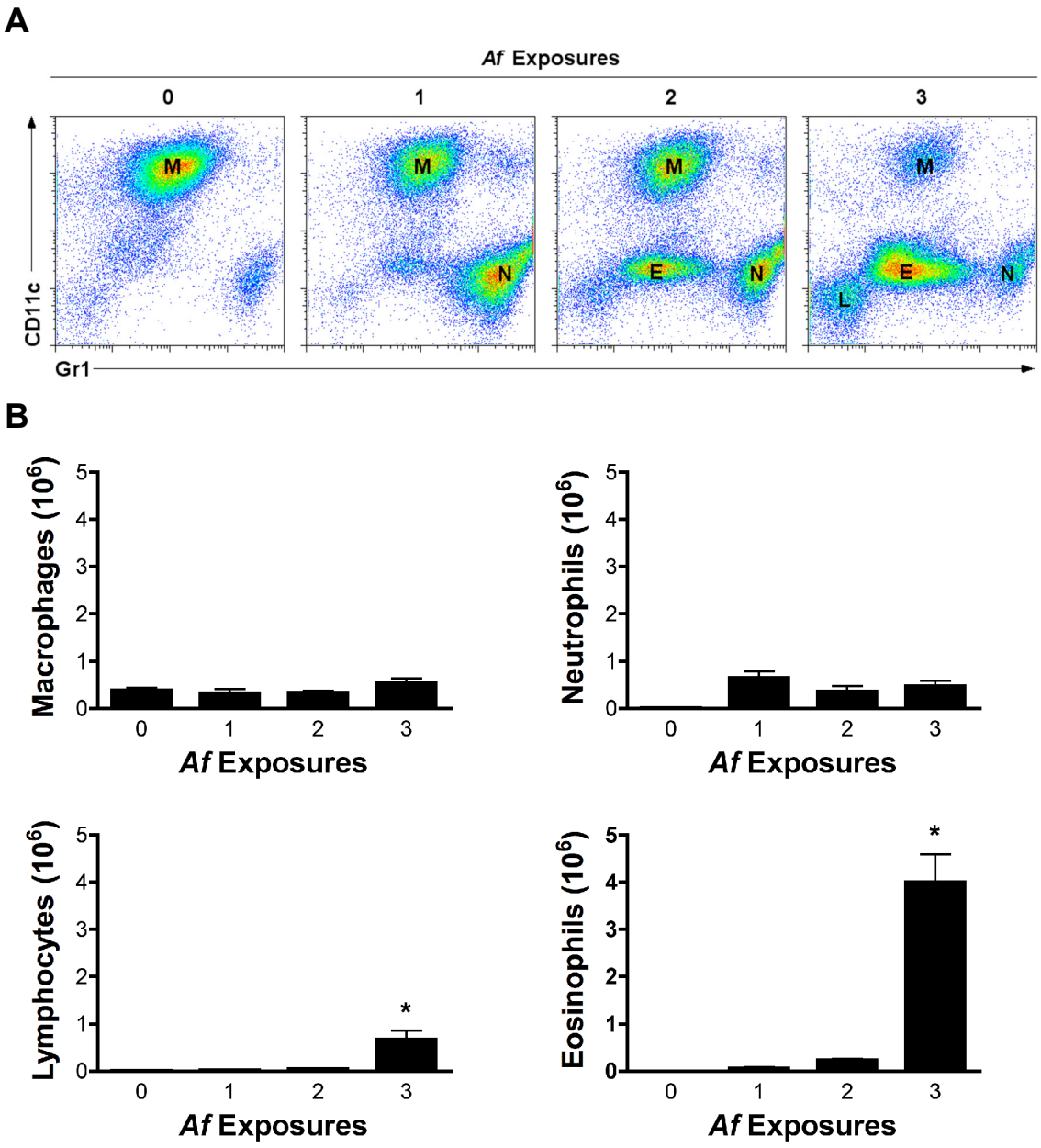

Figure 3-4. The innate immune system responds to a single exposure and the adaptive immune system responds after several exposures.
Cells were recovered from the airway, and leukocyte differentials were performed by flow cytometry according to the method described in Appendix 1. A) Representative density plots show the expression of CD11c and Gr1 for the total cell populations recovered. The central densities of individual leukocyte subpopulations are labeled (M=macrophage, N=neutrophil, L=lymphocyte, and E=eosinophil). B) The numbers of recovered cells belonging to each leukocyte subset are presented on the bar graphs (see y-axis labels). Mean (+SEM) of cell numbers compiled from the means of two independent experiments are shown. * $p < 0.05$ for 3 exposures compared to 0 or 1 exposures (lymphocytes); $p < 0.01$ for 3 exposures compared to all other groups (eosinophils)

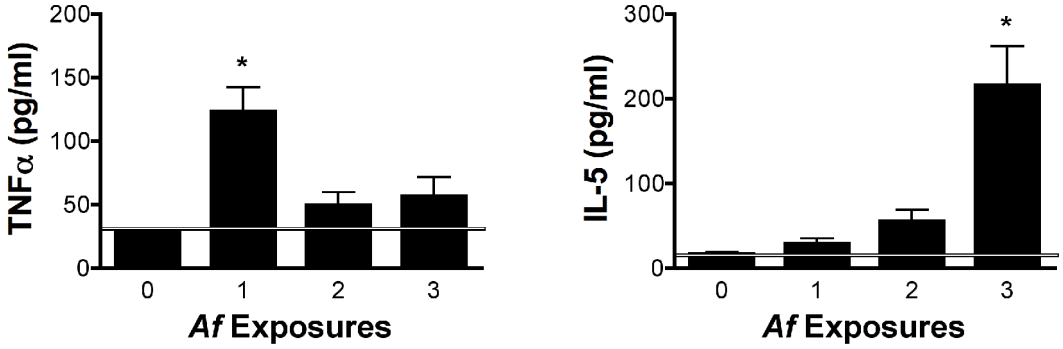

Figure 3-5. Peak levels of innate inflammatory and T_H2 cytokines coincide with the pattern of leukocyte recruitment.
Cytokines present in the cell-free bronchoalveolar lavage fluid were quantified by ELISA. The bar graphs depict the mean (+SEM) for individual samples collected from two independent experiments (n=3 per group per experiment; "0 exposures" group included in one of the two experiments but consistent with additional independent experiments). The limit of detection for each assay is indicated with a horizontal line. *$p < 0.01$ compared to 0 exposures and $p < 0.05$ compared to 2 and 3 exposures (TNFα); $p < 0.01$ compared to all other groups (IL-5)

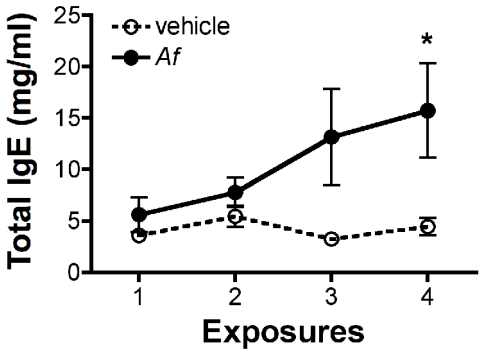

Figure 3-6. Increased serum IgE is a component of the allergic response to repeated exposure.
Mice were exposed to vehicle control or *A. fumigatus* conidia (*Af*) on a weekly basis. Blood was collected serially from the tail vein of each mouse 72h after every exposure. Total IgE levels in the serum were quantified by ELISA. *$p < 0.03$ for *Af* vs. vehicle after 4 exposures

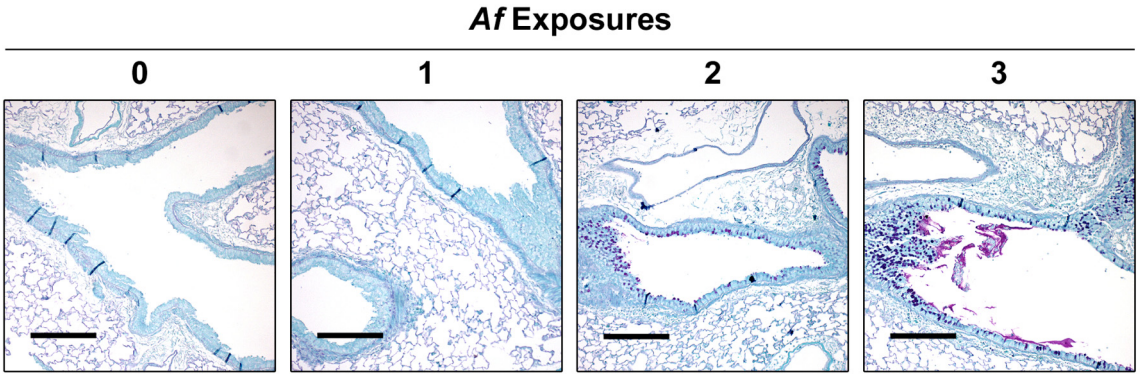

Figure 3-7. Development of goblet cell metaplasia and mucous hypersection is evident in the upper airways.
Histological sections of lung tissue were stained with PAS in order to detect mucous, which is stained purple. Representative photomicrographs include conducting airways from mice exposed to *A. fumigatus* 0, 1, 2 or 3 times at weekly intervals. Black bars are 200μm in length.

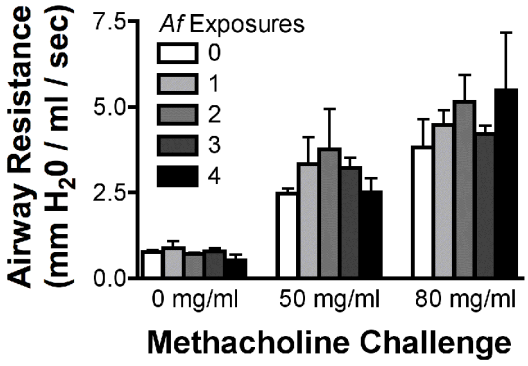

Figure 3-8. Airway hyperresponsiveness does not develop despite the co-existence of many features of allergic airway disease.
As described in the material and methods, bronchial resistance was measured in a whole body plethysmograph 24h after a given number of exposures (see bar graph legend). Briefly, resistance values were calculated in real-time for anesthetized and ventilated mice at baseline and after direct respiratory challenge with 20μl of a nebulized methacholine solution (see x-axis labels) at doses previously determined to elicit significant responses in hyperreactive mice. Mean (+SEM) for five mice per group are shown. An independent experiment, including groups exposed 0 and 4 times, produced similar results.

DISCUSSION

The data presented in this chapter demonstrated that a hypersensitivity response to *A. fumigatus* developed after repeated inhalation of viable conidia in the absence of fungal growth or persistence. Many features of the hypersensitivity response were similar to prototypical features of atopic asthma, an AAD. These features included the presence of peribronchial and peribronchiolar cellular infiltrate, significant airway eosinophilia, the presence of T_H2 cytokines in the airway, the increased production of IgE, and goblet cell metaplasia with mucus hypersecretion[7]. In spite of the characteristic AAD, hypersensitive mice did not exhibit increased airway resistance after inhalation of conidia.

The growth of *A. fumigatus* was prevented in the lungs of C57BL/6 mice throughout the study. Of the few, sporadic conidia detected in silver-stained lung sections, the majority appeared to be small, resting conidia residing inside macrophage cells. However, rare germinating conidia or hyphae were also detected. The germination of resting conidia is a critical event in the development of innate and adaptive immune responses to *A. fumigatus*. During germination, fungal molecules, such as β-glucans, are exposed and recognized by pattern recognition receptors of the innate immune system[8, 9]. In response to germinating, but not resting conidia, macrophages produced pro-inflammatory mediators including TNFα[8, 9]. The inhalation of viable, but not nonviable, resting conidia also promoted a T_H1 response[4, 10]. It is suspected that the majority of *A. fumigatus* allergens, that are the target of a T_H2 response, are likely expressed

by the organism during germination[11]. Finally, the intratracheal delivery of *A. fumigatus* hyphae resulted in the priming of T_H2 cells in the draining lymph nodes[12]. Based on these data, we suspect that germination of the viable conidia after inhalation resulted in the initiation of the immune response that resulted in hypersensitivity to the fungus.

After a single exposure to conidia, an innate immune response was evidenced by increased TNFα secretion and neutrophil recruitment. Growth of the inhaled conidia was prevented throughout the period of study, and the amount of fungal material detected by histological examination was similar 24 hours after the first and the third exposures. It is well known that the innate immune system of immunocompetent mice readily clears the lungs of inhaled conidia of *A. fumigatus*[13]. Both TNFα and neutrophils were previously reported to participate in the innate host defense response to inhaled *A. fumigatus* conidia[14, 15]. The ability of the innate host defense response to prevent the growth of inhaled conidia suggested that the robust allergic airway response that developed with repeated exposure was likely unnecessary and potentially harmful to the host.

The hypersensitivity response documented in the present study contained many prototypical features of a T_H2 AAD. The evidence of an AAD included a peribronchial-peribronchiolar pattern of inflammation, significant airway eosinophilia, increased BALF IL-5, elevated serum IgE levels, and airway mucus hyperproduction. On the other hand, features of HP that were not detected in this study included alveolitis, a granulocytic response primarily consisting of

neutrophils, and a low $CD4^+/CD8^+$ T cell ratio (see Appendix 2, Figure A2-3). It is suspected that $CD4^+$ T_H1 cells contribute to the hypersensitive inflammatory response in HP[16]. A single inhalation of *A. fumigatus* conidia resulted in the priming of $CD4^+$ T_H1 cells[4, 12]. In the present study, the presence of $CD4^+$ T_H1 cells was not determined directly, but indirect evidence of a robust $CD4^+$ T_H1 response was absent. For instance, robust $CD8^+$ T cell recruitment, present in T_H1-associated HP, was not observed. Instead, indirect evidence of a substantial $CD4^+$ T_H2 response was apparent based on the development of many features of AAD.

In the present study, C57BL/6 mice did not develop a significant increase in airway resistance after repeated inhalation of *A. fumigatus* conidia. In several studies comparing airway hyperresponsiveness (AHR) among different strains of mice, C57BL/6 mice were characterized as a low-responder strain[17-19]. Also, systemic allergen priming with adjuvant is employed commonly in laboratory mice to promote increased AHR after subsequent allergen exposure. Based on the extent of the AAD induced in this study, it is possible that similar treatment of a different laboratory strain of mice with a stronger genetic predisposition would result in significant AHR. Alternately, initial systemic allergen priming with adjuvant may enhance the AHR phenotype. However, these data demonstrated that viable *A. fumigatus* conidia, a natural aeroallergen in its native form, induced a robust hypersensitivity response upon re-exposure in the airway in the absence of systemic priming.

The generation of an experimental AAD by repeated inhalation of viable *A. fumigatus* conidia represented a unique addition to the published literature, but at least three other groups have reported *A. fumigatus*-induced AAD models[20-22]. In the first model, characteristic AAD resulted from repeated intraperitoneal sensitization with *A. fumigatus* antigen extract admixed with alum followed by repeated intranasal exposure to *A. fumigatus* antigen[21]. In the second model, significant AAD developed at week three after repeated inhalation of *A. fumigatus* antigen extract three times a week[22]. In the third model, a robust AAD resulted after systemic sensitization to *A. fumigatus* antigen extract with adjuvant, followed by intranasal exposure to extract and intratracheal delivery of viable conidia[20]. We elected to repeatedly expose mice to viable *A. fumigatus* conidia via the intranasal route, because we aimed to recapitulate the pathogenesis of clinical hypersensitivity responses that develop as a consequence of the exposure to allergens at the respiratory mucosa.

In conclusion, repeated inhalation of viable *A. fumigatus* conidia resulted in the development of a hypersensitivity response manifesting as an AAD. Currently, there is a paucity of animal models for AAD that result from a natural route of exposure to a natural aeroallergen in its native form[6]. Our model affords the opportunity for further investigation into the immunopathogenesis of respiratory allergies.

References

1. Kurup, V. P., Shen, H. D. & Banerjee, B. Respiratory fungal allergy. Microbes Infect 2, 1101-10 (2000).
2. Latge, J. P. Aspergillus fumigatus and aspergillosis. Clin Microbiol Rev 12, 310-50 (1999).
3. Kheradmand, F. et al. A protease-activated pathway underlying Th cell type 2 activation and allergic lung disease. J Immunol 169, 5904-11 (2002).
4. Rivera, A. et al. Innate immune activation and CD4+ T cell priming during respiratory fungal infection. Immunity 25, 665-75 (2006).
5. Rogers, D. F. Airway mucus hypersecretion in asthma: an undervalued pathology? Curr Opin Pharmacol 4, 241-50 (2004).
6. Epstein, M. M. Do mouse models of allergic asthma mimic clinical disease? Int Arch Allergy Immunol 133, 84-100 (2004).
7. Kay, A. B. Allergy and allergic diseases. Second of two parts. N Engl J Med 344, 109-13 (2001).
8. Hohl, T. M. et al. Aspergillus fumigatus triggers inflammatory responses by stage-specific beta-glucan display. PLoS Pathog 1, e30 (2005).
9. Steele, C. et al. The beta-glucan receptor dectin-1 recognizes specific morphologies of Aspergillus fumigatus. PLoS Pathog 1, e42 (2005).
10. Brieland, J. K. et al. Cytokine networking in lungs of immunocompetent mice in response to inhaled Aspergillus fumigatus. Infect Immun 69, 1554-60 (2001).
11. Denning, D. W., O'Driscoll, B. R., Hogaboam, C. M., Bowyer, P. & Niven, R. M. The link between fungi and severe asthma: a summary of the evidence. Eur Respir J 27, 615-26 (2006).
12. Bozza, S. et al. Dendritic cells transport conidia and hyphae of Aspergillus fumigatus from the airways to the draining lymph nodes and initiate disparate Th responses to the fungus. J Immunol 168, 1362-71 (2002).
13. Schaffner, A., Douglas, H. & Braude, A. Selective protection against conidia by mononuclear and against mycelia by polymorphonuclear phagocytes in resistance to Aspergillus. Observations on these two lines of defense in vivo and in vitro with human and mouse phagocytes. J Clin Invest 69, 617-31 (1982).
14. Mehrad, B., Strieter, R. M. & Standiford, T. J. Role of TNF-alpha in pulmonary host defense in murine invasive aspergillosis. J Immunol 162, 1633-40 (1999).
15. Bonnett, C. R., Cornish, E. J., Harmsen, A. G. & Burritt, J. B. Early neutrophil recruitment and aggregation in the murine lung inhibit germination of Aspergillus fumigatus Conidia. Infect Immun 74, 6528-39 (2006).
16. Patel, A. M., Ryu, J. H. & Reed, C. E. Hypersensitivity pneumonitis: current concepts and future questions. J Allergy Clin Immunol 108, 661-70 (2001).

17. Levitt, R. C. & Mitzner, W. Expression of airway hyperreactivity to acetylcholine as a simple autosomal recessive trait in mice. Faseb J 2, 2605-8 (1988).
18. Takeda, K., Haczku, A., Lee, J. J., Irvin, C. G. & Gelfand, E. W. Strain dependence of airway hyperresponsiveness reflects differences in eosinophil localization in the lung. Am J Physiol Lung Cell Mol Physiol 281, L394-402 (2001).
19. Chiba, Y., Yanagisawa, R. & Sagai, M. Strain and route differences in airway responsiveness to acetylcholine in mice. Res Commun Mol Pathol Pharmacol 90, 169-72 (1995).
20. Hogaboam, C. M. et al. Chronic airway hyperreactivity, goblet cell hyperplasia, and peribronchial fibrosis during allergic airway disease induced by Aspergillus fumigatus. Am J Pathol 156, 723-32 (2000).
21. Kurup, V. P., Mauze, S., Choi, H., Seymour, B. W. & Coffman, R. L. A murine model of allergic bronchopulmonary aspergillosis with elevated eosinophils and IgE. J Immunol 148, 3783-8 (1992).
22. Wang, J. M., Denis, M., Fournier, M. & Laviolette, M. Experimental allergic bronchopulmonary aspergillosis in the mouse: immunological and histological features. Scand J Immunol 39, 19-26 (1994).

Chapter 4

Hypersensitivity Response to *Aspergillus fumigatus*: Phenotype and Function of $CD4^+$ T Cells

Introduction

Rationale

$CD4^+$ T_H2 cells are widely recognized as central mediators to the pathogenesis of allergic airway disease (AAD)[1, 2], but the phenotype and function of $CD4^+$ T cells in the hypersensitivity response to viable *Aspergillus fumigatus* conidia requires further investigation. The role of T_H1 cells in AAD is somewhat controversial, because conflicting reports suggested that T_H1 responses may abrogate or augment T_H2-mediated AAD[3]. Several studies reported that inhalation of viable *A. fumigatus* conidia resulted in an innate pro-inflammatory response and a $CD4^+$ T_H1 cell response[4-7]. Previous reports indicated that the induction of a T_H2 response to *A. fumigatus* required the use of purified antigens with or without systemic priming[8-11]. When exposed to chitin, a fungal product, or proteases purified from *Aspergillus* species, recent reports demonstrated that innate immune cells were capable of mediating components of the allergic response, including the recruitment of eosinophils, in the absence of an adaptive immune system[12, 13].

Hypothesis

$CD4^+$ T cells mediate the hypersensitivity response to inhaled viable *A. fumigatus* conidia upon re-exposure.

Objectives

1. To determine the association of $CD4^+$ T_H cells with the development of the hypersensitivity response to *A. fumigatus*.
2. To determine the necessity for $CD4^+$ T cell involvement in the development of the hypersensitivity response to *A. fumigatus*.
3. To determine the sufficiency of $CD4^+$ T cells to mediate the development of the hypersensitivity response to *A. fumigatus*.

RESULTS

To determine if $CD4^+$ T cells mediated the hypersensitivity response to *A. fumigatus* conidia the phenotype and functional role of $CD4^+$ T cells was examined with a variety of methods. The kinetics of $CD4^+$ T cell accumulation in the airway after repeated inhalation of conidia was determined by flow cytometric analysis of cells recovered by bronchoalveolar lavage (BAL) (Figure 4-1). Very few $CD4^+$ T cells were detected in naïve mice or after one exposure, and there was a modest increase in $CD4^+$ T cells after the second exposure. A substantial, significant accumulation of $CD4^+$ T cells was detected after the third exposure, coinciding with the onset of the AAD.

$CD4^+$ T cell activation was examined by flow cytometric analysis of cells harvested from the spleen, lung-draining lymph node (LDLN), and BAL (Figure 4-2). Spleen samples from naïve mice were included as a control population of naïve $CD4^+$ T cells. There was very little difference in surface activation marker expression among $CD4^+$ lymphocyte populations isolated from the spleen of naïve mice and the spleen and LDLN of mice exposed to conidia four times. In contrast, the $CD4^+$ lymphocytes recovered from the airway (BAL) exhibited an activated phenotype. BAL $CD4^+$ T cells were uniformly CD44-positive while greater than 75% of $CD4^+$ T cells from the other tissues were CD44-negative. The populations expressing CD69 and CD69 plus CD25 were more than doubled in frequency in the BAL sample compared to those recovered from the secondary lymphoid tissues.

CD25 is also expressed by a majority of natural T regulatory cells (T_{Reg}) that co-express the transcription factor Foxp3[14]. Intracellular staining for Foxp3 was performed to distinguish $CD4^+CD25^+$ T_{Reg} from activated $CD4^+$ T cells (see Appendix 2, Figure A2-4). A similar frequency of $CD4^+$ T cells in the BAL expressed Foxp3 (14.3%) as compared to the spleens or LDLN (17.4-19.4%). T_{Reg} frequency within the total airway $CD4^+$ T cell population was roughly equivalent to that seen in the secondary lymphoid tissues.

The production of IL-4 and IFNγ by $CD4^+$ lymphocytes was examined by intracellular flow cytometric analysis performed after a brief period of *in vitro* stimulation as described in the methods (Figure 4-3). There was an absence of cytokine-producing effector $CD4^+$ T cells isolated from the spleens of naïve mice and from the spleens and LDLN of mice exposed to *A. fumigatus* four times. In contrast, $IL\text{-}4^+$ and $IFN\gamma^+$ $CD4^+$ T cells were routinely recovered from the airway in roughly equal frequencies (~11-12%). It is noted that there is a background frequency of $IFN\gamma^+$ cells (~3%) in the secondary lymphoid tissues, including the naïve spleen, but that IL-4 production was only measured in the BAL cells in this assay.

In order to deplete $CD4^+$ T cells, anti-CD4 antibody was administered prior to and throughout the period of exposure to exposure to *A. fumigatus*. Greater than 99% of $CD4^+$ T cells were depleted as determined by flow cytometric analysis of spleen, LDLN and BAL cells (see Appendix 2, Figure A2-5).

The ability of $CD4^+$ T cell-depleted mice to prevent an *A. fumigatus* infection was confirmed by histological examination of silver-stained lung tissues.

Fungal growth was not observed in control or $CD4^+$ T cell-depleted mice that repeatedly inhaled conidia (Figure 4-4).

After three exposures to conidia, cellular inflammation in the lung was examined in H&E stained lung tissue sections (Figure 4-5). Substantial leukocytic infiltration was apparent in the peribronchial and peribronchiolar areas of control mice, but inflammation was markedly attenuated in anti-CD4 treated mice.

The number of cells recruited to the airways was quantified after the recovery of cells by BAL (Figure 4-6). Depletion of $CD4^+$ cells abrogated the accumulation of cells in the airways that was noted in control mice after the third exposure to conidia.

To characterize the airway cellular infiltrate, flow cytometric leukocyte differential analysis was performed on cells recovered after three exposures to *A. fumigatus* conidia from control or anti-CD4-treated mice (Figure 4-7). In the absence of $CD4^+$ cells, the innate immune response remained intact as evidenced by the recruitment of neutrophils. On the other hand, the hypersensitivity response, as evidenced by the influx of lymphocytes and eosinophils, was dependent on the presence of $CD4^+$ cells.

The levels of cytokines in the BAL fluid (BALF), collected from control and anti-CD4-treated mice, were measured by ELISA (Figure 4-8). The innate pro-inflammatory cytokine TNFα was detected in the airways of both control and anti-CD4 treated mice after repeated exposure to *A. fumigatus*. The T_H2 cytokine IL-5 was only detected when $CD4^+$ cells were present. The production of another

T_H2 cytokine, IL-4, exhibited a pattern similar to that of IL-5 (see Appendix 2, Figure A2-6). None of the aforementioned cytokines were detectable in the airways of naïve mice (previous observations).

The capacity of $CD4^+$ T cells to drive the AAD was tested by the adoptive transfer of naïve or *A. fumigatus*-primed $CD4^+$ T cells into a naïve recipient that was subsequently exposed to conidia two times. Control, naïve $CD4^+$ T cells were purified from the spleens of naïve mice. *A. fumigatus*-primed $CD4^+$ T cells were purified from the combined lung and lung-draining lymph node tissues of mice previously exposed to conidia three times. $CD4^+$ T cells were purified to greater than 90% with a combination of negative and positive selection with magnetic beads (see Appendix 2, Figure A2-7). $0.8\text{-}1\times10^7$ purified $CD4^+$ T cells were transferred to naïve recipients, and on the same day they received the first of two weekly exposures to conidia. A recipient control group received only a PBS vehicle i.v. injection. Airway cellular inflammation in the recipient mice was quantified after the recovery of cells by BAL 24 hours after the second inhalation of conidia (Figure 4-9). Vehicle control- and naïve $CD4^+$ T cell-recipient mice had similar numbers of airway leukocytes that were comparable to the response seen in previous experiments in naïve mice after two exposures. By comparison, *A. fumigatus*-primed $CD4^+$ T cell-recipient mice had a several-fold, significant increase in the number of airway cells.

To characterize the leukocytic infiltrate, the cells recovered from the airways of recipient mice were analyzed by flow cytometric leukocyte differential analyses (Figure 4-10). The adoptive transfer of *A. fumigatus*-primed $CD4^+$ T

cells, but not vehicle or naïve $CD4^+$ T cells, promoted the allergic airways response, evidenced by significantly greater numbers of lymphocytes and eosinophils.

Transferred $CD4^+$ T cells were labeled with CFSE in order to monitor their trafficking and proliferation in the recipient mice (Figure 4-11). Approximately 5% of the total $CD4^+$ T cell population was identified by the CFSE label in the mice that received *A. fumigatus*-primed $CD4^+$ T cells. The CFSE profile indicated that the cells had undergone various rounds of cell division, thereby diluting the CFSE stain. It is possible that additional donor *A. fumigatus*-primed $CD4^+$ T cells were not distinguished from host $CD4^+$ T cells, because the CFSE had been diluted to the background level of unstained cells. In marked contrast, less than 0.5% of the total $CD4^+$ cell population was $CFSE^+$ in the mice that received naïve $CD4^+$ T cells. Furthermore, the $CFSE^+$ cells from the naïve donors did not exhibit any sign of proliferation in the recipients after exposure to *A. fumigatus*.

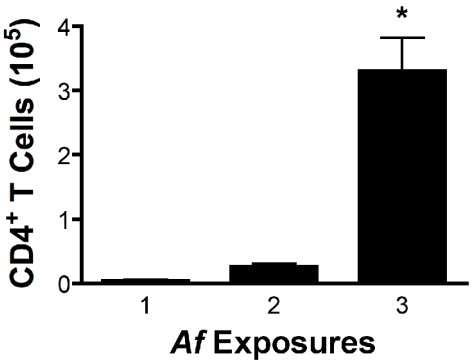

Figure 4-1. A significant increase in airway $CD4^+$ T cells corresponds to the onset of the allergic airways disease.
Cells recovered from the airway were analyzed for expression of CD4 on lymphocytes as described in the materials and methods. Mean (+SEM) of cell numbers compiled from the means of two independent experiments are shown. Note: In previous experiments, the number of $CD4^+$ T cells present in the airways of unchallenged mice was essentially nil. *$p < 0.05$ compared to all other groups

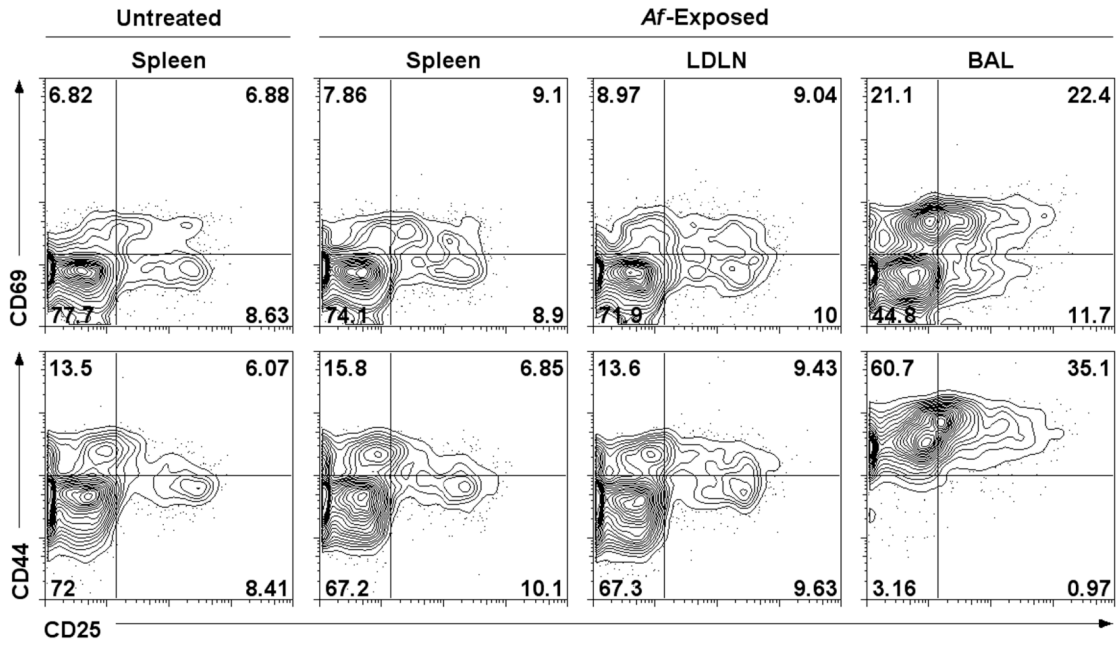

Figure 4-2. Activated CD4$^+$ T cells are localized exclusively to the effector site.

As described in the materials and methods, cells were collected from various tissues (including spleen, lung draining-lymph nodes (LDLN), and airway (BAL)) from untreated mice and mice exposed to *A. fumigatus* four times (n=3 per group) as indicated above the figure. Cells were pooled for analysis. Gated CD4$^+$ lymphocytes were analyzed for expression of the activation markers CD25, CD44 and CD69 by flow cytometry (see axes labels for contour plots). Quadrants were set with isotype control-stained CD4$^+$ lymphocytes (not shown) and the percentage of CD4$^+$ lymphocytes in each quadrant is included on each plot. An independent, repeat experiment produced similar results.

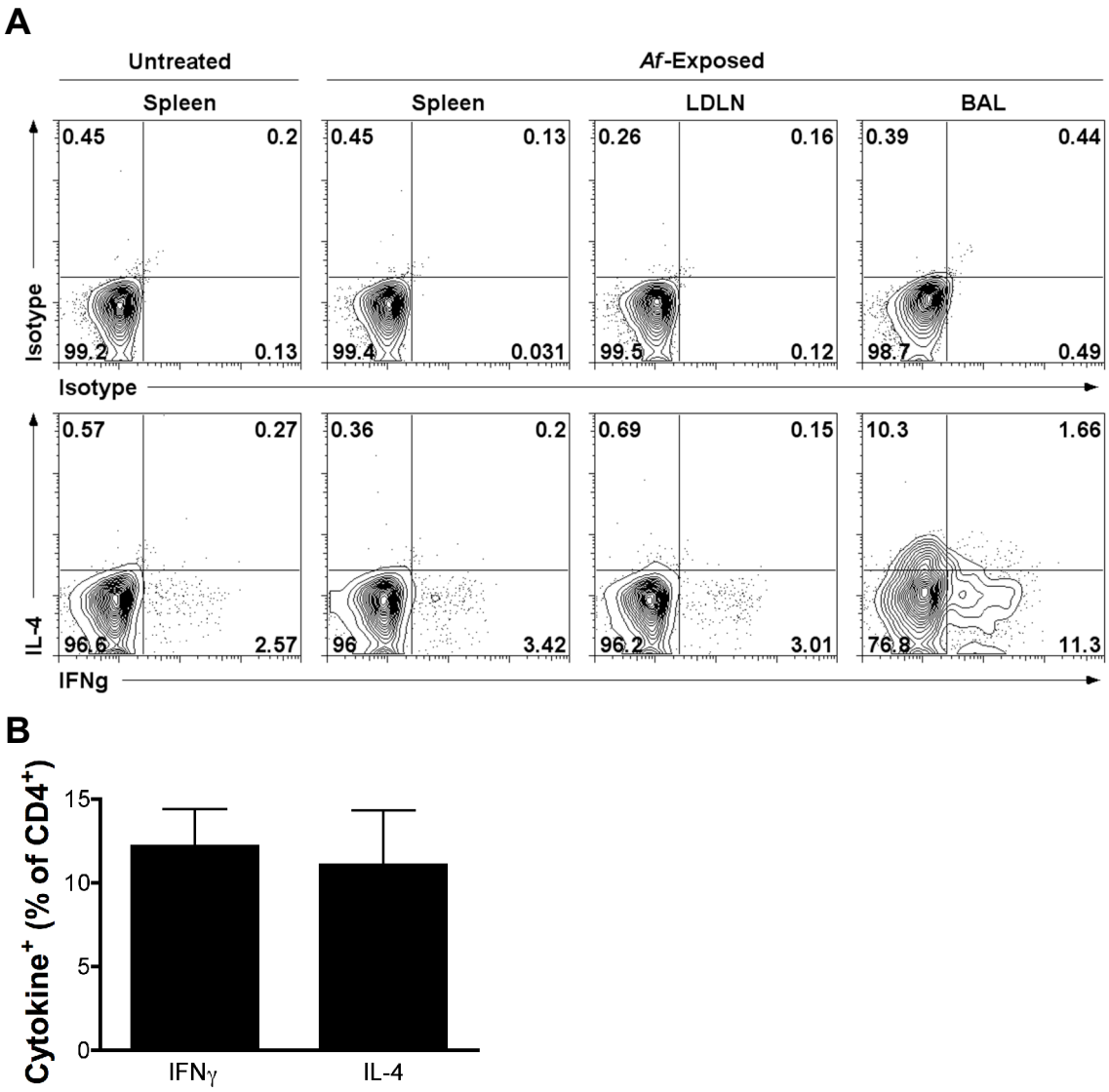

Figure 4-3. CD4$^+$ T cells exhibit a mixed T_H1/T_H2 subset profile at the effector site. As described in the materials and methods, cells were collected from various tissues from untreated mice and mice exposed to *A. fumigatus* four times (n=3 per group) and analyzed for cytokine production by flow cytometry. Pooled cells for each group were briefly activated *in vitro* for 5h with PMA and ionomycin in the presence of monensin in order to enhance cytokine production and block its secretion, respectively. A) Gated CD4$^+$ lymphocytes were analyzed for the intracellular accumulation IFNγ and IL-4 (see axes labels for contour plots). Quadrants were set with intracellular isotype control-stained CD4$^+$ lymphocytes (top row) and the percentage of CD4$^+$ lymphocytes in each quadrant is included on each plot. An independent, repeat experiment produced similar results. B) The bar graph depicts data collected from four independent experiments with cells recovered by BAL from mice exposed to *A. fumigatus* three or four times (note three and four exposures produced similar data). The data show the mean (+SEM) percentage of CD4$^+$ lymphocytes expressing the specific cytokine.

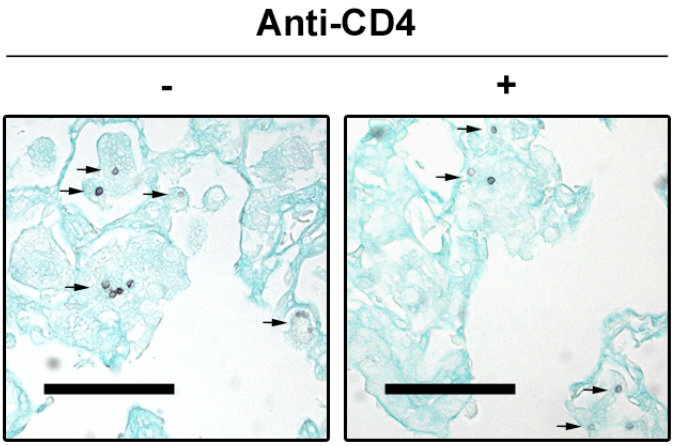

Figure 4-4. In the absence of $CD4^+$ T cells, *Aspergillus fumigatus* does not escape host protection in the lungs of mice after repeated, weekly inhalation of viable conidia.
As described in the materials and methods, one group of mice was treated with anti-CD4 antibody prior to and throughout the period of three exposures, while another group was exposed but not treated with depleting antibody. Histological sections of lung tissue were stained with Gomori Methenamine Silver in order to detect fungal material, which is stained black. Representative photomicrographs are shown. Black bars are 50μm in length.

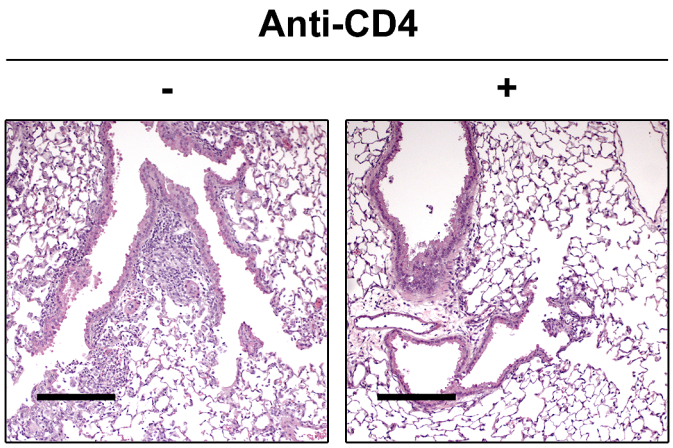

Figure 4-5. The absence of $CD4^+$ T cells results in severely attenuated inflammation of the lungs.
Mice in both groups were exposed to *A. fumigatus* three times, and not treated or treated with anti-CD4. Histological sections of lung tissues stained were with H&E. Representative micrographs include terminal bronchioles. Black bars are 200μm in length.

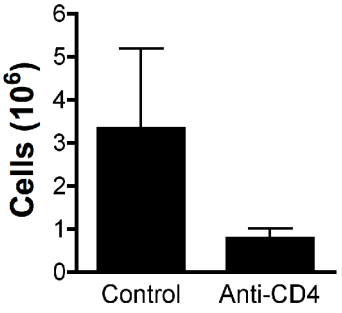

Figure 4-6. $CD4^+$ cells mediate the accumulation of leukocytes in the airway to a large extent.
Mice in both groups were exposed to *A. fumigatus* three or four times, and not treated or treated with anti-CD4 (note: three or four exposures produced similar results). Cells were recovered from the airway and enumerated under a microscope with a hemacytometer. Mean (+SEM) of cell numbers compiled from the means of three independent experiments are shown.

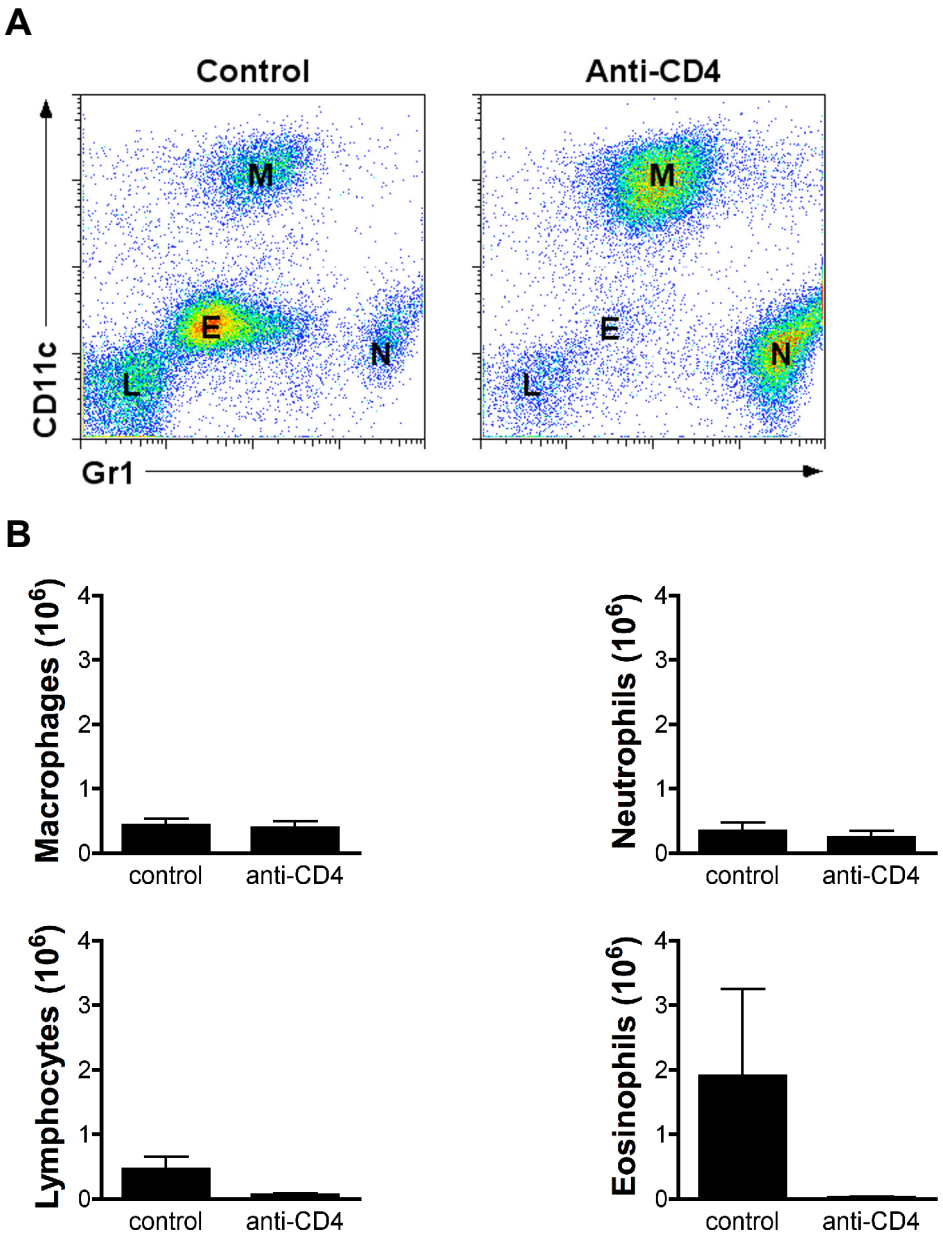

Figure 4-7. CD4$^+$ T cells are necessary for the manifestation of cellular allergic airway inflammation.
Mice in both groups were exposed to *A. fumigatus* three or four times, and not treated or treated with anti-CD4 (note: three or four exposures produced similar results). Cells were recovered from the airway and a leukocyte differential was performed with flow cytometry according to the method described in Appendix 1. A) Representative density plots show expression of CD11c and Gr1 for the entire airway cell populations. The central densities of individual leukocyte subpopulations are labeled (M=macrophage, N=neutrophil, L=lymphocyte, and E=eosinophil). B) The product of the percentage of each leukocyte subset and the total airway cell number gives the cell numbers for each leukocyte subset present in the airways (see y-axis labels). Mean (+SEM) of cell numbers compiled from the means of three independent experiments are shown.

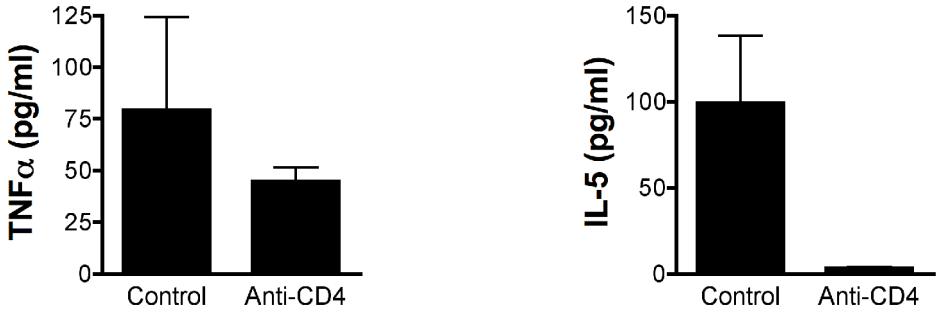

Figure 4-8. $CD4^+$ T cells are necessary for the production of a T_H2 cytokine but not an innate inflammatory cytokine.
Mice in both groups were exposed to *A. fumigatus* three times, and not treated or treated with anti-CD4. Cytokines present in the cell-free BALF were quantified by ELISA. The graph depicts the mean (+SEM) for individual samples (n=3 per group). An independent, repeat experiment produced similar results. Note: In previous experiments, both cytokines were undetectable in BALF from naïve mice.

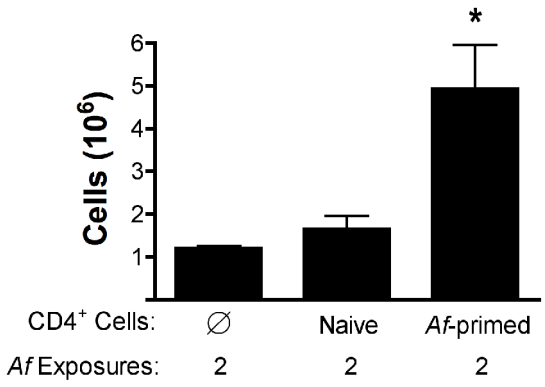

Figure 4-9. The transfer of *A. fumigatus*-primed, but not naïve, $CD4^+$ T cells promotes a significantly enhanced cellular response to inhaled conidia. After the adoptive transfer of vehicle control (∅) or 0.8-1×10^7 purified $CD4^+$ T cells, recipient mice were exposed to conidia on the day of transfer and a week later, 24h before cells were collected from the airway. As described in the methods, naïve $CD4^+$ T cells were purified from the spleens of naïve animals, and *Af*-primed $CD4^+$ T cells were purified from a pool of lung leukocytes and lung-draining lymph node cells harvested from mice exposed to conidia three times. The graph depicts the mean (+SEM) for individual samples (n=4 per group) of total cells recovered from the airways of recipient mice post *A. fumigatus* exposure. *$p < 0.05$ compared to both other groups

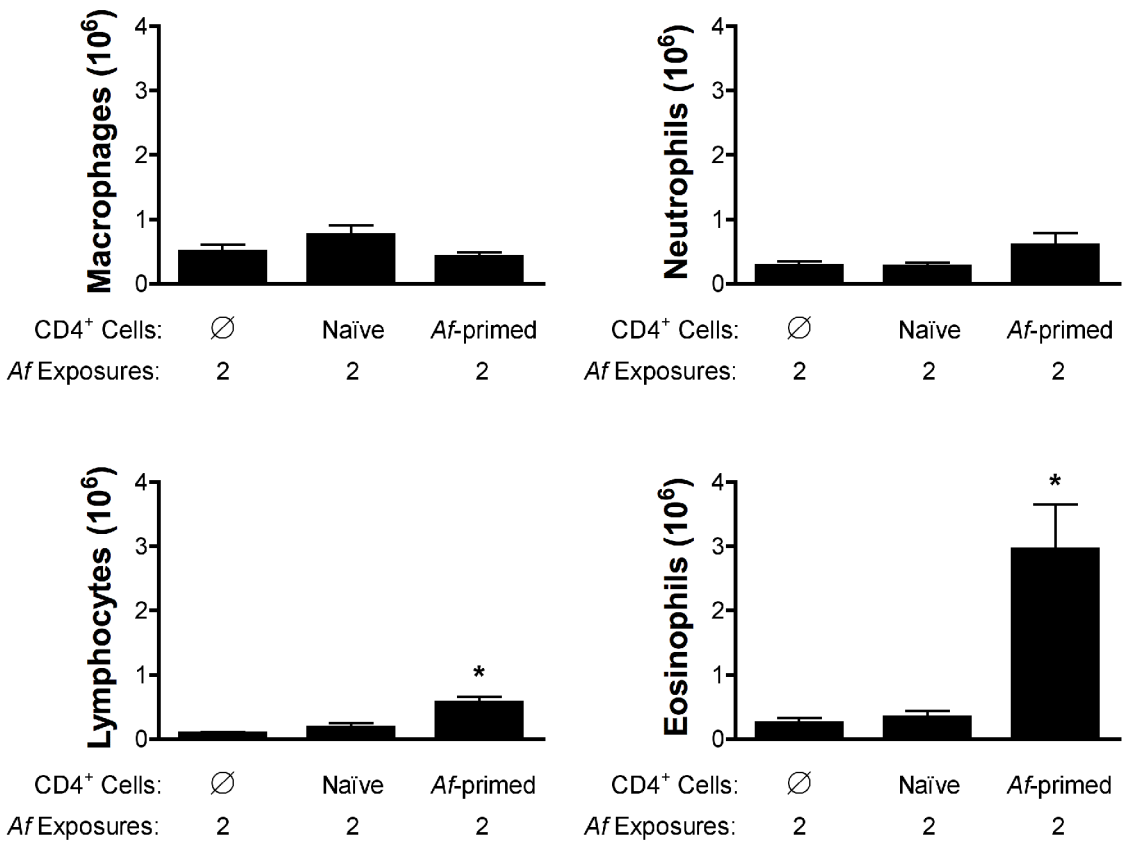

Figure 4-10. The transfer of *A. fumigatus*-primed, but not naïve, CD4+ T cells accelerates the development of the allergic airways response.
As described previously, recipient mice were exposed to conidia on days 0 and 7 after the adoptive transfer of vehicle control (∅) or 0.8-1×10^7 purified $CD4^+$ T cells. Cells were collected from the airways of recipient mice 24h after the second exposure, and leukocyte differential analyses were performed on individual samples. The graph depicts the mean (+SEM) number of cells for each leukocyte subset. *$p < 0.01$ compared to both other groups for that leukocyte subset

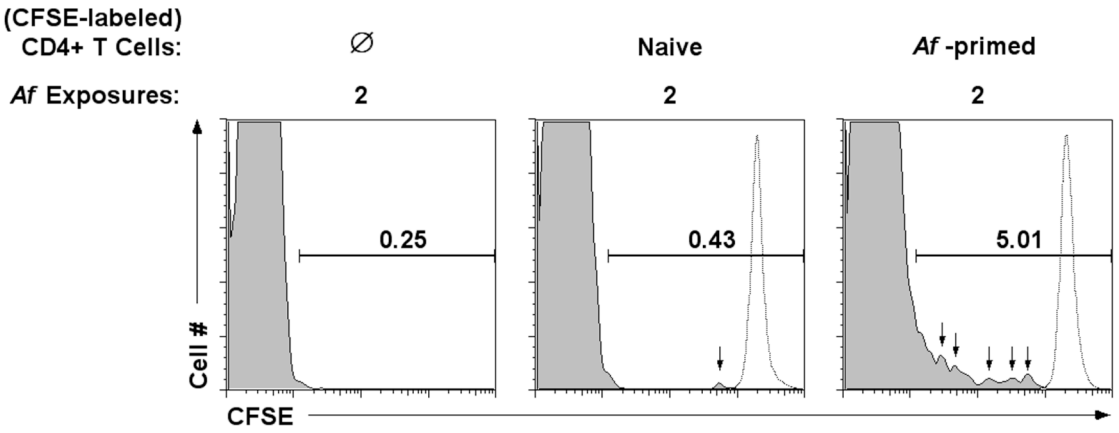

Figure 4-11. Transferred *A. fumigatus*-primed, but not naïve, CD4$^+$ T cells undergo cellular division and accumulate at the effector site.
As described previously, recipient mice were exposed to conidia on days 0 and 7 after the adoptive transfer of vehicle control (∅) or 0.8-1×10^7 purified, CFSE-labeled CD4$^+$ T cells. Cells were collected from the airways of recipient mice 24h after the second exposure and pooled for flow cytometric analyses. Shown above are the CFSE profiles of the gated CD4$^+$ T cell populations, including endogenous recipient cells and transferred donor cells (shaded histograms). Endogenous recipient cells are CFSE$^-$. Arrows point to distinct peaks of donor CFSE$^+$CD4$^+$ T cells, where peaks of reduced intensity are evidence of previous cell division. The CFSE intensity of each donor cell population at the time of transfer is overlayed onto each respective plot for reference (open histograms), but note that these cells were analyzed by flow cytometry at a previous, separate session due to the length of the experiment and the amplitude of the donor cell peak is not relevant. The percentage of CD4$^+$ T cells in the recipient airways that are CFSE$^+$ are labeled on each histogram, but note that additional donor cells may have blended in with the naïve CD4$^+$ T cell population after many rounds of division.

DISCUSSION

The data presented in this chapter demonstrated that $CD4^+$ T cells mediated the hypersensitivity response to *A. fumigatus* after repeated inhalation of viable conidia. After three weekly exposures, a significant increase in the number of activated, cytokine producing $CD4^+$ T_H cells in the airway coincided with the onset of the hypersensitivity response that manifested as an AAD. $CD4^+$ T cells were required for the pathogenesis of the hypersensitivity disease, because depletion of $CD4^+$ T cells throughout the period of exposure to conidia severely abrogated the AAD but did not affect fungal clearance. Finally, the adoptive transfer of *A. fumigatus*-primed, but not naïve, $CD4^+$ T cells augmented the development of the AAD.

In the present study, activated and terminal effector $CD4^+$ T cells were recovered exclusively from the airways. Specifically, BAL $CD4^+$ T cells, but not spleen or LDLN $CD4^+$ T cells, had increased expression of the activation markers CD25, CD44, and CD69 and an increased production of the effector cytokines IL-4 or IFNγ. These data on the compartmentalization of $CD4^+$ T cell activation and cytokine production are consistent with previous reports on the generation of $CD4^+$ T_H1 cell responses to pulmonary fungal infections[7, 15]. Recently, the priming of T_H1 cells was analyzed in the context of pulmonary infections with the fungi *Aspergillus fumigatus* and *Cryptococcus neoformans*[7, 15]. In both studies, the proliferative capacity of $CD4^+$ T cell population resided with those cells in the LDLN, but activated, IFNγ-producing effector $CD4^+$ T_H1 cells resided exclusively at the site of infection. The pattern of T_H1 differentiation during fungal infection

was similar to that reported in the context of a pulmonary infection with influenza virus[16]. Our findings suggested that $CD4^+$ T_H2 cell priming likely occurs in a similar fashion. It is interesting that activated, cytokine-producing T_H2 cells seem to be restricted to the lung during the allergic response considering the critical role of T_H2 cells and T_H2 cytokines in promoting IgE production by germinal center B cells residing in secondary lymphoid organs[17, 18]. While lymph node-resident dendritic cells prime $CD4^+$ T_H1 cells by antigen presentation and IL-12 production, dendritic cells do not produce IL-4, so the spatiotemporal organization of $CD4^+$ T_H2 priming is more complex and not currently well understood[19-21]. Our model provides further opportunity to study the regulation of the development of a T_H2 immune response to an inhaled allergen.

Repeated exposure to viable *A. fumigatus* conidia induced $CD4^+$ T_H2 and T_H1 cells. Several previous reports indicated that a single exposure to *A. fumigatus* conidia led primarily to the priming of $CD4^+$ T_H1 cells[6, 7], and exposure to *A. fumigatus* hyphae or antigen extracts led primarily to the priming of $CD4^+$ T_H2 cells[6, 9]. Systemic priming and airway exposure to *A. fumigatus* antigens established a T_H2-mediated AAD that was subsequently augmented by exposure to conidia, suggesting at least that pre-formed $CD4^+$ T_H2 cells would respond to conidia[8]. Differences in the $CD4^+$ T cell response to conidia likely depended on the dosing and frequency used in the various studies. In the aforementioned studies that resulted in primarily CD4+ T_H1 priming, 5 and 100 times the number of conidia used in our study were administered[6, 7]. A differential effect of dose and frequency of exposure to *A. fumigatus* conidia may have clinical relevance,

because T_H1-associated hypersensitivity pneumonitis results from very high-dose exposure, generally in an occupational setting[22-25].

It is interesting that in spite of the presence of T_H2 and T_H1 cells, the $CD4^+$ T cell-dependent hypersensitivity disease that developed after repeated exposure to conidia had many features of AAD, a T_H2 disease. Previously, T_H1 cells were reported to abrogate T_H2 cell-mediated AAD[26]. However, it is also noted that T_H1 responses to viral infections are known to exacerbate asthma symptoms[27, 28]. Furthermore, it was recently demonstrated in mice that a T_H1-promoting rhinovirus infection augmented a T_H2 allergic airway disease, and that the pre-existing T_H2 allergic airway disease augmented the T_H1 response to rhinovirus infection[29]. The data generated in the present study support the emerging understanding that asthma and allergic diseases are not simply the result of an imbalance in counterregulatory T_H1 and T_H2 responses[30]. Rather, current evidence suggests that T_H2 and T_H1 responses are both inflammatory, and are both subject to control by myriad regulatory mechanisms, such as those mediated by dedicated regulatory T cells.

In our experiments, clearance of *A. fumigatus* was not impaired by either $CD4^+$ T cell depletion or the development of a $CD4^+$ T_H2 cell response. It has been reported in murine models of invasive pulmonary aspergillosis that $CD4^+$ T_H1 cells enhance protection, and $CD4^+$ T_H2 cells enhance susceptibility[31-34]. It was likely that T_H1 cells were better able to promote the restoration of functional innate immunity following certain treatments that impaired macrophage or

neutrophil responses. The participation of $CD4^+$ T cells in the clearance of inhaled conidia is probably not required if the innate immune response is intact.

In the present study, we found that $CD4^+$ cell depletion throughout the period of *A. fumigatus* exposure ablated airway eosinophilia and BALF IL-5 production. It has been recognized for some time that production of IL-5 is critical for the orchestration of tissue eosinophilia[35-37]. In turn, T_H2 cells are widely regarded as the critical source of IL-5 in the allergic response[38]. However, recent evidence demonstrated that innate immune cells were able to promote tissue eosinophilia in response to chitin, a fungal product, and purified *Aspergillus oryzae* protease in RAG-deficient mice that lack functional $CD4^+$ T cells[12, 13]. In the present study, airway inflammation was examined after several weekly exposures to conidia, so it is possible we failed to detect an early wave of innate immune activity, including eosinophil recruitment.

The introduction of *A. fumigatus*-primed $CD4^+$ T cells into naïve mice augmented the development of the AAD in response to subsequent inhalation of conidia. In agreement with our previous observations (see Chapter 3), two exposures to conidia did not induce a robust allergic response. However, mice that received *A. fumigatus*-primed $CD4^+$ T cells, but not naïve $CD4^+$ T cells, exhibited a robust allergic response. The magnitude of the response was comparable to measured after naïve mice were exposed to conidia three or four times (see Chapter 3). Therefore, a rate-limiting step in the development of the AAD was the priming of the $CD4^+$ T cell response.

In conclusion, $CD4^+$ T cells mediated the hypersensitivity response to *A. fumigatus*. The $CD4^+$ T cell response was comprised of relatively equal frequencies of T_H2 and T_H1 cells. In addition, T_H17 cells were present at frequencies similar to those for T_H2 and T_H1 cells (see Figure 5-3). This model affords further opportunity for investigation into the T_H cell response to the inhalation of a natural respiratory allergen, including local T_H cell differentiation and unique T_H cell subset effects. In addition, this model affords the opportunity to investigate the chronic effects of a $CD4^+$ T cell-mediated hypersensitivity response to a natural aeroallergen encountered via the natural route of exposure.

References

1. Kay, A. B. Allergy and allergic diseases. Second of two parts. N Engl J Med 344, 109-13 (2001).
2. Kay, A. B. The role of T lymphocytes in asthma. Chem Immunol Allergy 91, 59-75 (2006).
3. van Oosterhout, A. J. & Motta, A. C. Th1/Th2 paradigm: not seeing the forest for the trees? Eur Respir J 25, 591-3 (2005).
4. Hohl, T. M. et al. Aspergillus fumigatus triggers inflammatory responses by stage-specific beta-glucan display. PLoS Pathog 1, e30 (2005).
5. Steele, C. et al. The beta-glucan receptor dectin-1 recognizes specific morphologies of Aspergillus fumigatus. PLoS Pathog 1, e42 (2005).
6. Bozza, S. et al. Dendritic cells transport conidia and hyphae of Aspergillus fumigatus from the airways to the draining lymph nodes and initiate disparate Th responses to the fungus. J Immunol 168, 1362-71 (2002).
7. Rivera, A. et al. Innate immune activation and CD4+ T cell priming during respiratory fungal infection. Immunity 25, 665-75 (2006).
8. Hogaboam, C. M. et al. Chronic airway hyperreactivity, goblet cell hyperplasia, and peribronchial fibrosis during allergic airway disease induced by Aspergillus fumigatus. Am J Pathol 156, 723-32 (2000).
9. Kheradmand, F. et al. A protease-activated pathway underlying Th cell type 2 activation and allergic lung disease. J Immunol 169, 5904-11 (2002).
10. Grunig, G. et al. Interleukin-10 is a natural suppressor of cytokine production and inflammation in a murine model of allergic bronchopulmonary aspergillosis. J Exp Med 185, 1089-99 (1997).
11. Kurup, V. P. et al. Immune responses to Aspergillus antigen in IL-4-/-mice and the effect of eosinophil ablation. Allergy 54, 420-7 (1999).
12. Kiss, A. et al. A new mechanism regulating the initiation of allergic airway inflammation. J Allergy Clin Immunol 120, 334-42 (2007).
13. Reese, T. A. et al. Chitin induces accumulation in tissue of innate immune cells associated with allergy. Nature 447, 92-6 (2007).
14. Sakaguchi, S. Naturally arising Foxp3-expressing CD25+CD4+ regulatory T cells in immunological tolerance to self and non-self. Nat Immunol 6, 345-52 (2005).
15. Lindell, D. M., Moore, T. A., McDonald, R. A., Toews, G. B. & Huffnagle, G. B. Distinct compartmentalization of CD4+ T-cell effector function versus proliferative capacity during pulmonary cryptococcosis. Am J Pathol 168, 847-55 (2006).
16. Roman, E. et al. CD4 effector T cell subsets in the response to influenza: heterogeneity, migration, and function. J Exp Med 196, 957-68 (2002).
17. Secord, E. A. et al. Reconstitution of germinal center formation in nude mice with Th1 and Th2 clones. Cell Immunol 174, 173-9 (1996).
18. Shang, X. Z. et al. Regulation of antigen-specific versus by-stander IgE production after antigen sensitization. Cell Immunol 229, 106-16 (2004).

19. Noben-Trauth, N., Hu-Li, J. & Paul, W. E. Conventional, naive CD4+ T cells provide an initial source of IL-4 during Th2 differentiation. J Immunol 165, 3620-5 (2000).
20. Liu, Z. et al. IL-2 and autocrine IL-4 drive the in vivo development of antigen-specific Th2 T cells elicited by nematode parasites. J Immunol 174, 2242-9 (2005).
21. Sokol, C. L., Barton, G. M., Farr, A. G. & Medzhitov, R. A mechanism for the initiation of allergen-induced T helper type 2 responses. Nat Immunol 9, 310-8 (2008).
22. Aebischer, C. C., Frey, U. & Schoni, M. H. Hypersensitivity pneumonitis in a five-year-old boy: an unusual antigen source. Pediatr Pulmonol 33, 77-8 (2002).
23. Enriquez-Matas, A. et al. Hypersensitivity pneumonitis caused by domestic exposure to molds. J Investig Allergol Clin Immunol 17, 126-7 (2007).
24. Patel, A. M., Ryu, J. H. & Reed, C. E. Hypersensitivity pneumonitis: current concepts and future questions. J Allergy Clin Immunol 108, 661-70 (2001).
25. Ruiz-Hornillos, F. J. et al. Occupational asthma due to esparto hypersensitivity in a building worker. Allergy Asthma Proc 28, 571-3 (2007).
26. Irifune, K. et al. Adoptive transfer of T-helper cell type 1 clones attenuates an asthmatic phenotype in mice. Eur Respir J 25, 653-9 (2005).
27. Beasley, R. et al. Viral respiratory tract infection and exacerbations of asthma in adult patients. Thorax 43, 679-83 (1988).
28. Mallia, P. & Johnston, S. L. How viral infections cause exacerbation of airway diseases. Chest 130, 1203-10 (2006).
29. Bartlett, N. W. et al. Mouse models of rhinovirus-induced disease and exacerbation of allergic airway inflammation. Nat Med 14, 199-204 (2008).
30. Wills-Karp, M., Santeliz, J. & Karp, C. L. The germless theory of allergic disease: revisiting the hygiene hypothesis. Nat Rev Immunol 1, 69-75 (2001).
31. Cenci, E. et al. T cell vaccination in mice with invasive pulmonary aspergillosis. J Immunol 165, 381-8 (2000).
32. Cenci, E. et al. Interleukin-4 causes susceptibility to invasive pulmonary aspergillosis through suppression of protective type I responses. J Infect Dis 180, 1957-68 (1999).
33. Cenci, E. et al. Cytokine- and T helper-dependent lung mucosal immunity in mice with invasive pulmonary aspergillosis. J Infect Dis 178, 1750-60 (1998).
34. Cenci, E. et al. Th1 and Th2 cytokines in mice with invasive aspergillosis. Infect Immun 65, 564-70 (1997).
35. Huffnagle, G. B., Boyd, M. B., Street, N. E. & Lipscomb, M. F. IL-5 is required for eosinophil recruitment, crystal deposition, and mononuclear cell recruitment during a pulmonary Cryptococcus neoformans infection in genetically susceptible mice (C57BL/6). J Immunol 160, 2393-400 (1998).

36. Mould, A. W., Matthaei, K. I., Young, I. G. & Foster, P. S. Relationship between interleukin-5 and eotaxin in regulating blood and tissue eosinophilia in mice. J Clin Invest 99, 1064-71 (1997).
37. Murali, P. S. et al. Aspergillus fumigatus antigen induced eosinophilia in mice is abrogated by anti-IL-5 antibody. J Leukoc Biol 53, 264-7 (1993).
38. Haczku, A. T cells and eosinophils in asthma. Acta Microbiol Immunol Hung 45, 19-29 (1998).

Chapter 5

Hypersensitivity Response to *Aspergillus fumigatus*: Chronic Airway Inflammation

INTRODUCTION

Rationale

Hypersensitivity responses can lead to severe disease when the inflammation becomes **chronic**. In humans, the pathogenesis of asthma is routinely described as a progression through the following stages: acute inflammation, chronic inflammation, and airway remodeling. Chronic inflammation is associated with nonspecific bronchial hyperreactivity, and chronic inflammation promotes airway remodeling. Airway remodeling is associated with reversible airways obstruction. Bronchial hyperreactivity and reversible airways obstruction result in the manifestation of the clinical disease asthma[1]. In Chapter 4, the **acute** allergic airway response to viable *Aspergillus fumigatus* conidia did not result in augmented airway hyperreactivity. Previously published murine models do not recapitulate all the clinical features of the human disease asthma, especially the maintenance of **chronic** inflammation[2].

Hypothesis

Due to the inherent allergenicity of viable *A. fumigatus* conidia, **chronic** exposure will result in progressive pathophysiological alterations to the lungs.

Objectives

1. To determine the strength and character of the local immune response after **chronic** exposure to viable *A. fumigatus* conidia via continued, weekly inhalation.
2. To determine the extent of histopathological alterations in the lung after **chronic** exposure to conidia.
3. To determine the extent of pathophysiological alterations in pulmonary function after **chronic** exposure to conidia.

RESULTS

To determine if chronic exposure to *A. fumigatus* conidia led to progressive inflammation, the extent of the allergic airway disease (AAD) was evaluated in mice 24 hours after the last of 4 and 8 weekly exposures. The severity of the inflammatory response was examined by the quantification of the airway leukocytes recovered by bronchoalveolar lavage (BAL) (Figure 5-1). Similar numbers of total cells were recovered from the airways after four and eight exposures. Cellular inflammation was persistent, but not progressive, during the transition from acute (4 exposures) to chronic (8 exposures) inflammation.

Leukocyte different counts were generated by flow cytometric analysis of cells recovered from the airway (Figure 5-2). There were no significant differences for any particular leukocyte subset, though macrophages were slightly increased and eosinophils were slightly decreased after eight as compared to four exposures. The numbers of neutrophils and lymphocytes were very similar at both time points.

The functional capacity of effector $CD4^+$ T_H cells to produce cytokines was analyzed by intracellular cytokine staining and flow cytometry with cells recovered from the airway (Figure 5-3). Only cells recovered from the airway (BAL), and not the lung-draining lymph nodes (LDLN), produced detectable amounts of cytokines as measured by this method (see Chapter 4). After four exposures, approximately 10-15% of $CD4^+$ T cells produced IL-4, IFNγ, or IL-17. The percent of IL-17-producing $CD4^+$ T cells significantly increased after long-

term exposure. There was a modest, but not significant, decrease in the frequency of $CD4^+$ T cells producing IL-4. Finally, the proportion of $CD4^+$ T cells producing IFNγ was similar after four or eight exposures. Note, the absolute numbers of $CD4^+$ T cells recovered from the airways after four and eight exposures was similar (see Appendix 2, Figure A2-8).

The levels of serum total IgE were measured by ELISA in blood samples collected at the time of harvest (Figure 5-4). An elevated level of total IgE, present after four exposures, persisted with chronic exposure.

Histological samples of lung tissue were stained with PAS to reveal mucus in the airways (Figure 5-5). Goblet cell metaplasia and mucus hypersecretion were prominent after four exposures and persisted with chronic exposure. Airways obstruction with mucus was not regularly detected and did not increase with chronic exposure.

Histological samples of lung tissue were stained with Masson's trichrome in order to examine the peribronchial collagen (Figure 5-6). In naïve control mice, a thin layer of blue-stained collagen supported the peribronchial smooth muscle. A single layer of mesenchymal cells, identified by their spindle-shaped nuclei, was associated with the collagen layer in naïve mice. After four exposures, there was increased collagen staining in the peribronchial area. After eight exposures, modest remodeling was noted in that there were often several layers of collagen-associated mesenchymal cells, identified by rows of nuclei adjacent to the epithelium.

Peribronchial smooth muscle was evaluated by immunohistochemistry of lung sections stained with anti-α smooth muscle actin (α-SMA) antibody (Figure 5-7). AAD resulting from repeated exposure to *A. fumigatus* did not result in remodeling of the peribronchial smooth muscle layer at early or late time points.

The airway response to methacholine provocation in mice exposed to conidia four and eight times was compared to the airway response in naïve mice (Figure 5-8). Mice with acute or chronic allergic airway inflammation did not exhibit an increase in airway hyperreactivity (AHR) compared to untreated mice.

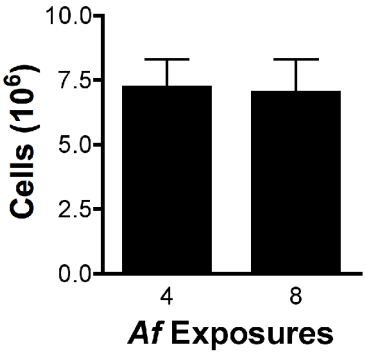

Figure 5-1. Cellular inflammation in the airway is maintained with chronic exposure to conidia.
Cells were recovered from the airway by bronchoalveolar lavage and enumerated under the microscope with a hemacytometer. These data were collected from four independent experiments for each group, containing three or mice per group per experiment. The mean value for each group in each experiment was compiled. The graph illustrates the mean (+ SEM) number of total cells present in the airways 24h after 4 or 8 weekly exposures.

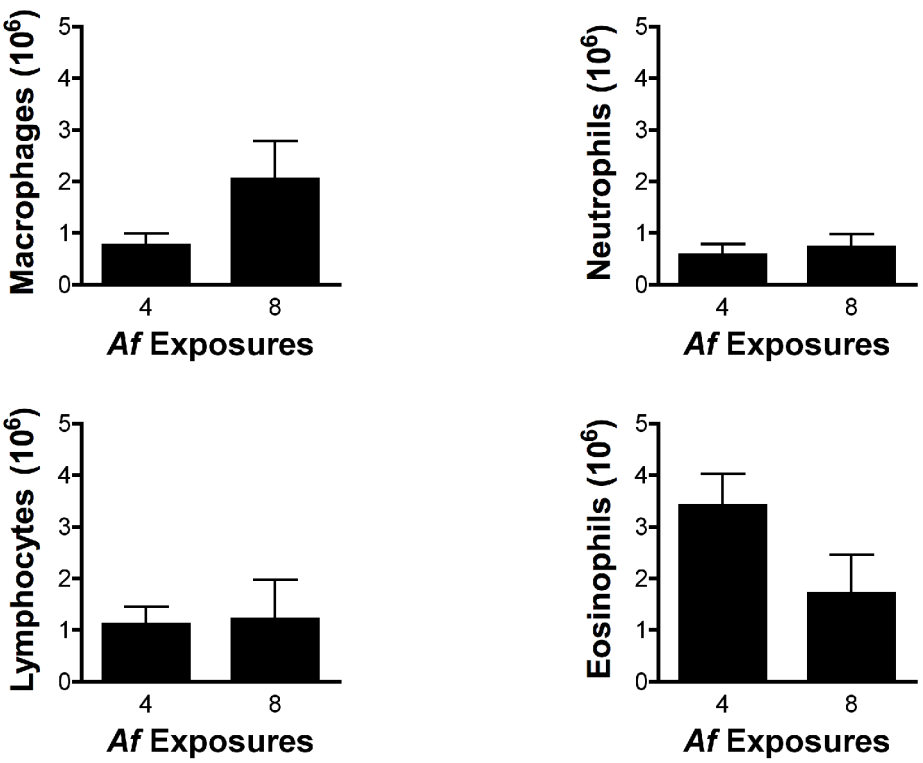

Figure 5-2. Subtle changes in airway leukocyte subsets result from chronic exposure.
After 4 or 8 weekly exposures to *A. fumigatus*, cells were recovered from the airways, and leukocyte differential analyses were performed with flow cytometry according to the method described in Appendix 1. The product of the percentage of each leukocyte subset and the total airway cell number gives the cell numbers for each leukocyte subset present in the airways (i-iv, see y-axis labels). Mean (+SEM) of cell numbers compiled from the means of three independent experiments are shown.

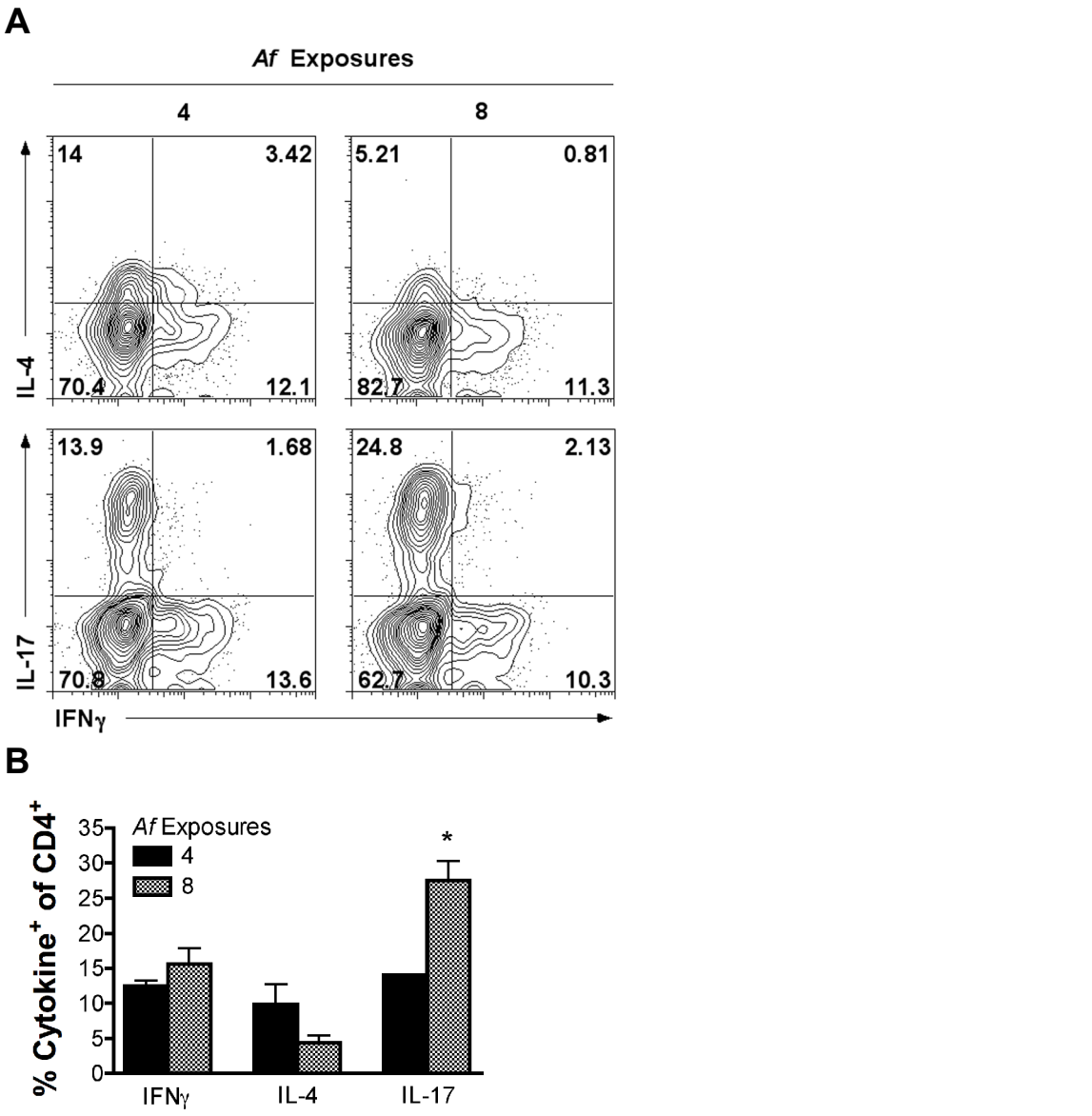

Figure 5-3. The frequency of airway T_H subsets is variably affected by chronic exposure. Cells were collected from the airways of mice exposed to *A. fumigatus* 4 or 8 times (n=3 per group) and analyzed for cytokine production by flow cytometry, as described in the materials and methods. Pooled cells for each group were briefly activated *in vitro* for 5h with PMA and ionomycin in the presence of monensin in order to enhance cytokine production and block its secretion, respectively. A) Gated $CD4^+$ lymphocytes were analyzed for the intracellular accumulation IFNγ, IL-4, and IL-17 (see axes labels for density plots). Quadrants were set with the aid of intracellular isotype control-stained $CD4^+$ lymphocytes (not shown) and the percentage of $CD4^+$ lymphocytes in each quadrant is included on each plot. An independent, repeat experiment produced similar results. B) The bar graph depicts data collected from three independent experiments (two experiments included IL-17). The data show the mean (+SEM) percentage of $CD4^+$ lymphocytes expressing the specific cytokine after four or eight exposures. *$p < 0.05$ compared to the 4 exposures group for the same cytokine

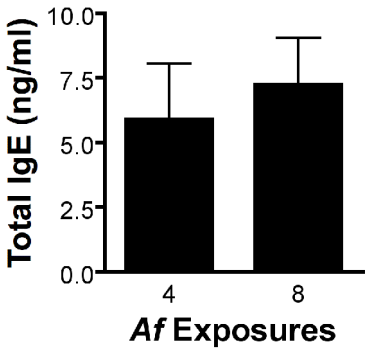

Figure 5-4. Elevated levels of serum IgE are maintained with chronic exposure.
Mice were exposed to *A. fumigatus* 4 or 8 times on a weekly basis. Blood was collected 24h after the final exposure. Total IgE levels in the serum were quantified by ELISA. Data for individual mice was compiled from 5 independent experiments (n=23 mice per group). The mean (+SEM) is shown for each group.

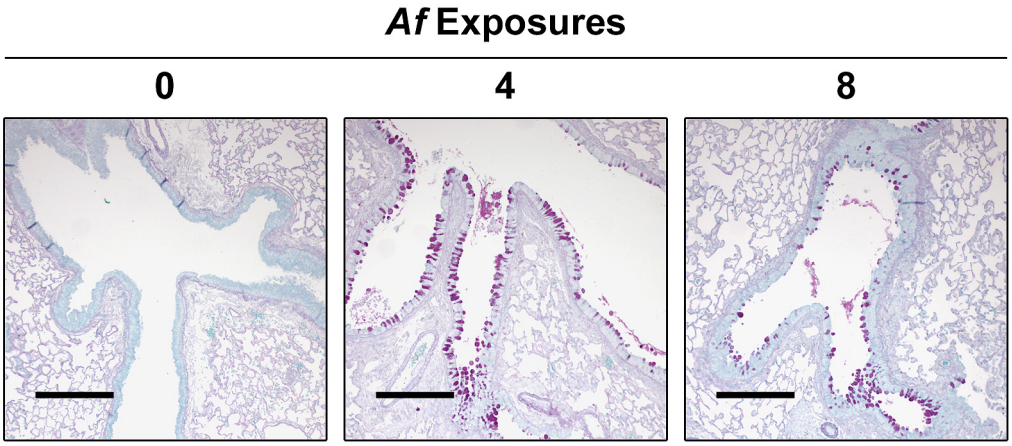

Figure 5-5. Goblet cell metaplasia and mucous hypersecretion persist with chronic exposure.
Histological sections of lung tissue were stained with PAS in order to detect mucous, which is stained purple. Representative photomicrographs include conducting airways from mice exposed to *A. fumigatus* 0, 4 or 8 times at weekly intervals. Black bars are 200μm in length.

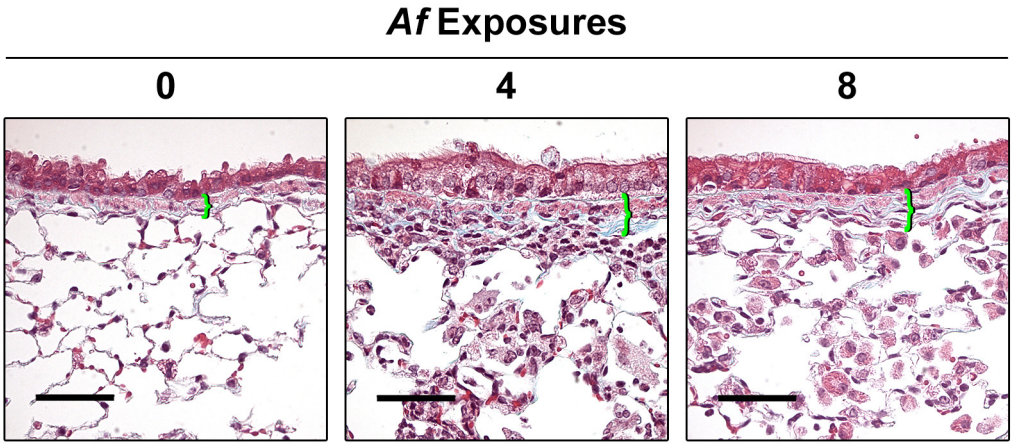

Figure 5-6. Remodeling of the peribronchial collagen layer develops after repeated exposure.
Histological sections of lung tissue were stained with Masson's trichrome in order to detect collagen, which is stained blue. Representative photomicrographs include conducting airways from mice exposed to *A. fumigatus* 0, 4 or 8 times at weekly intervals. Black bars are 50μm in length.

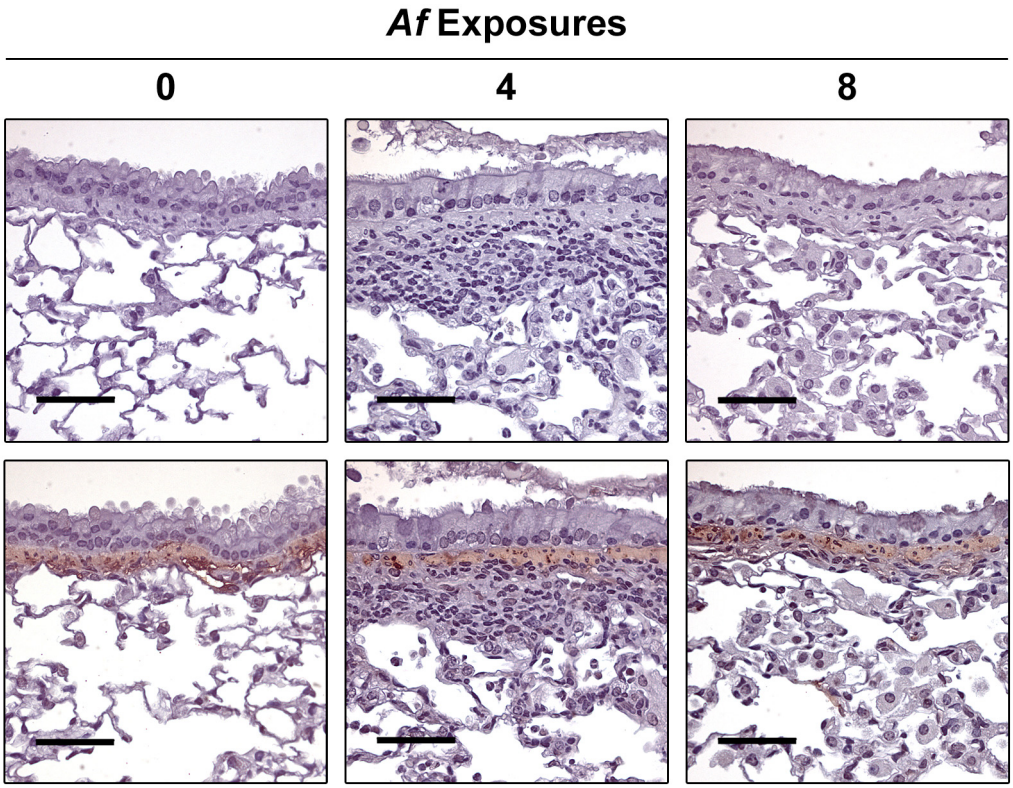

Figure 5-7. Thickening of the peribronchial smooth muscle layer does not occur after repeated exposure.
As described in the methods, histological sections of lung tissue were stained with standard immunohistochemistry techniques in order to identify smooth muscle cells, which are stained brown. The bottom row contains sections stained with anti-α smooth muscle actin and the appropriate secondary antibody while the top row contains adjacent sections stained with secondary antibody only. Representative photomicrographs include conducting airways from mice exposed to *A. fumigatus* 0, 4 or 8 times at weekly intervals. Black bars are 50μm in length.

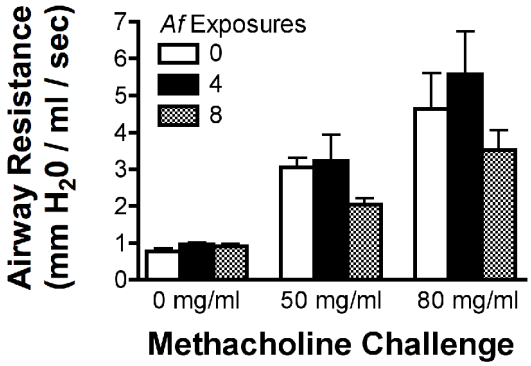

Figure 5-8. Airway hyperreactivity does not develop after repeated inhalation of *A. fumigatus* conidia.
As described in the methods, bronchial resistance was measured in a whole body plethysmograph 24h after a given number of exposures (see bar graph legend). Briefly, resistance values were calculated in real-time for anesthetized and ventilated mice at baseline and after direct respiratory challenge with 20μl of a nebulized methacholine solution (see x-axis labels) at doses previously determined to elicit significant responses in hyperreactive mice. Mean (+SEM) for four-to-five mice per group are shown. An independent experiment with unchallenged mice and mice exposed four times produced similar results.

DISCUSSION

The data presented in this chapter demonstrated that pulmonary inflammation persisted, but did not progress, with chronic exposure to viable *A. fumigatus* conidia. Features of the AAD that were similar in severity between the acute and chronic inflammatory phases included the number of leukocytes present in the airways, the level of serum total IgE, and the presence of mucus hypersecretion. While the total number of $CD4^+$ T cells in the airways was similar at both time points, the proportions of $CD4^+$ T_H subsets were dynamic. After four exposures, there were roughly equivalent frequencies of cytokine-producing T_H1, T_H2, and T_H17 cells (~10-15% of total $CD4^+$ T cells). However, by eight exposures, the frequency of T_H2 cells was moderately decreased, and the frequency of T_H17 cells was significantly increased. Evidence of mild airway remodeling was found, but remodeling was not progressive. As was the case with acute inflammation, chronic inflammation to *A. fumigatus* conidia did not result in increased AHR.

In the present study, airway eosinophilia persisted with chronic inflammation. While the total number of eosinophils was reduced compared to the peak levels detected during acute inflammation, the number of eosinophils present during the chronic phase of inflammation was higher than that seen in naïve mice (see Chapter 3). Attenuated airway eosinophilia with chronic exposure is a common finding in murine models of AAD. For instance, airway eosinophilia and increased AHR developed with acute exposure lasting 10 days in OVA-sensitized mice, but were attenuated with chronic exposure lasting more

than six weeks[3]. Likewise, acute airway eosinophilia peaked after ~3 weeks of repeated inhalation of *A. fumigatus* antigens, but airway eosinophilia declined at later time points with continued exposure[4, 5]. The effect of attenuated airway eosinophilia is not well understood, in part because the role of eosinophils in the mouse appears to be limited compared to their role in humans[6].

In our study, a modest, but insignificant, decline in the frequency of T_H2 cells within the airway population of $CD4^+$ T cells accompanied the modest reduction in the number of airway eosinophils during the progression from acute to chronic exposure. The attenuation of airway eosinophilia with chronic exposure to allergen in OVA-sensitized mice was associated with diminished T_H2 cell activities[7]. Chronic inflammation is central to the pathogenesis of asthma, because it induces airway remodeling. While T_H2 activity declined with continued exposure to viable conidia, T_H1 activity was maintained and T_H17 activity was increased, so $CD4^+$ T cell-mediated pro-inflammatory influences persisted.

In our study, chronic exposure to *A. fumigatus* led to mild, but not progressive, airway remodeling. Goblet cell metaplasia and mucus hypersecretion was detected in the acute and chronic phases of inflammation. We noted an increase in the peribronchial collagen, and an increase in the number of layers of parenchymal cells, possibly collagen-producing fibroblasts, associated with the peribronchial collagen layer. We did not detect thickening of the peribronchial smooth muscle layer at any point during the inflammatory response. Chronic inflammation and varying degrees of airway remodeling have been reported in other studies with mice[8-10]. In those reports, chronic

inflammation and peribronchial fibrosis were detected in OVA-sensitized and challenged mice, house dust mite (HDM) exposed mice, and *A. fumigatus* antigen-sensitized and conidia exposed mice. Increased peribronchial smooth muscle also was reported in the studies with OVA and HDM. In every case, airway remodeling was associated with persistent cellular inflammation and AHR. Airway remodeling is a central feature of asthma, but in general murine models of AAD have not exhibited a strong propensity towards airway remodeling.

Chronic exposure to *A. fumigatus* conidia in the present study did not result in interstitial fibrosis or fungal colonization of the airways. *A. fumigatus* is implicated in hypersensitivity pneumonitis (HP), a hypersensitivity disease associated with a T_H1 immune response to inhaled organic particles[11-13]. In HP, chronic inflammation can result in severe interstitial fibrosis[14, 15]. Those with asthma are at heightened risk for the development of allergic bronchopulmonary aspergillosis (ABPA), a severe T_H2-mediated hypersensitivity disease driven by the colonization of the airway with *A. fumigatus*. Chronic, repeated exposure to viable *A. fumigatus* conidia did not lead to the development of pathological features found in HP or ABPA.

In the present study, the progression from acute to chronic inflammation was accompanied by a significant increase in the frequency of T_H17 cells, but the number of neutrophils in the airway remained relatively constant. T_H17 cells are implicated in the pathogenesis of a variety of chronic inflammatory disorders, including autoimmune and allergic disorders[16]. It is clear that IL-17 has an important role in mediating pathology in a variety of diseases, but the mechanism

by which IL-17 acts is not well understood[17]. One important mechanism of action for IL-17 seems to be the recruitment of neutrophils to the site of inflammation[18]. In allergic airway disease, anti-IL-17 treatment simultaneously abrogated neutrophil recruitment and enhanced IL-5 production and eosinophil recruitment, suggesting these pathways may be reciprocally regulated[19]. In response to chronic exposure to *A. fumigatus* conidia, the increased T_H17 response was associated with a decreased T_H2 response. The pathological significance of the T_H17 response in this setting remains to be determined.

In conclusion, chronic exposure to viable *A. fumigatus* conidia resulted in persistent, but not progressive, airway inflammation. Polarized $CD4^+$ T_H1, T_H2, and T_H17 cells were present in the airway, and the relative frequencies of the T_H subsets were dynamically regulated during the progression from the acute to the chronic phase of inflammation. Our model provides a further opportunity to investigate the pathological effects of chronic pulmonary inflammation, and a further opportunity to study the regulation of T_H subset dynamics and the role of T_H17 cells in a novel *in vivo* model of chronic pulmonary inflammation.

References

1. Bousquet, J., Jeffery, P. K., Busse, W. W., Johnson, M. & Vignola, A. M. Asthma. From bronchoconstriction to airways inflammation and remodeling. Am J Respir Crit Care Med 161, 1720-45 (2000).
2. Finkelman, F. D. & Wills-Karp, M. Usefulness and optimization of mouse models of allergic airway disease. J Allergy Clin Immunol 121, 603-6 (2008).
3. Schramm, C. M. et al. Chronic inhaled ovalbumin exposure induces antigen-dependent but not antigen-specific inhalational tolerance in a murine model of allergic airway disease. Am J Pathol 164, 295-304 (2004).
4. Kurup, V. P., Choi, H., Resnick, A., Kalbfleisch, J. & Fink, J. N. Immunopathological response of C57BL/6 and C3H/HeN mice to Aspergillus fumigatus antigens. Int Arch Allergy Appl Immunol 91, 145-54 (1990).
5. Wang, J. M., Denis, M., Fournier, M. & Laviolette, M. Experimental allergic bronchopulmonary aspergillosis in the mouse: immunological and histological features. Scand J Immunol 39, 19-26 (1994).
6. Rothenberg, M. E. & Hogan, S. P. The eosinophil. Annu Rev Immunol 24, 147-74 (2006).
7. Swirski, F. K., D'Sa, A., Kianpour, S., Inman, M. D. & Stampfli, M. R. Prolonged ovalbumin exposure attenuates airway hyperresponsiveness and T cell function in mice. Int Arch Allergy Immunol 141, 130-40 (2006).
8. Hogaboam, C. M. et al. Chronic airway hyperreactivity, goblet cell hyperplasia, and peribronchial fibrosis during allergic airway disease induced by Aspergillus fumigatus. Am J Pathol 156, 723-32 (2000).
9. Johnson, J. R. et al. Continuous exposure to house dust mite elicits chronic airway inflammation and structural remodeling. Am J Respir Crit Care Med 169, 378-85 (2004).
10. McMillan, S. J. & Lloyd, C. M. Prolonged allergen challenge in mice leads to persistent airway remodelling. Clin Exp Allergy 34, 497-507 (2004).
11. Yoshida, K. et al. Hypersensitivity pneumonitis resulting from Aspergillus fumigatus in a greenhouse. Arch Environ Health 48, 260-2 (1993).
12. Quirce, S., Hinojosa, M., Blanco, R., Cespon, C. & Yoldi, M. Aspergillus fumigatus is the causative agent of hypersensitivity pneumonitis caused by esparto dust. J Allergy Clin Immunol 102, 147-8 (1998).
13. Aebischer, C. C., Frey, U. & Schoni, M. H. Hypersensitivity pneumonitis in a five-year-old boy: an unusual antigen source. Pediatr Pulmonol 33, 77-8 (2002).
14. Semenzato, G., Adami, F., Maschio, N. & Agostini, C. Immune mechanisms in interstitial lung diseases. Allergy 55, 1103-20 (2000).
15. Patel, A. M., Ryu, J. H. & Reed, C. E. Hypersensitivity pneumonitis: current concepts and future questions. J Allergy Clin Immunol 108, 661-70 (2001).

16. Schmidt-Weber, C. B., Akdis, M. & Akdis, C. A. TH17 cells in the big picture of immunology. J Allergy Clin Immunol 120, 247-54 (2007).
17. Ouyang, W., Kolls, J. K. & Zheng, Y. The biological functions of T helper 17 cell effector cytokines in inflammation. Immunity 28, 454-67 (2008).
18. Ye, P. et al. Requirement of interleukin 17 receptor signaling for lung CXC chemokine and granulocyte colony-stimulating factor expression, neutrophil recruitment, and host defense. J Exp Med 194, 519-27 (2001).
19. Hellings, P. W. et al. Interleukin-17 orchestrates the granulocyte influx into airways after allergen inhalation in a mouse model of allergic asthma. Am J Respir Cell Mol Biol 28, 42-50 (2003).

Chapter 6

Hypersensitivity Response to *Aspergillus fumigatus*: Pathogenesis of Pulmonary Arterial Remodeling

INTRODUCTION

Rationale

Emerging evidence suggests that chronic pulmonary inflammation associated with allergic airway disease (AAD) could represent a novel pathway for the pathogenesis of pulmonary arterial remodeling. In asthma patients, bronchial arteries exhibited an increase in intimal area, associated with smooth muscle proliferation and calcification of the elastica, and a corresponding decrease in luminal area[1]. In a murine model, recent data indicated that a prolonged T_H2 cell-mediated immune response to inhaled soluble antigen induced remodeling of pulmonary muscular arteries[2]. Another murine study demonstrated increased proliferation by various cellular components of small pulmonary arteries in the context of acute allergic inflammation[3]. Remodeling of small-to-medium-sized muscular arteries in the lung is central to the pathogenesis of pulmonary arterial hypertension (PAH). PAH is a disease with considerable morbidity and mortality owing to increased pressure within the pulmonary vasculature that can lead to right-sided heart failure. Chronic inflammation may play a role in the pathogenesis of PAH[4]. In Chapter 5, chronic exposure to viable *A. fumigatus* conidia resulted in persistent pulmonary inflammation.

Hypothesis

Immunopathological alterations in pulmonary arterial anatomy and physiology will result from chronic inflammation in the lung promoted by repeated, weekly inhalation of viable *A. fumigatus* conidia.

Objectives

1. To determine the association between the histopathogenesis of pulmonary arterial remodeling and the inflammatory response to viable *A. fumigatus* conidia during continued exposure.
2. To determine the extent of pathophysiological alterations in pulmonary circulation after chronic exposure to conidia.
3. To determine the necessity for $CD4^+$ T cell involvement in the pathogenesis of alterations in pulmonary artery anatomy and physiology after chronic exposure to conidia.

RESULTS

To determine if pathological alterations to pulmonary artery anatomy and physiology resulted from chronic allergic airways inflammation a kinetic study was performed on mice exposed weekly to viable *A. fumigatus* conidia for a total of 0, 2, 4 or 8 exposures. Using this protocol for exposure, the strength and character of the hypersensitivity response was measured previously by the analysis of bronchoalveolar lavage (BAL) contents (see Chapters 3, 4 and 5). In this study, the extent and composition of the cellular response was measured after leukocytes were recovered from the whole lung in order to sample all lung regions, including the perivascular area (Figure 6-1). Significant increases in total lung leukocytes were recorded after 4 or 8 exposures. In each case, the number of cells had more than doubled compared to the number of cells present in untreated mice.

Traditional leukocyte differential counts were performed on cells recovered form the lung (Figure 6-2). The number of macrophages was increased slightly after 4 and 8 exposures and decreased slightly after 2 exposures. There was a consistent increase in neutrophils throughout the period of study to roughly double the number found in untreated mice. Increased numbers of lymphocytes were present in the lung, particularly at the later two time points. The number of eosinophils increased significantly, many-fold higher than background, peaked after 4 exposures, and declined to approximately half the peak-level after 8 exposures. These data indicate that repeated exposure to conidia resulted in

persistent, but dynamic, allergic pulmonary inflammation. These data were similar to the data generated by analysis of BAL cells.

The inflammatory response to *A. fumigatus* induced substantial remodeling of small-to-medium-sized muscular arteries in the lung. Large pulmonary arteries and all pulmonary veins were not affected (see Appendix 2, Figure A2-9 and Figure 6-7). The remodeling process was progressive over the period of inflammation studied. Histological sections of lungs were analyzed after staining with H&E, anti-α smooth muscle actin (α-SMA) antibody, Masson's trichrome, and Verhoeff's-van Giesen's. At the conclusion of the chronic exposure period, the cellularity of the arterial walls was markedly increased, and the arterial lumen was oftentimes severely occluded (Figure 6-3). Multiple rows of structural-support cells, containing spindle-shaped nuclei, were apparent in the fully remodeled arteries (Figure 6-3). Intermediate stages of remodeling were appreciated after two and four exposures. During the intermediate period, nucleated cells accumulated on the luminal side of the arteries (Figure 6-3). Cells, probably smooth muscle cells and/or myofibroblasts, that were fully incorporated into the arterial wall after chronic exposure stained positive for α-smooth muscle actin (Figure 6-4). In contrast, cells associated with the arterial lumen during intermediate remodeling had primarily round nuclei and did not stain positive for α-smooth muscle actin (Figure 6-4).

Fibrosis of the fully remodeled arterial walls was severe as evidenced by a dense network of extracellular matrix material, probably collagen, that stained

with Masson's trichrome (Figure 6-5). On the other hand, fibrosis of the arterial wall was not extensive at the intermediate stages of remodeling (Figure 6-5).

Based on examination of elastin staining with Verhoeff's-van Giesen's, additional layers of cells in fully remodeled arteries were positioned on the luminal side of the interna elastica, indicative of neointimal formation (Figure 6-6). The elastic basement membranes were difficult to visualize in many remodeled arteries, probably because they were disrupted in the pathological process. However, it was concluded that neointimal formation was part of the remodeling spectrum based on the visualization of the interna elastica in a fraction of vessels.

The muscularization of small-to-medium-sized arteries throughout the lungs was quite extensive (Figure 6-7). Whole organ histopathological examination of lungs suggested that remodeling developed primarily in inflamed areas of the lung. Hyphal invasion of the arterial walls by the fungus was not detected with GMS stain though background staining of affected arteries was noted (see Appendix 2, Figure A2-10).

Our previous data indicated that $CD4^+$ T cells mediated the acute allergic inflammatory response to repeated inhalation of *A. fumigatus* conidia (see Chapter 4). To determine the role of $CD4^+$-mediated inflammation on the arterial pathology detected with chronic exposure, one group of mice was treated with anti-CD4 antibody throughout the period of eight exposures to conidia. Based on histological examination of the lung, the absence of $CD4^+$ T resulted in a severely attenuated inflammatory response (Figure 6-8).

In order to quantify the extent of lumen narrowing, morphometric analysis was undertaken (Figure 6-9). Arteries were selected from the lungs in random fashion using an automated microscope apparatus. The cross-sectional areas of the artery and the patent lumen were measured in a blinded fashion. Chronic exposure resulted in a significantly decreased ratio of patent lumen to total artery cross-sectional areas. In untreated mice, the lumen area was 58% ± 12% (mean ± SD). After eight exposures, the lumen area was reduced to 29% ± 14%. Anti-CD4 treatment throughout the period of exposure inhibited some, but not all, of the arterial remodeling. After eight exposures in the absence of $CD4^+$ cells, the lumen area was 40% ± 12%. In the *A. fumigatus*-exposed, anti-CD4-treated group, the luminal patency was significantly greater than that of the *A. fumigatus*-exposed group but significantly reduced compared to the untreated group. Anti-CD4 treatment protected the *A. fumigatus*-exposed mice from the most severe narrowing as evidenced by the relative paucity of arteries with less than 25% lumen area in the doubly treated group. These data suggest that $CD4^+$ T cells participated in the pathogenesis of arterial remodeling, but that some degree of remodeling was $CD4^+$ T cell-independent.

Significant pulmonary arterial lumen narrowing can lead to increased pulmonary arterial pressure. The systolic pressure within the right ventricle was measured in order to gauge pulmonary arterial pressure (Figure 6-10). In ventilated mice, the thoracic cavity was dissected, and a probe was inserted into the beating right ventricle. Mice with chronic inflammation did not exhibit a significant increase in pulmonary arterial pressure, but a higher range of

pressures was measured for mice within this group. The range of pressures recorded for untreated mice was 12-34 cm H_2O. The range of pressures recorded for mice with chronic pulmonary inflammation was 19-48 cm H_2O. In the absence of $CD4^+$ cells, right ventricular systolic pressure after chronic exposure was similar to that for untreated mice.

Increased pulmonary arterial pressure places extra burden on the muscle of the right ventricle and, over time, results in hypertrophy of the right ventricle. Chronic inflammation induced by continued exposure to *A. fumigatus* conidia did not lead to an increase in the mass of the right ventricle relative to the mass of the left ventricle and septum (Figure 6-11).

Chronic hypoxemia can induce arterial remodeling and pulmonary hypertension. It is very difficult to directly measure blood gases in mice. Therefore, the blood hemoglobin was measured as a surrogate marker of chronic hypoxemia (Figure 6-12). There were no differences between the blood hemoglobin levels in the various groups of mice, so evidence for compensation for chronic hypoxemia was not detected.

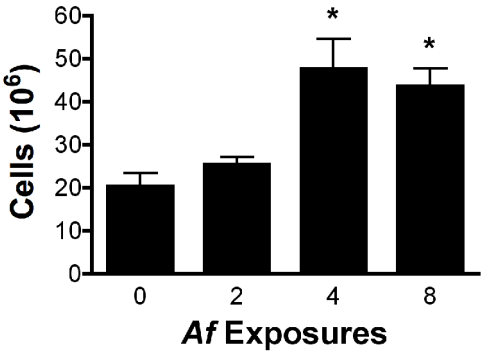

Figure 6-1. Leukocytes accumulate in the lung after several, repeated exposures to *A. fumigatus* conidia.
Leukocytes were recovered from the lung after mechanical disruption, enzymatic digestion and enrichment by a density gradient, as described in the methods. Lungs were harvested 24h after the final weekly exposure to *A. fumigatus* conidia, as indicated on the x-axis label. Cells from individual mice were enumerated under a microscope using a hemacytometer. The bar graph displays the mean (+SEM) number of cells recovered per mouse (n=6 per group). All data for this experiment was collected at the same time. These data are similar to independent experiments that compared each *A. fumigatus* group (2, 4 or 8 exposures) to an untreated control group. *$p < 0.01$ compared to 0 exposures and $p < 0.05$ compared to 2 exposures

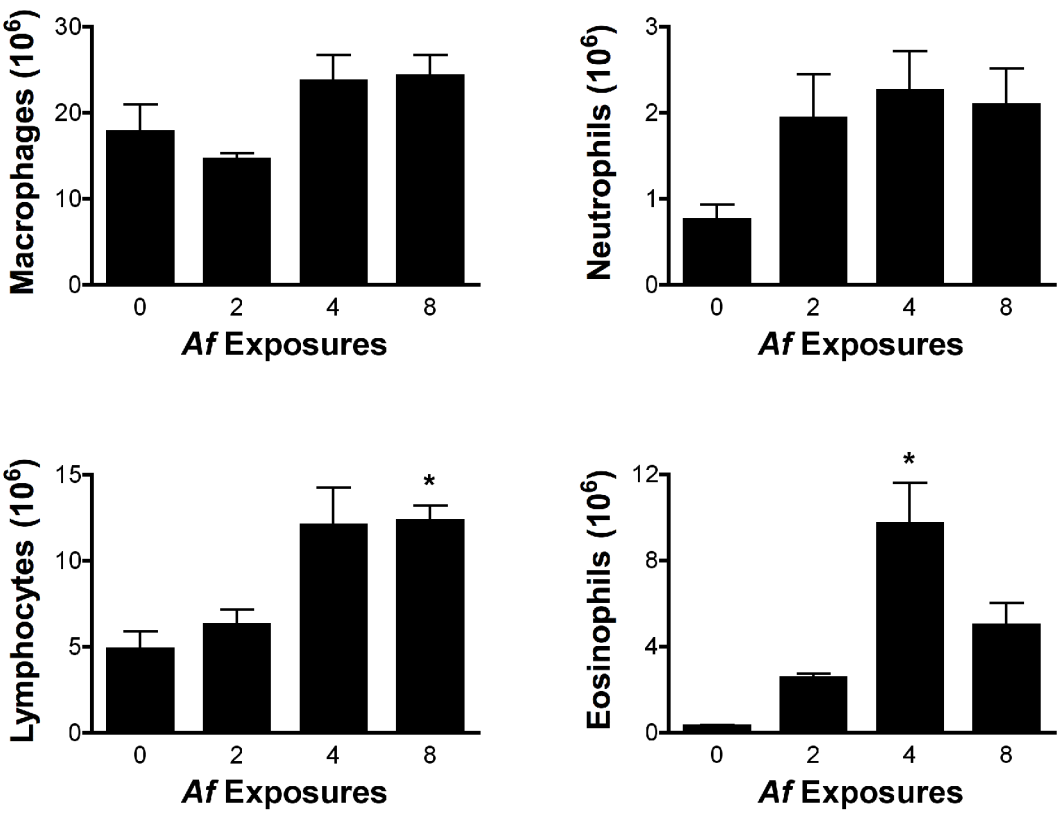

Figure 6-2. A dynamic pattern of leukocyte subset accumulation results from repeated exposures.
As described previously, lung leukocytes were recovered 24h after the final weekly exposure to *A. fumigatus* conidia. Leukocyte differential analyses were performed on individual samples using standard morphological criteria, as described in the methods. The bar graph displays the mean (+SEM) number of cells for each leukocyte subset recovered per mouse (n=6 per group). *$p < 0.05$ compared to 0 and 2 exposures (Lymphocytes); $p < 0.01$ compared to 0 and 2 exposures (Eosinophils)

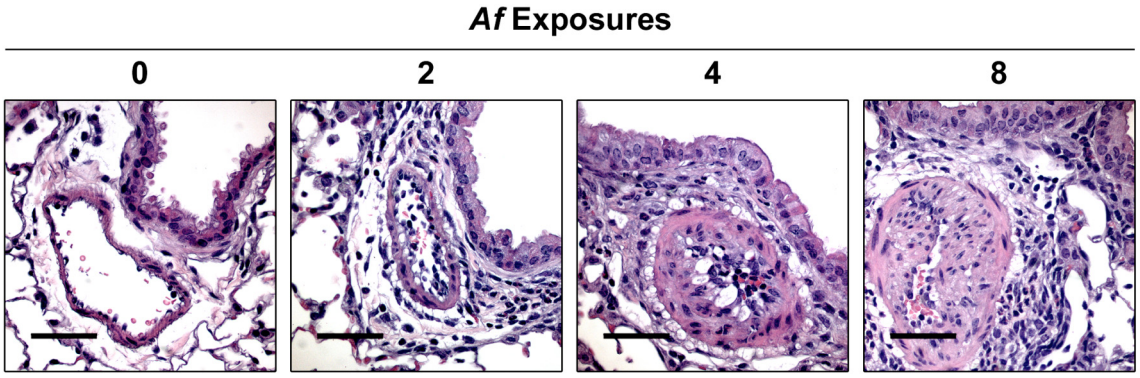

Figure 6-3. Substantial remodeling causes lumen narrowing and occlusion of small- to medium-sized muscular pulmonary arteries after long-term, repeated exposure.
Histological sections of lung tissues were stained with H&E. Representative photomicrographs include medium-sized muscular arteries adjacent to conducting airways. Images depict the extent of arterial remodeling present in an untreated sample (0) and 24h after the second, fourth or eighth weekly exposures (2, 4 and 8, respectively). Black bars are 50μm in length.

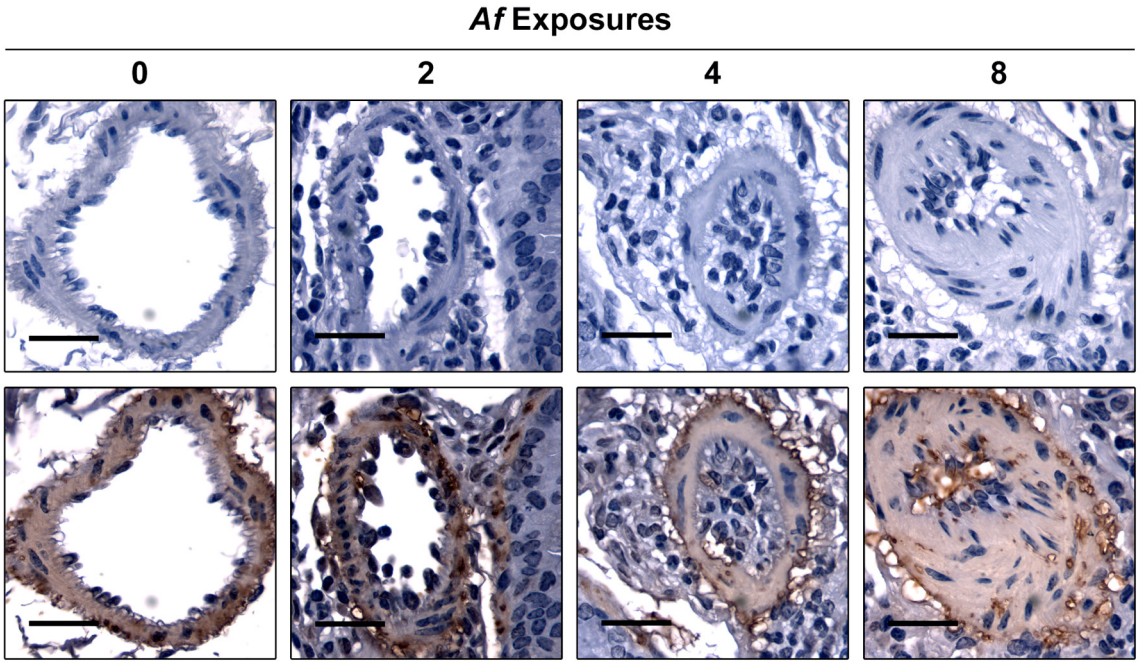

Figure 6-4. Smooth muscle cell hyperplasia is a component of arterial thickening.
As described in the methods, histological sections of lung tissue were stained with standard immunohistochemistry techniques in order to identify smooth muscle cells, which are stained brown. The bottom row contains sections stained with anti-α smooth muscle actin and the appropriate secondary antibody while the top row contains adjacent sections stained with secondary antibody only. Representative photomicrographs include medium-sized muscular arteries adjacent to conducting airways. Images depict the extent of muscularization of the arteries present in an untreated sample (0) and 24h after the second, fourth or eighth weekly exposures (2, 4 and 8, respectively). Black bars are 20μm in length.

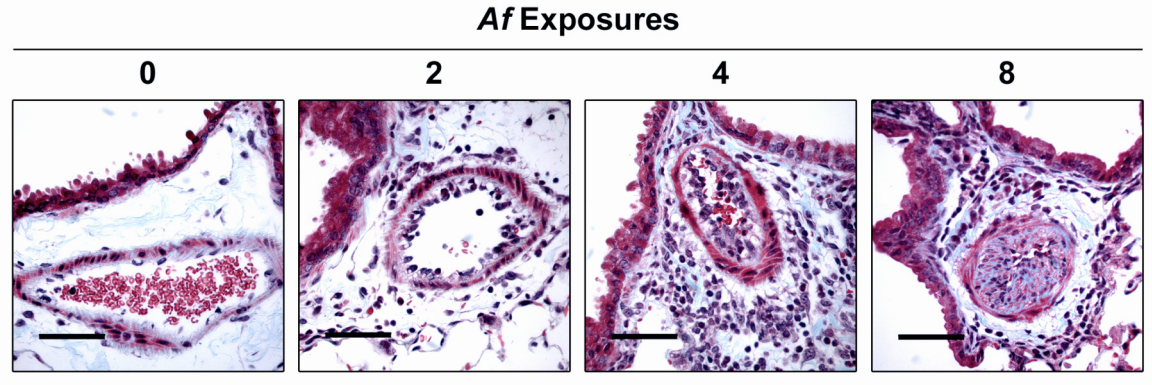

Figure 6-5. Deposition of extracellular matrix material follows the luminal accumulation of nucleated cells during arterial remodeling.
Histological sections of lung tissues were stained with Masson's trichrome in order to detect collagen, which is stained blue. Representative photomicrographs include medium-sized muscular arteries adjacent to conducting airways. Images depict the extent of collagen-containing, extracellular matrix deposition in the walls of the muscular arteries present in an untreated sample (0) and 24h after the second, fourth or eighth weekly exposures (2, 4 and 8, respectively). Black bars are 50μm in length.

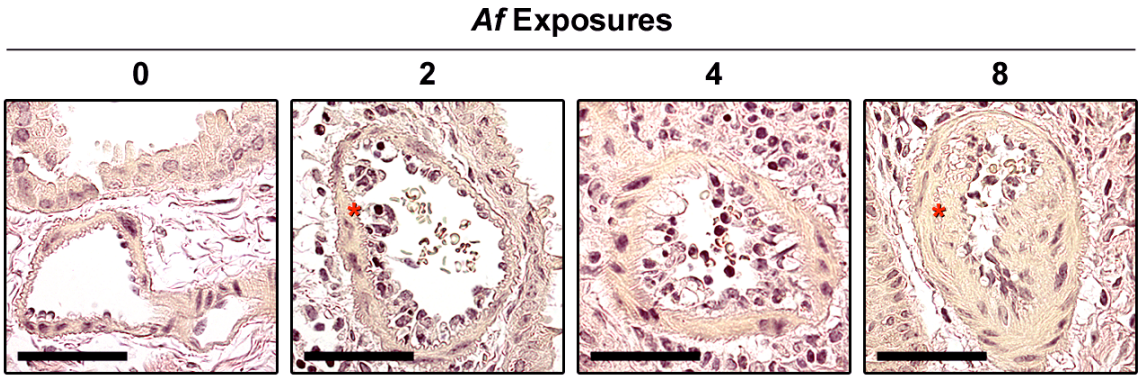

Figure 6-6. Neointimal formation contributes to arterial remodeling. Histological sections of lung tissues were stained with Verhoeff's-van Giesen's in order to visualize elastin. Representative photomicrographs include medium-sized muscular arteries adjacent to conducting airways. Images depict the localization of remodeling relative to the elastic basement membranes that differentiate the layers of the arterial wall in an untreated sample (0) and 24h after the second, fourth or eighth weekly exposures (2, 4 and 8, respectively). The interna elastica is labeled with red asterisks in the 2 and 8 *Af* exposures photomicrographs. Black bars are 20μm in length.

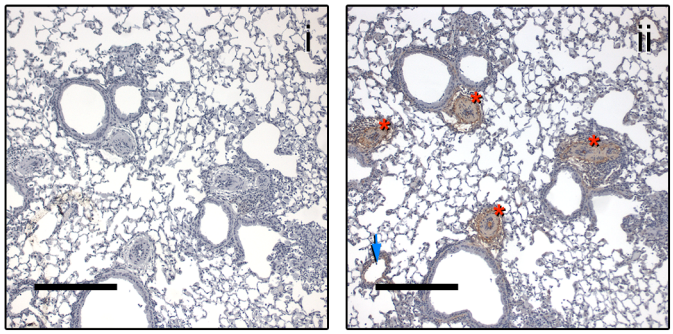

Figure 6-7. Muscularization of small- to medium-sized arteries in the lung is extensive.
Histological sections of lung tissue were stained with standard immunohistochemistry techniques as described previously. Smooth muscle cells appear brown in the section stained with anti-α smooth muscle actin (ii), but not in the adjacent control section stained with secondary antibody only (i). Representative photomicrographs highlight the extent of artery involvement (red asterisks). Notice that unaffected veins appear in the upper right and lower left corners of the field (blue arrow at lower left). Black bars are 200μm in length.

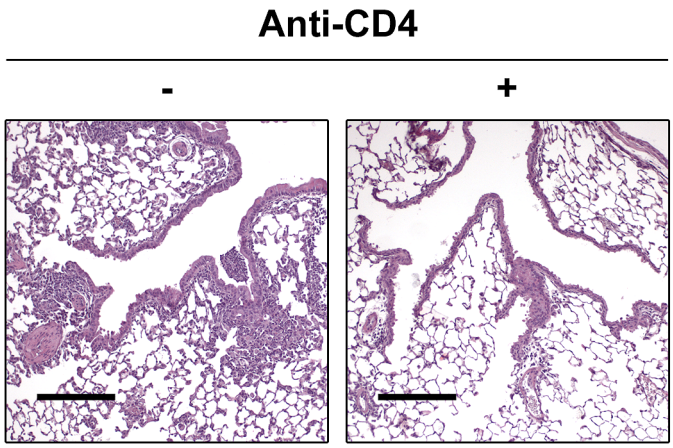

Figure 6-8. The absence of $CD4^+$ T cells results in severely attenuated inflammation of the lung.
Mice in both groups were exposed to *A. fumigatus* eight times, and not treated or treated with anti-CD4, as described in the methods. Histological sections of lung tissues stained were with H&E. Representative micrographs include terminal bronchioles. Black bars are 200μm in length.

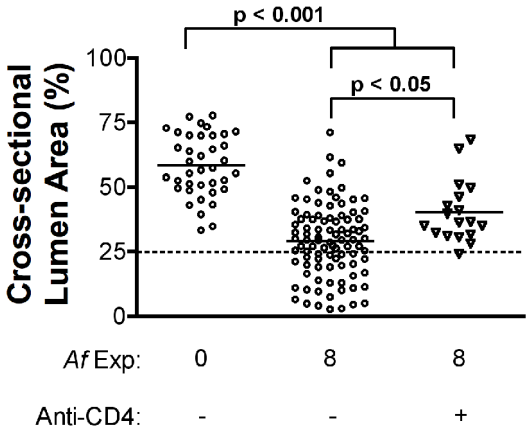

Figure 6-9. Arterial remodeling from repeated exposure to conidia results in significant lumen narrowing and is mediated at least in part by $CD4^+$ T cells.

Morphometric analyses were performed on histological sections of lung tissues in order to quantify the extent of arterial lumen narrowing. Lung samples were collected from mice exposed or not to *A. fumigatus* 8 times at weekly intervals and treated or not with depleting anti-CD4 antibody throughout the experiment. An automated set-up was used to select random fields of the left lung from each sample and all muscular arteries obtained were measured, as described in the methods. The data are presented as the cross-sectional area of the lumen divided by the total cross-sectional area of the vessel for all vessels with a length-to-width ratio less-than-or-equal-to 2.5, thereby excluding tangential artery sections. Also, very small and large arteries were excluded, as explained in the methods. These data were collected in two independent experiments (n=4 per group per experiment; except n=2-3 per group per experiment for the αCD4-treated group). Each artery is represented by a symbol on the scatter plot, and the mean for each group is indicated by a horizontal line. The dashed line at the y-axis value of 25% is included to aid in the comparison between groups. The percentage of arteries at or below the y-axis value of 25% for each group left to right is 0%, 37%, and 6%. Significant differences between groups are labeled on the plot.

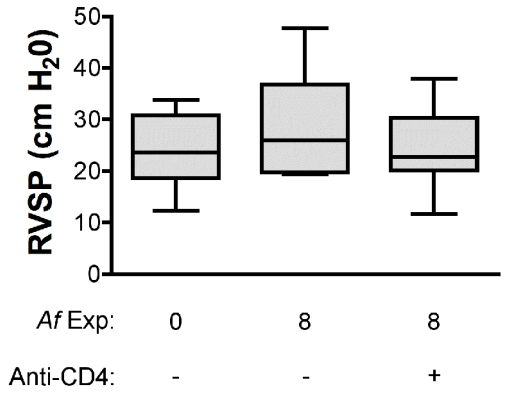

Figure 6-10. Significant pulmonary arterial remodeling does not promote pulmonary arterial hypertension.
Pulmonary arterial pressure was measured in the right ventricle on ventilated mice using an open chest technique, as described in the methods. Pressure was measured in mice exposed or not to *A. fumigatus* 8 times at weekly intervals and treated or not with depleting anti-CD4 antibody throughout the experiment. The average systolic pressure was calculated from six consecutive heart beats for each mouse. Values were only accepted from mice whose heart rate was above 300 beats per minute in order to exclude any mice exhibiting cardiopulmonary distress, as explained in the methods. Data were pooled from two independent experiments (n=4-5 per group). Boxes designate the median and the 25th and 75th percentiles, while the whiskers designate the range.

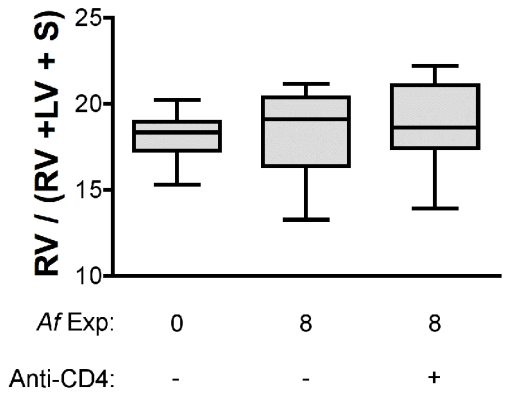

Figure 6-11. Right ventricular hypertrophy does not develop during chronic *A. fumigatus*-induced hypersensitivity disease.
The mass of the right ventricular free wall was determined in order to detect possible right ventricular hypertrophy, as described in the methods. Tissue mass was measured in mice exposed or not to *A. fumigatus* 8 times at weekly intervals and treated or not with depleting anti-CD4 antibody throughout the experiment. The heart was dissected out and the atria were removed. The right ventricular free wall was dissected away from the left ventricle and septum. The tissues were weighed, and the data are presented as the mass of the right ventricular free wall divided by the combined mass of the right and left ventricles and the septum. These data were collected in two independent experiments (n=4 per group per experiment; except n=2-3 per group per experiment for the αCD4-treated group). Boxes designate the median and the 25th and 75th percentiles, while the whiskers designate the range.

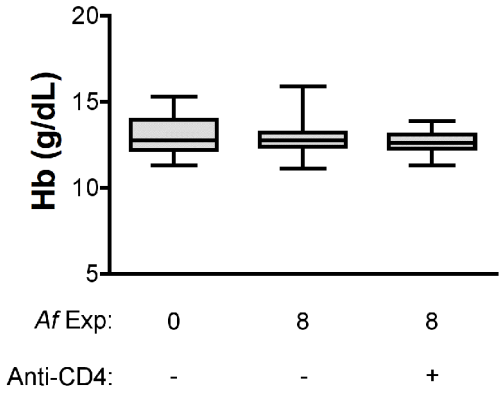

Figure 6-12. Chronic allergic airway disease does not augment blood hemoglobin levels.
The blood hemoglobin level was measured in order to detect potential compensation for chronic hypoxemia, as described in the methods. Hemoglobin levels were measured in mice exposed or not to *A. fumigatus* 8 times at weekly intervals and treated or not with depleting anti-CD4 antibody throughout the experiment. These data were collected in two independent experiments (n=4 per group per experiment; except n=2-3 per group per experiment for the αCD4-treated group). Boxes designate the median and the 25th and 75th percentiles, while the whiskers designate the range.

DISCUSSION

That data presented in this chapter demonstrated that significant remodeling of pulmonary arteries resulted from a chronic hypersensitivity response to *A. fumigatus*. The remodeled arteries had markedly increased muscularization and fibrosis of the arterial wall, and remodeled arteries showed signs of neointimal formation. $CD4^+$ T cells were required for the full manifestation of pulmonary inflammation and arterial remodeling. Though mice developed severe arterial muscularization, arterial fibrosis, and significant luminal narrowing, mice did not develop PAH as a result.

The detection of pulmonary arterial remodeling in the present study joins a few other recent reports in detailing a novel mechanism for the pathogenesis of arterial remodeling. In 2006, Green et al. reported that bronchial arterial remodeling was present in asthma patients[1]. In 2008, Rydell-Tormanen et al. reported evidence of the induction of pulmonary arterial remodeling in mice with chronic allergic airway inflammation[5]. Also in 2008, Daley et al. reported substantial pulmonary arterial muscularization developed in mice with chronic allergic airway inflammation[2]. The present study uniquely demonstrated severe and extensive remodeling that was quantified by morphometric analysis of randomly selected lung fields.

In the present study, arterial remodeling, associated with the inflammatory response to *A. fumigatus*, shared many features with arterial remodeling seen in PAH, including severe thickening of the arterial wall and narrowing of the arterial lumen. Arterial remodeling in PAH is complex, because 1) it involves all layers of

the arterial wall: intima, media and adventitia; and 2) pathological changes to all layers result in an abnormal, heterogeneous collection of cell types[6]. Another component of PAH is the disorganized proliferation of endothelial cells leading to plexiform lesions. Such lesions were not observed in mice chronically exposed to conidia, but other murine models of PAH generally fail to recapitulate this clinical feature, as well[7].

In this study, fully remodeled arteries contained multiple layers of cells expressing α-SMA, likely smooth muscle cells or myofibroblasts. In contrast, pulmonary arteries in untreated mice contained only a single layer of smooth muscle cells. Green et al. detected smooth muscle hyperplasia associated with intimal thickening in bronchial arteries of asthma patients[1]. After chronic exposure to house dust mite allergens, Rydell-Tormanen et al. measured increased proliferation of smooth muscle cells in walls of pulmonary arteries[5]. Daley et al. demonstrated severe arterial musclarization, very similar to that reported in this study, in small-to-medium-sized pulmonary arteries in allergic mice chronically exposed to OVA of *A. fumigatus* antigens[2]. Smooth muscle cell hyperplasia and myofibroblast participation are central components of arterial remodeling in PAH that facilitate augmented vasoconstriction[4].

Extracellular matrix, possibly collagen, was deposited extensively in the remodeled arterial walls after chronic exposure to viable conidia. Green et al. detected intimal fibrosis in the bronchial arteries of asthma patients[1]. Rydell-T Tormanen et al. also detected increased collagen in the intima of pulmonary

arteries in allergic mice[5]. In PAH, extensive fibrosis of the arterial wall limits the vasodilatory capacity of the vessel, contributing to increased arterial pressure.

In the present study, neointimal formation was a component of arterial remodeling with chronic inflammation as evidenced by the presence of multiple layers of cells on the luminal side of the interna elastica. In untreated mice, the intima was composed of the interna elastica and a single layer of thin endothelial cells that lined the arterial lumen. In many remodeled vessels, the interna elastica was difficult to visualize. This result may be due to the finding that elastase activity is increased during vessel remodeling, and elastase may participate in the remodeling process by degrading the elastic membranes[8]. Nonetheless, neointimal formation is a hallmark of severe pulmonary arterial hypertension[7]. Collectively, the data presented in this study indicate that pulmonary arterial remodeling associated with the chronic inflammatory response to *A. fumigatus* was severe and shared many features with the arterial remodeling described in PAH.

In the absence of $CD4^+$ T cells, pulmonary inflammation was attenuated and pulmonary arterial remodeling was significantly abrogated after chronic exposure to *A. fumigatus* conidia. However, the arterial lumens were significantly narrowed in doubly anti-CD4 treated and conidia exposed mice compared to naïve, healthy mice as determined by morphometric analysis of randomly selected vessels. Daley et al. demonstrated that arterial remodeling, as measured by a histological scoring system, was largely abolished in the absence of $CD4^+$ T cells after chronic exposure to *A. fumigatus* antigens[2]. The

discrepancy in detecting $CD4^+$ T cell-independent remodeling may lie in differences between the innate responses to *A. fumigatus* conidia and antigen extracts. Alternatively, the scoring system in the their study may not have reflected a degree of arterial lumen narrowing that was measured in our study by morphometry. Nonetheless, these data imply that $CD4^+$ T cell-mediated chronic inflammation contributes to the pathogenesis of pulmonary arterial remodeling.

In the present study, severe arterial remodeling associated with chronic allergic airway inflammation did not result in a significant increase in pulmonary arterial pressure or in right ventricular hypertrophy. Daley et al. presented arterial histopathology that was very similar to that presented in the present study, and they also did not detect pulmonary arterial hypertension or right ventricular hypertrophy as a result[2]. PAH is a complex disease involving genetic susceptibility, augmented vasoconstriction and arterial remodeling[9]. It is possible that C57BL/6 mice lack a necessary genetic predilection for the development of pulmonary arterial hypertension. Alternatively, it is possible that pulmonary hypertension did not develop in the present study because pathophysiological vasoconstriction was absent.

In conclusion, the chronic pulmonary hypersensitivity response to *A. fumigatus* promoted the pathogenesis of pulmonary arterial remodeling reminiscent of the histopathological appearance of the remodeled arteries seen in PAH. PAH is a severe disease that leads to right heart failure and death, and there is no cure for PAH. The pathogenesis of arterial remodeling in PAH is poorly understood, but mounting evidence suggests inflammation may play an

important role[10]. This study contributes to a growing recognition that inflammation associated with chronic AAD may represent a novel mechanism for pulmonary arterial remodeling. However, this study is the first to demonstrate that pulmonary arterial remodeling can result from a natural route of exposure to a natural aeroallergen in its native form. The physiologically relevant model for progressive pulmonary arterial remodeling described in this study provides future opportunities to investigate the immunopathogenesis of pulmonary arterial remodeling.

References

1. Green, F. H., Butt, J. C., James, A. L. & Carroll, N. G. Abnormalities of the bronchial arteries in asthma. Chest 130, 1025-33 (2006).
2. Daley, E. et al. Pulmonary arterial remodeling induced by a Th2 immune response. J Exp Med 205, 361-72 (2008).
3. Rydell-Tormanen, K., Uller, L. & Erjefalt, J. S. Remodeling of extra-bronchial lung vasculature following allergic airway inflammation. Respir Res 9, 18 (2008).
4. Chan, S. Y. & Loscalzo, J. Pathogenic mechanisms of pulmonary arterial hypertension. J Mol Cell Cardiol 44, 14-30 (2008).
5. Rydell-Tormanen, K., Johnson, J. R., Fattouh, R., Jordana, M. & Erjefalt, J. S. Induction of Vascular Remodeling in the Lung by Chronic House Dust Mite Exposure. Am J Respir Cell Mol Biol (2008).
6. Jeffery, T. K. & Morrell, N. W. Molecular and cellular basis of pulmonary vascular remodeling in pulmonary hypertension. Prog Cardiovasc Dis 45, 173-202 (2002).
7. Perros, F., Dorfmuller, P. & Humbert, M. Current insights on the pathogenesis of pulmonary arterial hypertension. Semin Respir Crit Care Med 26, 355-64 (2005).
8. Rabinovitch, M. Elastase and the pathobiology of unexplained pulmonary hypertension. Chest 114, 213S-224S (1998).
9. Chin, K. M. & Rubin, L. J. Pulmonary arterial hypertension. J Am Coll Cardiol 51, 1527-38 (2008).
10. Dorfmuller, P., Perros, F., Balabanian, K. & Humbert, M. Inflammation in pulmonary arterial hypertension. Eur Respir J 22, 358-63 (2003).

Chapter 7

Hypersensitivity Response to *Aspergillus fumigatus*: The Roles of the Cytokines IL-4, IFNγ, and IL-10

INTRODUCTION

Rationale

$CD4^+$ T helper (T_H) cells coordinate the adaptive immune response largely through the production of cytokines. For this reason, various T_H subsets are categorized by the cytokines they produce. T_H1 cells produce IFNγ, T_H2 cells produce IL-4, IL-5, and IL-13, and T_H17 cells produce IL-17. Likewise, $CD4^+$ regulatory T cells (T_{Reg}) are recognized for the production of cytokines with anti-inflammatory activity, including IL-10 and TGFβ. T_H cytokines are central to the promotion of particular adaptive immune response "programs" that likely developed evolutionarily to counter particular pathogenic threats. As reported Chapters 3-6, repeated exposure to *Aspergillus fumigatus* conidia resulted in the pathogenesis of $CD4^+$ T cell-dependent allergic airway disease (AAD) and pulmonary arterial remodeling. The acute and chronic phases of the inflammatory response exhibited a dynamic involvement of T_H1, T_H2, T_H17, and T_{Reg} cells.

Hypothesis

During continued exposure to viable *A. fumigatus* conidia, the IL-4-dependent T_H2 immune response mediates the immunopathogenesis of allergic airway disease and pulmonary arterial remodeling, and both the IFNγ-dependent

T_H1 response and the IL-10-dependent anti-inflammatory response antagonize the manifestation and outcome of the T_H2 response.

Objectives

1. To determine the roles for IL-4, IFNγ, and IL-10 in the pathogenesis of allergic airway disease resulting from inhalation of viable *A. fumigatus* conidia.
2. To determine the roles for IL-4, IFNγ, and IL-10 in the pathogenesis of pulmonary arterial remodeling resulting from inhalation of viable *A. fumigatus* conidia.
3. To determine the necessity for IL-5 and, by extension, eosinophil involvement in the T_H2-dependent immunopathogenesis of pulmonary arterial remodeling resulting from inhalation of viable *A. fumigatus* conidia.

RESULTS

To determine the role of critical $CD4^+$ T cell cytokines in the $CD4^+$ T cell-dependent hypersensitivity response to *A. fumigatus* prominent features of the hypersensitivity disease were evaluated in IL-4, IFNγ, and IL-10 cytokine-deficient mice. Cellular inflammation was evaluated in wild-type and cytokine-deficient mice at the peak of allergic airway response after four exposures to *A. fumigatus* conidia (Figure 7-1). Compared to C57BL/6, the number of cells recovered from the airway by BAL was similar in $IFN\gamma^{-/-}$ mice, reduced by about two-fold in $IL\text{-}4^{-/-}$ mice, and slightly reduced in $IL\text{-}10^{-/-}$ mice. As was the case for C57BL/6 mice, silver-stained histological lung sections indicated that *A. fumigatus* did not grow in the lungs of cytokine-deficient mice (see Appendix 2, Figure A2-11).

Airway leukocyte differential counts were performed on cells recovered by bronchoalveolar lavage (BAL) at the peak of allergic inflammation (Figure 7-2). Compared to C57BL/6 mice, the number of airway eosinophils was similar in $IFN\gamma^{-/-}$ mice and significantly reduced by about eight-fold in $IL\text{-}4^{-/-}$ and $IL\text{-}10^{-/-}$ mice. There were only mild and not significant differences in the numbers of other leukocyte subsets present in the airway between wild-type and cytokine-deficient mice.

As determined by flow cytometric analysis, the number of $CD4^+$ T cells recovered from the airway by BAL was slightly increased in $IFN\gamma^{-/-}$ and $IL\text{-}10^{-/-}$ mice and slightly decreased in $IL\text{-}4^{-/-}$ mice, all in comparison to C57BL/6 mice (Figure 7-3). The production of T_H cytokines was examined in wild-type and

cytokine-deficient mice by flow cytometry after a brief period of *in vitro* stimulation (Figure 7-4). Note that in previous studies, we detected cytokine production only in $CD4^+$ T cells recovered from the effector site, the airway, and not from the draining lymph nodes or spleen (see Chapter 4). The percent of $CD4^+$ T cells producing IFNγ in IL-$4^{-/-}$ mice and the percent of $CD4^+$ T cells producing IL-4 in IFN$\gamma^{-/-}$ mice were essentially equal to those populations in C57BL/6 mice. These data suggested that T_H1 and T_H2 did not counterregulate one another in wild-type mice through the production of IFNγ and IL-4, respectively. Interestingly, in IL-$10^{-/-}$ mice the frequency of IFNγ-producing T_H1 cells was similar to C57BL/6, but the frequency of IL-4-producing T_H2 cells was significantly reduced by greater than four-fold compared to C57BL/6. IL-$10^{-/-}$ mice develop spontaneous intestinal inflammation[1], but the reduced T_H2 response was detected in IL-$10^{-/-}$ mice that did not exhibit overt colitis based on histological evaluation or increased serum TNFα levels measured by ELISA (see Appendix 2, Figure A2-12). These data suggested that IL-10 contributed to the development of a T_H2 response in wild-type mice, or that in the absence of IL-10 a T_H2-inhibitory mechanism, not active in wild-type mice, was activated.

Pulmonary arterial remodeling associated with chronic inflammation was evaluated in wild-type and cytokine-deficient mice after eight weekly exposures to *A. fumigatus* conidia (Figure 7-5). In addition to IL-$4^{-/-}$, IFN$\gamma^{-/-}$, and IL-$10^{-/-}$ mice, IL-$5^{-/-}$ mice were included. IL-5 is critical for the bone marrow development and tissue recruitment of eosinophils, and IL-$5^{-/-}$ mice developed T_H2 cells but not airway eosinophilia (see Appendix 2, Figure A2-13). After chronic exposure to *A.*

fumigatus, remodeled arteries were detected in C57BL/6, IFN$\gamma^{-/-}$, and IL-5$^{-/-}$ mice but not in IL-4$^{-/-}$ and IL-10$^{-/-}$ mice. So, arterial remodeling was associated only with those mice that developed a CD4^{+} T_H2 cell response to *A. fumigatus*.

In order to quantify the extent of arterial lumen narrowing, morphometric analysis was employed (Figure 7-6). Arteries were selected from the lungs in random fashion using an automated microscope apparatus. The cross-sectional areas of the artery and the patent lumen were measured in a blinded fashion. C57BL/6 mice had significantly greater arterial lumen narrowing compared to IL-4$^{-/-}$ and IL-10$^{-/-}$ mice, but not compared to IFN$\gamma^{-/-}$ and IL-5$^{-/-}$ mice. Lumen patency in IL-4$^{-/-}$ and IL-10$^{-/-}$ mice after chronic exposure was similar to lumen patency in naïve wild-type mice as previously determined. While IFN$\gamma^{-/-}$ mice exhibited severe remodeling, the proportion of affected vessels was slightly reduced compared to C57BL/6 or IL-5$^{-/-}$ mice, suggesting that IFNγ was not required for, but may have contributed to, arterial remodeling. In all likelihood, the type of inflammation and not just the extent of inflammation influenced these results, because whole lung and perivascular inflammation in IL-10$^{-/-}$ mice were comparable in extent to that seen in C57BL/6 mice (see Appendix 2, Figure A2-14).

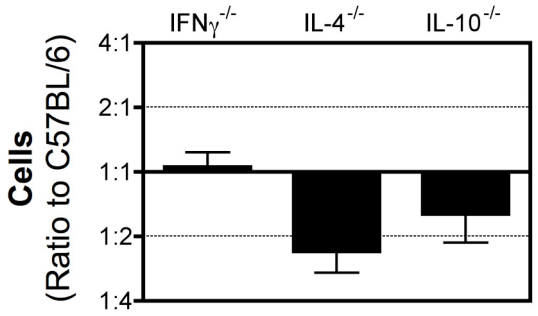

Figure 7-1. Fewer cells are recruited to the airway in the absence of IL-4, and to a lesser extent IL-10, after repeated inhalation of conidia.
Mice were exposed to *A. fumigatus* four times on a weekly basis to induce the maximal allergic airway disease. Cells were recovered by bronchoalveolar lavage and enumerated under a microscope with a hemacytometer. Each cytokine-deficient mice group was included in three independent experiments along with a C57BL/6 control mice group. The mean number of cells recovered from each cytokine-deficient mice group was normalized to the mean number of cells recovered from the control mice group in each particular experiment in order to address experiment to experiment variation in the extent of cellular inflammation. This bar graph depicts the mean (+SEM) of the ratios generated from three independent experiments per group.

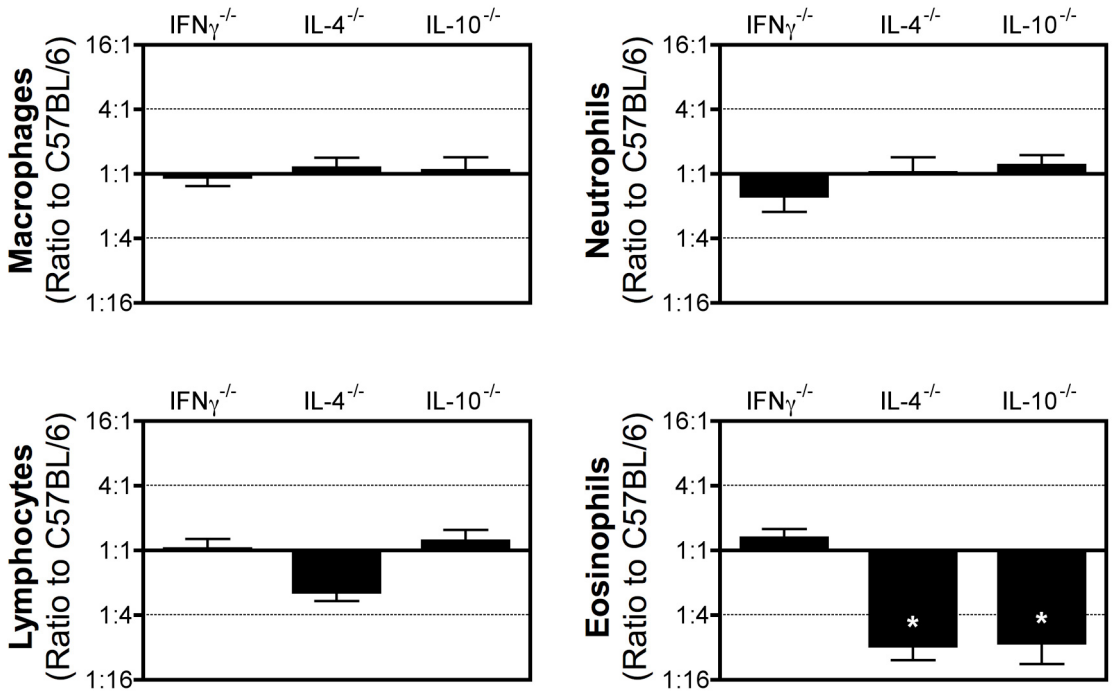

Figure 7-2. Airway eosinophilia is significantly abrogated in mice lacking IL-4 or IL-10 in comparison to either C57BL/6 or IFNγ-deficient mice. Mice were exposed to *A. fumigatus* four times on a weekly basis to induce the maximal allergic airway disease. Leukocyte differential analyses of airway cells were performed with flow cytometry, as described in Appendix 1. The mean number of cells recovered from each cytokine-deficient mice group was normalized to the mean number of cells recovered from the control mice group in each particular experiment in order to address experiment to experiment variation in the extent of cellular inflammation. This bar graph depicts the mean (+SEM) of the ratios generated for each leukocyte subset from three independent experiments per group. *$p < 0.01$ compared to IFNγ$^{-/-}$; $p < 0.05$ compared to C57BL/6 when C57BL/6 value set as 1 for each experiment

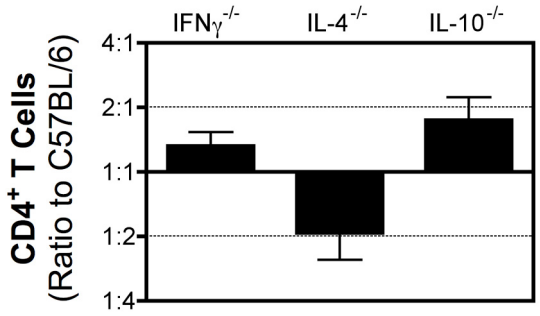

Figure 7-3. The absence of select cytokines results in slight differences in airway $CD4^+$ T cell numbers.
Mice were exposed to *A. fumigatus* four times on a weekly basis to induce the maximal allergic airway disease. $CD4^+$ T cells present in the airway cell population were identified by flow cytometric analyses. The mean number of cells recovered from each cytokine-deficient mice group was normalized to the mean number of cells recovered from the control mice group in each particular experiment in order to address experiment to experiment variation in the extent of cellular inflammation. This bar graph depicts the mean (+SEM) of the ratios generated for the number of $CD4^+$ T cells from three independent experiments per group.

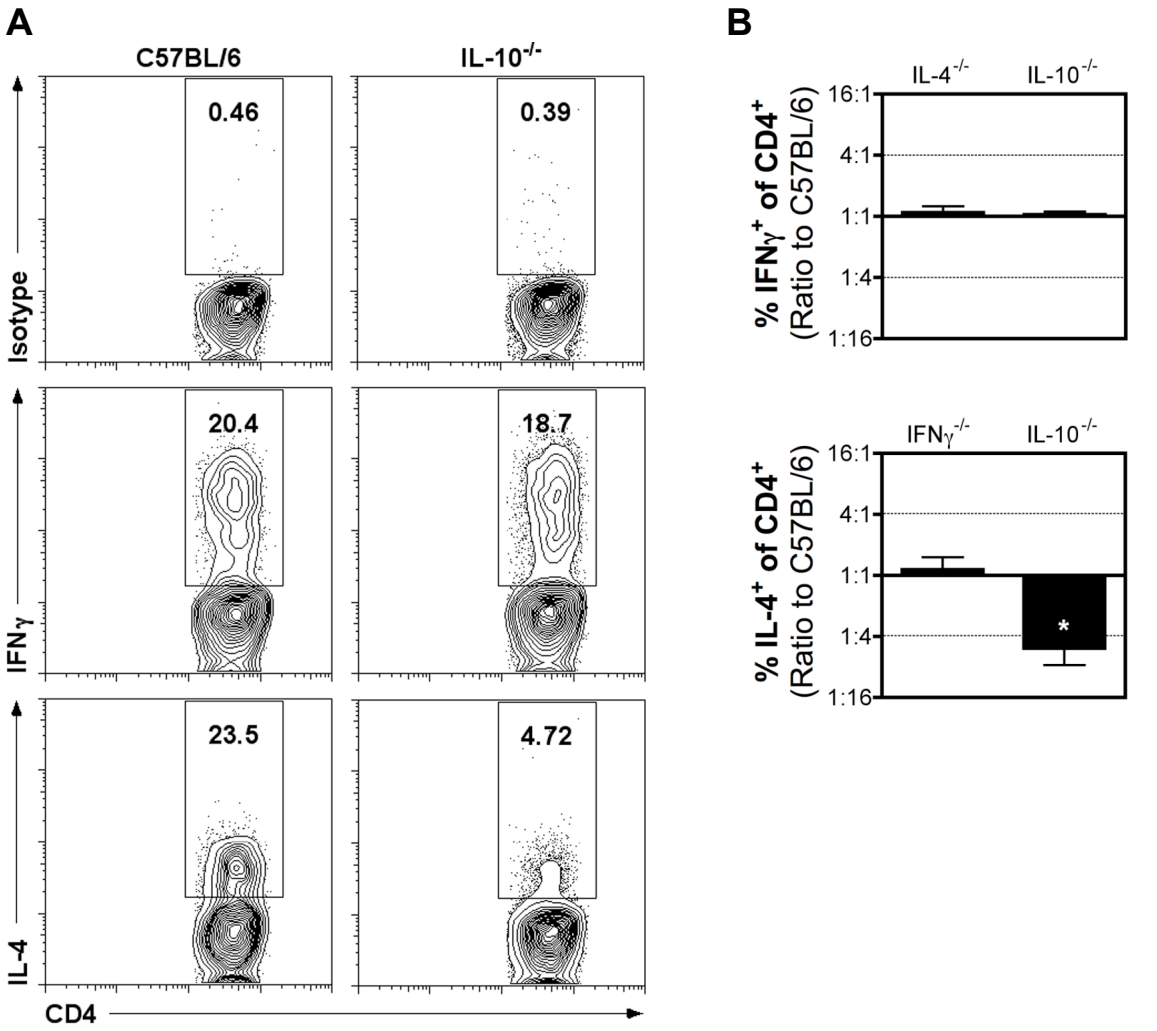

Figure 7-4. IL-4$^+$ T_H2 CD4$^+$ T cells were significantly diminished in IL-10-deficient mice.

Mice were exposed to *A. fumigatus* four times on a weekly basis to induce the maximal allergic airway disease. Airway cells were analyzed for cytokine production by flow cytometry, as detailed in the materials and methods. Pooled cells for each group were briefly activated *in vitro* for 5h with PMA and ionomycin in the presence of monensin in order to enhance cytokine production and block its secretion, respectively. A) Gated CD4$^+$ lymphocytes were analyzed for the intracellular accumulation IFNγ and IL-4 (see axes labels for density plots). Quadrants were set with intracellular isotype control-stained CD4$^+$ lymphocytes (not shown) and the percentage of CD4$^+$ lymphocytes in each quadrant is included on each plot. B) The value determined for each cytokine-deficient mice group was normalized to the value determined for the control mice group in each particular experiment in order to address experiment to experiment variation. This bar graph depicts the mean (+SEM) of the ratios generated from three independent experiments per group for the percent of CD4$^+$ T cells positive for the particular cytokine. *$p < 0.05$ compared to C57BL/6 with the value for C57BL/6 set to 1 for each experiment

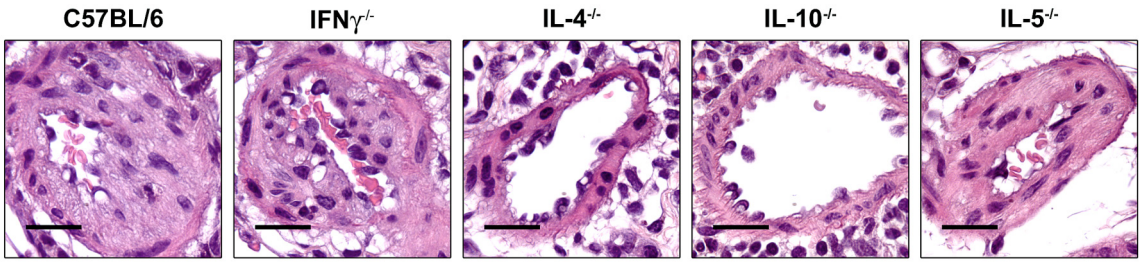

Figure 7-5. Cytokine-deficient mice that do not develop a T_H2 response to *A. fumigatus* do not exhibit arterial remodeling in the lung.
To induce arterial remodeling in the lung, mice were exposed to *A. fumigatus* once a week for eight total exposures. Histological sections of lung tissues were stained with H&E. Representative photomicrographs include medium-sized muscular arteries adjacent to conducting airways. Images depict the extent of arterial remodeling present in C57BL/6 and select cytokine-deficient mice. Black bars are 20μm in length.

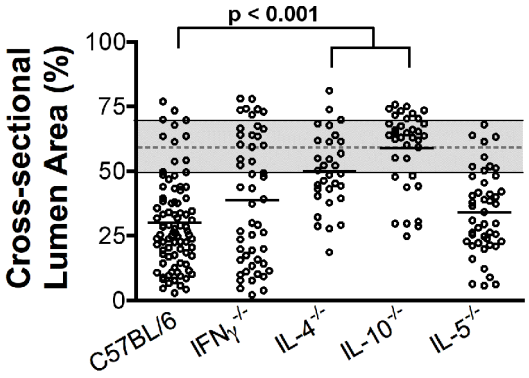

Figure 7-6. Significant arterial wall thickening is absent from cytokine-deficient mice that do not develop a T_H2 response to *A. fumigatus*.
To induce arterial remodeling in the lung, mice were exposed to *A. fumigatus* once a week for eight total exposures. In order to quantify the extent of arterial lumen narrowing, morphometric analyses were performed on histological sections of lung tissues from C57BL/6 and select cytokine-deficient mice. An automated set-up was used to select random fields of the left lung from each sample and all muscular arteries obtained were measured, as described in the methods. The data are presented as the cross-sectional area of the lumen divided by the total cross-sectional area of the vessel for all vessels with a length-to-width ratio less-than-or-equal-to 2.5, thereby excluding tangential artery sections. Also, very small and large arteries were excluded, as explained in the methods. For each cytokine-deficient mice group, data were collected from at least two independent experiments including C57BL/6 controls, and at least six mice total per group were analyzed. Each artery is represented by a symbol on the scatter plot, and the mean for each group is indicated by a horizontal line. Arteries from untreated C57BL/6 were measured in a previous study (n=38 arteries from 8 mice), and the mean and the 25th and 75th quartiles from that study are included for reference (dashed and solid lines and grey bar). Significant differences between groups are labeled on the plot.

DISCUSSION

The data presented in this chapter demonstrated that IL-4 and IL-10 were critical to the immunopathogenesis of both an AAD and pulmonary arterial remodeling that resulted from repeated inhalation of viable *Aspergillus fumigatus* conidia. In IL-$4^{-/-}$ and IL-$10^{-/-}$ mice, $CD4^+$ T_H2 cell responses were significantly reduced compared to C57BL/6 and IFN$\gamma^{-/-}$ mice. These date were consistent with a critical role for T_H2 cells in mediating the immunopathogenesis of AAD and pulmonary arterial remodeling.

The T_H2 immune response to inhaled *A. fumigatus* conidia was not affected by the presence or absence of IFNγ, a critical T_H1 cytokine. During the acute inflammatory phase in the present study, airway eosinophilia was greatly reduced in IL-$4^{-/-}$ compared to C57BL/6 mice, but airway eosinophilia was similar in IFN$\gamma^{-/-}$ and C57BL/6 mice. Also, the frequency of IL-4-producing T_H2 cells within the airway $CD4^+$ T cell population was similar in IFN$\gamma^{-/-}$ and C57BL/6 mice, and the frequency of IFNγ-producing T_H1 cells in the airway $CD4^+$ T cell population was similar in C57BL/6 and IL-$4^{-/-}$ mice. Due to a number of conflicting reports, further clarification of the impact of T_H1 cells on T_H2-mediated AAD is necessitated. In rodent models of allergic airway disease, T_H1 cells were reported to inhibit the ability of T_H2 cells to promote allergic disease in an IFNγ-dependent manner[2, 3]. Airway administration of IFNγ or IL-12, a T_H1-promoting cytokine, also diminished the manifestations of T_H2-mediated allergic airway responses[4, 5]. However, other research studies indicated that T_H1 cells augmented airway inflammation in cooperation with allergy-inducing T_H2 cells[6, 7].

Data produced in the present study suggested that T_H2 and T_H1 priming were independent events, and that a T_H1/T_H2 counterregulatory mechanism was not active.

In the present study, the T_H2 cell response in mice possessing a genetic deficiency for IL-10 was significantly attenuated compared to IL-10-sufficient control mice. On the other hand, the airway T_H1 cell response was similar in IL-$10^{-/-}$ and C57BL/6 mice. The principle role of IL-10 is to limit and ultimately terminate inflammatory responses[8]. In an animal model of AAD, IL-10 gene transfer to the airway suppressed the development of allergic airway sensitization[9]. In previous reports on the immune response to *A. fumigatus*, IL-$10^{-/-}$ mice developed an exaggerated T_H1 response to viable conidia[10], and the allergic response to antigen extracts was similar in IL-$10^{-/-}$ and wild-type mice[11]. Disparities between the preparation, dose, and frequency of *A. fumigatus* used in those studies and the present one may explain the different findings. Similar to the present study, other reports described the attenuation of T_H2 responses in IL-10-deficient mice. Those studies included investigations of a pulmonary infection with the fungus *Cryptococcus neoformans*[12], an OVA sensitization and challenge model of AAD[13], and a murine model of allergic dermatitis[14]. Clearly, IL-10 is a pleiotropic cytokine that has immunomodulatory and anti-inflammatory properties. The requirement for IL-10 in the development of T_H2 responses in certain settings, such as that described in the present study, necessitates further investigation into this functional capacity of IL-10.

In the present study, arterial remodeling did not develop in those mice that did not mount a T_H2 response to *A. fumigatus*. Severe arterial remodeling was detected in C57BL/6 and IFN$\gamma^{-/-}$ mice, but not in IL-4$^{-/-}$ and IL-10$^{-/-}$ mice. Recent studies have reported that prolonged allergic inflammation in the lung resulted in arterial remodeling, suggesting a possible pathogenic role for chronic T_H2-mediated inflammation in the process[15, 16]. Daley et al. demonstrated that arterial remodeling associated with AAD was significantly abrogated in the absence of CD4$^+$ T cells, in IL-4-deficient mice, and in mice treated with an IL-13 blockade reagent[15]. Our study confirmed the role of CD4$^+$ T cells (see Chapter 6) and IL-4 in the pathogenesis of arterial remodeling in the context of chronic AAD. The critical role of T_H2 cells in arterial remodeling was further supported by data presented here from the study of IL-10$^{-/-}$ mice. Compared to C57BL/6 mice, IL-10$^{-/-}$ mice had significantly attenuated levels of pulmonary arterial remodeling and T_H2 cells, but IL-10$^{-/-}$ mice had comparable levels of pulmonary inflammation, T_H1 cells, and T_H17 cells (see this Chapter and Appendix 2, Figures A2-14 and 15). Finally, the present study indicated that IL-5, and by extension eosinophils (see Appendix 2, Figure A2-13)[17], were not a critical component of the T_H2 response that promoted arterial remodeling. These data strongly support a pathogenic role for T_H2-mediated inflammation in the development of pulmonary arterial remodeling.

In conclusion, the study of cytokine-deficient mice elucidated the critical role of the T_H2 immune response for the immunopathogenesis of AAD and pulmonary arterial remodeling in the context of a hypersensitivity response to *A.*

fumigatus. The contribution of IL-10 was required for the development of T_H2 cells in this study, illustrating an underappreciated regulatory function of this pleiotropic cytokine. Along with several recent reports, the data presented in this study provide evidence for a novel mechanism whereby chronic T_H2-mediated allergic pulmonary inflammation induces arterial remodeling. These observations should stimulate further investigation into the immunopathogenesis of AAD and pulmonary arterial remodeling.

References

1. Kuhn, R., Lohler, J., Rennick, D., Rajewsky, K. & Muller, W. Interleukin-10-deficient mice develop chronic enterocolitis. Cell 75, 263-74 (1993).
2. Cohn, L., Homer, R. J., Niu, N. & Bottomly, K. T helper 1 cells and interferon gamma regulate allergic airway inflammation and mucus production. J Exp Med 190, 1309-18 (1999).
3. Huang, T. J. et al. Allergen-specific Th1 cells counteract efferent Th2 cell-dependent bronchial hyperresponsiveness and eosinophilic inflammation partly via IFN-gamma. J Immunol 166, 207-17 (2001).
4. Gavett, S. H. et al. Interleukin 12 inhibits antigen-induced airway hyperresponsiveness, inflammation, and Th2 cytokine expression in mice. J Exp Med 182, 1527-36 (1995).
5. Lack, G. et al. Nebulized IFN-gamma inhibits the development of secondary allergic responses in mice. J Immunol 157, 1432-9 (1996).
6. Hansen, G., Berry, G., DeKruyff, R. H. & Umetsu, D. T. Allergen-specific Th1 cells fail to counterbalance Th2 cell-induced airway hyperreactivity but cause severe airway inflammation. J Clin Invest 103, 175-83 (1999).
7. Randolph, D. A., Stephens, R., Carruthers, C. J. & Chaplin, D. D. Cooperation between Th1 and Th2 cells in a murine model of eosinophilic airway inflammation. J Clin Invest 104, 1021-9 (1999).
8. Moore, K. W., de Waal Malefyt, R., Coffman, R. L. & O'Garra, A. Interleukin-10 and the interleukin-10 receptor. Annu Rev Immunol 19, 683-765 (2001).
9. Stampfli, M. R. et al. Interleukin-10 gene transfer to the airway regulates allergic mucosal sensitization in mice. Am J Respir Cell Mol Biol 21, 586-96 (1999).
10. Del Sero, G. et al. Antifungal type 1 responses are upregulated in IL-10-deficient mice. Microbes Infect 1, 1169-80 (1999).
11. Grunig, G. et al. Interleukin-10 is a natural suppressor of cytokine production and inflammation in a murine model of allergic bronchopulmonary aspergillosis. J Exp Med 185, 1089-99 (1997).
12. Hernandez, Y. et al. Distinct roles for IL-4 and IL-10 in regulating T2 immunity during allergic bronchopulmonary mycosis. J Immunol 174, 1027-36 (2005).
13. Yang, X., Wang, S., Fan, Y. & Han, X. IL-10 deficiency prevents IL-5 overproduction and eosinophilic inflammation in a murine model of asthma-like reaction. Eur J Immunol 30, 382-91 (2000).
14. Laouini, D. et al. IL-10 is critical for Th2 responses in a murine model of allergic dermatitis. J Clin Invest 112, 1058-66 (2003).
15. Daley, E. et al. Pulmonary arterial remodeling induced by a Th2 immune response. J Exp Med 205, 361-72 (2008).
16. Rydell-Tormanen, K., Johnson, J. R., Fattouh, R., Jordana, M. & Erjefalt, J. S. Induction of Vascular Remodeling in the Lung by Chronic House Dust Mite Exposure. Am J Respir Cell Mol Biol (2008).

17. Foster, P. S., Hogan, S. P., Ramsay, A. J., Matthaei, K. I. & Young, I. G. Interleukin 5 deficiency abolishes eosinophilia, airways hyperreactivity, and lung damage in a mouse asthma model. J Exp Med 183, 195-201 (1996).

Chapter 8

Summary, Interpretation, Critical Review, and Future Directions

Summary

In this study, repeated inhalation of viable *A. fumigatus* conidia resulted in a hypersensitivity response after several weeks of exposure. Twenty-four hours after the first exposure an innate immune response appeared, characterized by the production of TNFα and the recruitment of neutrophils. In the absence of fungal growth, the magnitude of the inflammatory response increased significantly after the third exposure, 15 days after the initial exposure, and many prototypical features of an allergic airway response were evident. These features included the presence of peribronchial and peribronchiolar cellular infiltrates, significant airway eosinophilia, the presence of T_H2 cytokines in the airway, the increased production of IgE, and goblet cell metaplasia with mucus hypersecretion. In spite of the characteristic allergic airway disease (AAD), the mice exposed repeatedly to *A. fumigatus* did not exhibit increased airway hyperreactivity (AHR).

Coincident with the onset of the AAD, the number of $CD4^+$ T cells in the airway increased significantly. Activated, cytokine-producing effector $CD4^+$ T_H cells were present in the airway, but they were not detected in the draining lymph nodes or spleen. In the absence of $CD4^+$ T cells, the allergic airway response was severly attenuated, including airway eosinophilia and BALF T_H2 cytokine levels. However, the innate immune response remained intact, as evidenced by

neutrophil recruitment and TNFα secretion, and *A. fumigatus* did not grow in the lungs. The adoptive transfer of *A. fumigatus*-primed, but not naïve, $CD4^+$ T cells augmented the development of the AAD.

Pulmonary inflammation persisted with chronic exposure to viable *Aspergillus fumigatus* conidia. Several parameters of the AAD were similar in severity during the acute and chronic inflammatory phases, including the number of leukocytes present in the airways, the level of serum total IgE, and the presence of mucus hyperproduction. While the total number of $CD4^+$ T cells in the airways was similar at both time points, the proportions of $CD4^+$ T_H subsets were not static. After four exposures to conidia, the frequencies of cytokine-producing T_H1, T_H2, and T_H17 cells (~10-15% of total $CD4^+$ T cells) were roughly equivalent. However, after eight exposures, the frequency of T_H17 cells was significantly increased, and the frequency of T_H2 cells was moderately decreased. Goblet cell metaplasia and mild peribronchial fibrosis were detected at both time points, but remodeling was not progressive. In spite of persistent inflammation, chronic exposure to *A. fumigatus* conidia did not result in increased AHR.

The chronic hypersensitivity response to *Aspergillus fumigatus* did result in severe remodeling of pulmonary arteries and in significant narrowing of arterial lumens. The remodeled arterial walls were muscularized, fibrotic, and accompanied by signs of neointimal formation. $CD4^+$ T cells were required for the full manifestation of pulmonary inflammation and arterial remodeling. Though

mice developed severe arterial muscularization, arterial fibrosis, and significant luminal narrowing, mice did not develop pulmonary hypertension as a result.

In IL-$4^{-/-}$ and IL-$10^{-/-}$ mice, $CD4^+$ T_H2 cell responses were significantly reduced compared to C57BL/6 and IFN$\gamma^{-/-}$ mice. IL-$4^{-/-}$ and IL-$10^{-/-}$ mice did not exhibit acute airway eosinophilia or chronic pulmonary arterial remodeling. Like C57BL/6 mice, IFN$\gamma^{-/-}$ and IL-$5^{-/-}$ mice did develop remodeled arteries, but eosinophils were not a component of the T_H2 response in IL-$5^{-/-}$ mice.

Interpretation

$CD4^+$ T_H2 cells were primed by respiratory exposure to *A. fumigatus* conidia and mediated an allergic hypersensitivity response to *A. fumigatus* conidia upon re-exposure. Therefore, this study introduces a novel, physiologically relevant murine model for the study of allergic airway disease. Prolonged exposure to *A. fumigatus* conidia resulted in chronic $CD4^+$ T_H2 cell activity that coordinated the pathogenic remodeling of pulmonary arteries. The T_H2-mediated pathogenesis of arterial remodeling did not require eosinophils, and a component of the pathogenic response was $CD4^+$ T cell-independent. These data support and further an emerging, novel pathway for the pathogenesis of pulmonary arterial remodeling, the primary abnormality in pulmonary arterial hypertension, a severe and poorly understood human disease. IL-10 was required to support the IL-4-dependent induction of the allergic T_H2 response. This is further evidence of a role for IL-10 in the induction of T_H2 immunity separate from the well-defined anti-inflammatory role of IL-10. A T_H17 response

was positively correlated with continued exposure to *A. fumigatus* conidia, but the T_H17 response did not mediate pulmonary arterial remodeling in the absence of a T_H2 response. These data advance the nascent understanding of the physiological role(s) of T_H17 cells.

Critical Review

In all likelihood, the dose and frequency of exposure to viable *A. fumigatus* conidia utilized in this study had a major impact on the strength and character of the inflammatory response. Therefore, the data presented are representative of the response to this dose and frequency of conidia, and should not be generalized to *A. fumigatus* without regard to this fact.

Due in large part to the complex nature of this living, eukaryotic allergen, antigen-specific adaptive immune responses were not measured in this study. The growth of the fungus in cultures generated from conidia-exposed tissues hampered *in vitro* studies, although voriconazole was not used in this study and is reported to prevent fungal growth[1]. Commercially available *A. fumigatus* antigens induced low or undetectable levels of cytokines in co-culture experiments with secondary lymphoid tissues, and serum antibody levels were low to undetectable when measured against the antigens. Because purified antigens were produced from a growing fungal mycelium, it is possible that the purified antigens did not contain high concentrations of the antigens that provoked a response after inhalation of conidia *in vivo*.

In spite of the presence of multiple features of AAD, mice repeatedly exposed to conidia did not exhibit a significant increase in airway hyperreactivity (AHR). While mice do not develop a breathing disorder similar to asthma, increased airway resistance is often demonstrated by methacholine challenge[2]. The strain of mouse used in this study, C57BL/6, is widely recognized as a low-responder strain for the manifestation of AHR[3-5]. The utility of this model of AAD for studies on the development and treatment of AHR would be enhanced by a demonstration of increased AHR in a more susceptible strain of mice.

In the present study, silver-stained histological lung sections did not reveal morphological evidence of *A. fumigatus* hyphae in the remodeled arteries though background staining was increased (see Appendix 2, Figure A2-10). *A. fumigatus* hyphae have a marked tropism for blood vessels, and angioinvasion is a component of invasive aspergillosis seen in immunocompromised individuals[6]. Angioinvasion results in endothelial cell injury, thrombosis, and tissue infarction[7]. Endothelial cell injury and thrombosis are also features of arterial remodeling in PAH[8]. However, we never found any evidence of an infectious outcome resulting from repeated exposure to viable conidia. Therefore, it cannot be entirely discounted that the tropism for blood vessels attributed to *A. fumigatus* was involved in the pathogenesis of arterial remodeling, but angioinvasion likely was not involved.

Severe pulmonary arterial remodeling did not result in an elevation of pulmonary arterial pressure. Increased pulmonary arterial pressure has been measured in murine models of pulmonary arterial hypertension resulting from

chronic hypoxia or genetic modification[9-11]. Hypoxia and germline mutations affect the entire lung in a uniform manner. In the present study, many arteries were completely occluded and arterial involvement throughout the lung was extensive. Nonetheless, inflammation and arterial remodeling throughout the lung was not uniformly distributed, and irregularities in the vascular involvement may have prevented an increase in pressure for the whole system. It is also possible that remodeling did not involve critical regions along the vascular tree that promote pulmonary arterial hypertension. In a study of pulmonary arterial remodeling in response to chronic hypoxia, the authors concluded that increased vascular resistance was due to small artery muscularization and decreased vascular impedance was due to proximal artery fibrosis[12]. Finally, it is possible that the pathological process in the present study did not involve additional mediators that promote vasoconstriction or limit vasodilation.

Future Directions

- The mechanism of $CD4^+$ T_H2 cell development in response to *in vivo* exposure to a respiratory allergen could be further examined in this model. Several transgenic mice were described that would be particularly useful for this study. In 2001, the Locksley group engineered mice to express enhanced green fluorescent (EGFP) protein linked to IL-4, so all IL-4-producing cells were detectable by the fluorescent marker[13]. These mice were proven extremely useful in studies on the role of IL-4 in T_H2 and allergic responses[14-22]. In 2006, *A. fumigatus*-specific, $CD4^+$ TCR-

transgenic mice were developed by the Pamer group. In response to a single intranasal dose of 1×10^7 viable conidia, *A. fumigatus*-specific $CD4^+$ T_H1, but not T_H2, cells were primed locally. These transgenic mice would be useful in the examination of the development of the $CD4^+$ T_H2 cell response described in this study. Alternatively, MHC-antigen-tetramer reagents also would be useful to follow the responding $CD4^+$ T cells.

- The mechanism by which IL-17 mediates pathological inflammation is not well understood[23]. IL-17 promotes the recruitment of neutrophils[24], and anti-IL-17 treatment simultaneously abrogated neutrophil recruitment and enhanced IL-5 production and eosinophil recruitment, in a model of AAD[25]. In the present study, chronic inflammation also was associated with a decline in T_H2 responses and pulmonary arterial remodeling. IL-23 sustains chronic T_H17 inflammatory responses, and IL-23 is composed of a unique p19 subunit and a p40 subunit that is shared with IL-12[26]. While IL-23 is not necessary for the development of T_H17 cells, IL-23-deficient ($p19^{-/-}$) mice exhibited attenuated T_H17 responses[27]. These mutant mice would be useful for an investigation of the role of T_H17 cells in the AAD to *A. fumigatus* conidia. Additionally, *in vivo* IL-17 neutralization with anti-IL-17 antibody would complement the use of IL-$23p19^{-/-}$ mice[28]. A potential pitfall of this study would be if IL-17 reduction prevents neutrophil recruitment leading to a pulmonary infection with *A. fumigatus*. In this event, *A. fumigatus* antigens, which also promoted pulmonary arterial

remodeling in a chronic AAD model, would be substituted for viable conidia.

- Noverr et al. demonstrated that disruptions in the gastrointestinal microbiota influenced the allergic response to *A. fumigatus* conidia[29, 30]. IL-10$^{-/-}$ mice develop colitis that is dependent of the presence of the microbiota and is associated with enhanced production of IL-12 and IL-23[31, 32]. Selective production of IL-12 and IL-23 by antigen presenting cells (APC) may result in promotion of T_H1 and T_H17 responses at the expense of the T_H2 response. Experiments would test the possibility that spontaneous colitis and/or IL-12 and/or IL-23 prevented the development of the T_H2 response to *A. fumigatus* conidia. Broad spectrum antibiotic treatment limited colitis[33], and would be used to inhibiting colitis in IL-10$^{-/-}$ mice. Anti-IL-12p35, anti-IL-23p19, or anti-IL-12p40 antibodies would be used in IL-10$^{-/-}$ mice to block IL-12, IL-23, or both, respectively. Different combinations of antibiotic and antibody treatments would reveal T_H2 limiting factors that may be some combination of colitis, IL-12, and IL-23. Negative results would indicate the IL-10 works through some other direct or indirect mechanism to support the development of CD4$^+$ T_H2 cells in this model.

- Alternatively-activated macrophages (AAMϕ) are polarized during T_H2 immune responses by IL-4 or IL-13, and AAMϕ promote cell proliferation

and collagen deposition, two likely features of arterial remodeling in the present study[34]. In 2004, the Brombacher group developed macrophage/neutrophil-specific IL-4 receptor alpha-deficient mice and demonstrated that AAMϕ did not develop in these mice during prototypical T_H2 responses[35]. These mice would be useful for testing the hypothesis that AAMϕ are mediators of pathologic T_H2-driven arterial remodeling. A potential drawback to this approach is that unopposed T_H1 cytokine polarization of classically-activated macrophages may result in unexpectedly severe pulmonary inflammation. A well-controlled study with the addition of anti-IFNγ antibody might address this issue.

- In PAH patients, one study reported increased frequencies of certain polymorphisms in the fractalkine receptor, CX_3CR1[36], and another study reported increased levels of fractalkine and CX_3CR1^+ leukocytes[37]. Unlike other chemokines, endothelial cell-anchored fractalkine can mediate rapid and firm adhesion to CX_3CR1-expressing cells under high blood flow[38]. A recent study identified a novel patrolling behavior of blood monocytes, whereby $Gr1^-$ monocytes exhibited long-range crawling interactions with healthy endothelium, including that of arteries, and CX_3CR1-dependent extravasation in response to endothelial damage and tissue inflammation[39]. Interestingly, recently recruited CX_3CR1^+ monocytes rapidly differentiated into Mϕ expressing genes associated with the AAMϕ phenotype[39]. During the acute inflammatory response to *A. fumigatus*

conidia, we detected the intravascular accumulation of cells with a leukocyte appearance that preceded arterial remodeling. Anti-CX_3CR1 neutralizing antibody, administered during the period of respiratory exposure to conidia, would be used to test the role of fractalkine-CX_3CR1 interactions in mediating pulmonary arterial remodeling, after preliminary experiments detected the accumulation of CX_3CR1^+ monocytes in the arteries. If the intravascular cells were not identified as CX_3CR1^+ monocytes, laser-capture microscopy would be used to isolate the cells of interest for gene expression analysis and identification.

References

1. Rivera, A. et al. Innate immune activation and CD4+ T cell priming during respiratory fungal infection. Immunity 25, 665-75 (2006).
2. Epstein, M. M. Do mouse models of allergic asthma mimic clinical disease? Int Arch Allergy Immunol 133, 84-100 (2004).
3. Levitt, R. C. & Mitzner, W. Expression of airway hyperreactivity to acetylcholine as a simple autosomal recessive trait in mice. Faseb J 2, 2605-8 (1988).
4. Takeda, K., Haczku, A., Lee, J. J., Irvin, C. G. & Gelfand, E. W. Strain dependence of airway hyperresponsiveness reflects differences in eosinophil localization in the lung. Am J Physiol Lung Cell Mol Physiol 281, L394-402 (2001).
5. Chiba, Y., Yanagisawa, R. & Sagai, M. Strain and route differences in airway responsiveness to acetylcholine in mice. Res Commun Mol Pathol Pharmacol 90, 169-72 (1995).
6. Denning, D. W. Invasive aspergillosis. Clin Infect Dis 26, 781-803; quiz 804-5 (1998).
7. Fraser, R. S. Pulmonary aspergillosis: pathologic and pathogenetic features. Pathol Annu 28 Pt 1, 231-77 (1993).
8. Chin, K. M. & Rubin, L. J. Pulmonary arterial hypertension. J Am Coll Cardiol 51, 1527-38 (2008).
9. Steudel, W. et al. Sustained pulmonary hypertension and right ventricular hypertrophy after chronic hypoxia in mice with congenital deficiency of nitric oxide synthase 3. J Clin Invest 101, 2468-77 (1998).
10. Eddahibi, S. et al. Attenuated hypoxic pulmonary hypertension in mice lacking the 5-hydroxytryptamine transporter gene. J Clin Invest 105, 1555-62 (2000).
11. Beppu, H. et al. BMPR-II heterozygous mice have mild pulmonary hypertension and an impaired pulmonary vascular remodeling response to prolonged hypoxia. Am J Physiol Lung Cell Mol Physiol 287, L1241-7 (2004).
12. Tuchscherer, H. A., Vanderpool, R. R. & Chesler, N. C. Pulmonary vascular remodeling in isolated mouse lungs: effects on pulsatile pressure-flow relationships. J Biomech 40, 993-1001 (2007).
13. Mohrs, M., Shinkai, K., Mohrs, K. & Locksley, R. M. Analysis of type 2 immunity in vivo with a bicistronic IL-4 reporter. Immunity 15, 303-11 (2001).
14. Shinkai, K., Mohrs, M. & Locksley, R. M. Helper T cells regulate type-2 innate immunity in vivo. Nature 420, 825-9 (2002).
15. Stetson, D. B., Mohrs, M., Mallet-Designe, V., Teyton, L. & Locksley, R. M. Rapid expansion and IL-4 expression by Leishmania-specific naive helper T cells in vivo. Immunity 17, 191-200 (2002).
16. Voehringer, D., Shinkai, K. & Locksley, R. M. Type 2 immunity reflects orchestrated recruitment of cells committed to IL-4 production. Immunity 20, 267-77 (2004).

17. Mohrs, K., Wakil, A. E., Killeen, N., Locksley, R. M. & Mohrs, M. A two-step process for cytokine production revealed by IL-4 dual-reporter mice. Immunity 23, 419-29 (2005).
18. Ohmura, K., Nguyen, L. T., Locksley, R. M., Mathis, D. & Benoist, C. Interleukin-4 can be a key positive regulator of inflammatory arthritis. Arthritis Rheum 52, 1866-75 (2005).
19. Scheu, S. et al. Activation of the integrated stress response during T helper cell differentiation. Nat Immunol 7, 644-51 (2006).
20. Voehringer, D., Reese, T. A., Huang, X., Shinkai, K. & Locksley, R. M. Type 2 immunity is controlled by IL-4/IL-13 expression in hematopoietic non-eosinophil cells of the innate immune system. J Exp Med 203, 1435-46 (2006).
21. Reese, T. A. et al. Chitin induces accumulation in tissue of innate immune cells associated with allergy. Nature 447, 92-6 (2007).
22. Voehringer, D., van Rooijen, N. & Locksley, R. M. Eosinophils develop in distinct stages and are recruited to peripheral sites by alternatively activated macrophages. J Leukoc Biol 81, 1434-44 (2007).
23. Ouyang, W., Kolls, J. K. & Zheng, Y. The biological functions of T helper 17 cell effector cytokines in inflammation. Immunity 28, 454-67 (2008).
24. Ye, P. et al. Requirement of interleukin 17 receptor signaling for lung CXC chemokine and granulocyte colony-stimulating factor expression, neutrophil recruitment, and host defense. J Exp Med 194, 519-27 (2001).
25. Hellings, P. W. et al. Interleukin-17 orchestrates the granulocyte influx into airways after allergen inhalation in a mouse model of allergic asthma. Am J Respir Cell Mol Biol 28, 42-50 (2003).
26. Langrish, C. L. et al. IL-23 drives a pathogenic T cell population that induces autoimmune inflammation. J Exp Med 201, 233-40 (2005).
27. Zelante, T. et al. IL-23 and the Th17 pathway promote inflammation and impair antifungal immune resistance. Eur J Immunol 37, 2695-706 (2007).
28. Romani, L. et al. Defective tryptophan catabolism underlies inflammation in mouse chronic granulomatous disease. Nature 451, 211-5 (2008).
29. Noverr, M. C., Noggle, R. M., Toews, G. B. & Huffnagle, G. B. Role of antibiotics and fungal microbiota in driving pulmonary allergic responses. Infect Immun 72, 4996-5003 (2004).
30. Noverr, M. C., Falkowski, N. R., McDonald, R. A., McKenzie, A. N. & Huffnagle, G. B. Development of allergic airway disease in mice following antibiotic therapy and fungal microbiota increase: role of host genetics, antigen, and interleukin-13. Infect Immun 73, 30-8 (2005).
31. Kamada, N. et al. Abnormally differentiated subsets of intestinal macrophage play a key role in Th1-dominant chronic colitis through excess production of IL-12 and IL-23 in response to bacteria. J Immunol 175, 6900-8 (2005).
32. Yen, D. et al. IL-23 is essential for T cell-mediated colitis and promotes inflammation via IL-17 and IL-6. J Clin Invest 116, 1310-6 (2006).

33. Hoentjen, F. et al. Antibiotics with a selective aerobic or anaerobic spectrum have different therapeutic activities in various regions of the colon in interleukin 10 gene deficient mice. Gut 52, 1721-7 (2003).
34. Gordon, S. Alternative activation of macrophages. Nat Rev Immunol 3, 23-35 (2003).
35. Herbert, D. R. et al. Alternative macrophage activation is essential for survival during schistosomiasis and downmodulates T helper 1 responses and immunopathology. Immunity 20, 623-35 (2004).
36. Marasini, B. et al. Polymorphism of the fractalkine receptor CX3CR1 and systemic sclerosis-associated pulmonary arterial hypertension. Clin Dev Immunol 12, 275-9 (2005).
37. Balabanian, K. et al. CX(3)C chemokine fractalkine in pulmonary arterial hypertension. Am J Respir Crit Care Med 165, 1419-25 (2002).
38. Fong, A. M. et al. Fractalkine and CX3CR1 mediate a novel mechanism of leukocyte capture, firm adhesion, and activation under physiologic flow. J Exp Med 188, 1413-9 (1998).
39. Auffray, C. et al. Monitoring of blood vessels and tissues by a population of monocytes with patrolling behavior. Science 317, 666-70 (2007).

Chapter 9

Significance

In this dissertation, I tested the following hypotheses:

1. Pulmonary hypersensitivity disease will result from repeated inhalation of viable *A. fumigatus* conidia, a natural aeroallergen in its native form.
2. $CD4^+$ T cells mediate the hypersensitivity response to inhaled viable *A. fumigatus* conidia upon re-exposure.
3. Due to the inherent allergenicity of viable *A. fumigatus* conidia, chronic exposure will result in progressive pathophysiological alterations to the lungs.
4. Immunopathological alterations in pulmonary arterial anatomy and physiology will result from chronic inflammation in the lung promoted by repeated, weekly inhalation of viable *A. fumigatus* conidia.
5. During continued exposure to viable *A. fumigatus* conidia, the IL-4-dependent T_H2 immune response mediates the immunopathogenesis of allergic airway disease and pulmonary arterial remodeling, and both the IFNγ-dependent T_H1 response and the IL-10-dependent anti-inflammatory response antagonize the manifestation and outcome of the T_H2 response.

I conclude that the research presented in this dissertation producing the following significant contributions to the field:

- This study introduced a unique, physiologically relevant model of AAD. Inhalation of *A. fumigatus* conidia, a natural aeroallergen ubiquitous in the environment, promoted a $CD4^+$ T_H2 cell mediated AAD. Sensitization to this natural aeroallergen was achieved through a natural route of exposure by repeated inhalation without any form of systemic sensitization. In the absence of fungal growth or accumulation detected by silver-stained histological sections of lung, the allergic response developed after 3 exposures, appearing 15 days after the initial exposure. Prototypical features of AAD that were increased included airway IL-4-producing T_H2 cells, airway T_H2 cytokine levels, airway eosinophils, serum total IgE, and goblet cell metaplasia with mucus hyperproduction. Previous reports documented other AAD disease models that featured repeated respiratory exposure to natural allergens, including *A. fumigatus* antigen extracts, ragweed antigen extracts and house dust mite (HDM) antigen extracts, in previously unsensitized mice[1-4]. In spite of a robust AAD, mice exposed repeatedly to conidia did not develop increased airway hyperreactivity in the present study, in contrast to the models that relied on antigen extracts mentioned above. In terms of *A. fumigatus*, conidia represent the likeliest form of the fungus encountered in the environment.

- This study provided novel insight into the mechanism by which respiratory antigens promote the differentiation of $CD4^+$ T_H2 cells. Activated, IL-4-producing effector $CD4^+$ T_H2 cells, implicated in the allergic response to inhaled conidia, were found exclusively in the airway and not in the lung-draining lymph nodes or spleen. IL-4 is a critical cytokine for the differentiation of $CD4^+$ T_H2 cells and the promotion of B cell class switching to IgE[5, 6]. The source of IL-4 in the priming of $CD4^+$ T_H2 cells is an area of debate, because dendritic cells do not produce IL-4 themselves[7]. Furthermore, the location of $CD4^+$ T_H2 cell priming in atopic disease remains to be elucidated[7]. T_H2 cytokines were produced in the lung and secondary lymphoid tissue by $CD4^+$ T_H2 cells that were primed *in vitro* and transferred to naïve mice that were subsequently challenged with antigen[8]. Interestingly, other studies demonstrated that $CD4^+$ T_H2 cell priming occurred in the lung in the absence of lymph nodes[9-11]. The pattern of $CD4^+$ T_H2 cell activation and effector function acquisition in the present study was similar to the pattern observed for $CD4^+$ T_H1 cells in response to respiratory fungal infection with *A. fumigatus* or *Cryptococcus neoformans*[12, 13].

- This study contributed novel information regarding the potential role of $CD4^+$ T_H17 cells in chronic pulmonary hypersensitivity diseases. $CD4^+$ T_H17 cells were significantly increased during the transition from the acute to the chronic inflammatory response to *A. fumigatus* conidia. $CD4^+$ T_H17

cells are a recently recognized subset of $CD4^+$ T_H cells that are implicated in chronic inflammation, particularly in autoimmunity[14, 15]. A single inhalational challenge with *A. fumigatus* conidia or *Candida albicans* induced IL-17 production, and IL-17 promoted inflammation and negatively impacted the IFNγ-mediated host defense response to the fungi[16, 17].

- This study provided evidence that the pathogenesis of respiratory allergies may be aided by IL-10, a cytokine heralded as a therapeutic option to inhibit allergic inflammation. The T_H2-mediated AAD was abrogated in IL-$10^{-/-}$ compared to C57BL/6 mice after repeated exposure to conidia. The absence of IL-10 resulted in diminished airway IL-4-producing $CD4^+$ T_H2 cells, airway eosinophils, and pulmonary arterial remodeling. On the other hand, IL-$10^{-/-}$ and C57BL/6 mice were similar in terms of the frequency of airway IFNγ-producing $CD4^+$ T_H1 cells, the frequency of airway IL-17-producing T_H17 cells (Appendix 2), and the overall extent of pulmonary inflammation. IL-10 is widely recognized as an anti-inflammatory cytokine that acts on most hematopoietic cells[18]. Forced expression of IL-10 in the airway suppressed the development of allergic airway sensitization[19], and IL-10-producing $CD4^+$ T_{Reg} cells are regarded to possess immunotherapeutic potential for the treatment of allergic diseases[20]. In addition to the present study, other reports indicated that the absence of IL-10 resulted in an attenuated T_H2 immune response[21-23].

- This study provided evidence to support a novel pathway for the pathogenesis of pulmonary arterial remodeling. Severe fibromuscular remodeling of small-to-medium-sized pulmonary arteries developed as a result of chronic exposure to a respiratory allergen. The arterial lumens were significantly narrowed and often fully occluded. The arterial walls with greatly thickened by hyperplasia of α-smooth muscle actin-staining cells and stiffened by extensive fibrosis. Neointimal formation was evident. The pathology of the remodeled arteries was very similar to the description of arterial remodeling associated with pulmonary arterial hypertension (PAH)[24]. Currently, allergic hypersensitivity disease is not recognized for an association with PAH, but recent evidence indicates that chronic inflammation likely contributes to the pathogenesis of arterial remodeling in PAH[25]. Earlier this year, Daley et al. published the first report to demonstrate that pulmonary artery muscularization developed with an inflammatory response to inhaled antigen[26]. Intraperitoneal sensitization followed by ~4 weeks of intranasal challenge with *A. fumigatus* antigens yielded arterial pathology very similar to that presented in this study, as analyzed in H&E and α-smooth muscle actin-stained tissue sections. In the current study, we provided further evidence of neointimal development and arterial wall fibrosis, and we provided morphometric analysis of arterial lumen narrowing.
    - This study demonstrated that arterial modeling was mediated, at least in part, by $CD4^+$ T_H2 cell-mediated immunity. Arterial

remodeling was partially abrogated in the absence of $CD4^+$ T cells throughout the period of exposure to conidia. The absence of arterial remodeling in IL-$4^{-/-}$ or IL-$10^{-/-}$ mice, strongly implicated a pathological role for the T_H2-mediated response. Finally, we showed that IL-5, and by extension eosinophils, were not a necessary component of the immunopathological T_H2 response. Daley et al. also demonstrated the requirement for T_H2-mediated inflammation based on data collected in the absence of $CD4^+$ T cells, IL-4, and IL-13 signaling. Collectively, these data provide strong evidence for a novel immunopathological mechanism for pulmonary arterial remodeling.

References

1. Wang, J. M., Denis, M., Fournier, M. & Laviolette, M. Experimental allergic bronchopulmonary aspergillosis in the mouse: immunological and histological features. Scand J Immunol 39, 19-26 (1994).
2. Kheradmand, F. et al. A protease-activated pathway underlying Th cell type 2 activation and allergic lung disease. J Immunol 169, 5904-11 (2002).
3. Cates, E. C. et al. Effect of GM-CSF on immune, inflammatory, and clinical responses to ragweed in a novel mouse model of mucosal sensitization. J Allergy Clin Immunol 111, 1076-86 (2003).
4. Johnson, J. R. et al. Continuous exposure to house dust mite elicits chronic airway inflammation and structural remodeling. Am J Respir Crit Care Med 169, 378-85 (2004).
5. Kopf, M. et al. Disruption of the murine IL-4 gene blocks Th2 cytokine responses. Nature 362, 245-8 (1993).
6. Kopf, M., Le Gros, G., Coyle, A. J., Kosco-Vilbois, M. & Brombacher, F. Immune responses of IL-4, IL-5, IL-6 deficient mice. Immunol Rev 148, 45-69 (1995).
7. Georas, S. N., Guo, J., De Fanis, U. & Casolaro, V. T-helper cell type-2 regulation in allergic disease. Eur Respir J 26, 1119-37 (2005).
8. Harris, N. L., Watt, V., Ronchese, F. & Le Gros, G. Differential T cell function and fate in lymph node and nonlymphoid tissues. J Exp Med 195, 317-26 (2002).
9. Constant, S. L. et al. Resident lung antigen-presenting cells have the capacity to promote Th2 T cell differentiation in situ. J Clin Invest 110, 1441-8 (2002).
10. Gajewska, B. U. et al. Generation of experimental allergic airways inflammation in the absence of draining lymph nodes. J Clin Invest 108, 577-83 (2001).
11. Moyron-Quiroz, J. E. et al. Role of inducible bronchus associated lymphoid tissue (iBALT) in respiratory immunity. Nat Med 10, 927-34 (2004).
12. Lindell, D. M., Moore, T. A., McDonald, R. A., Toews, G. B. & Huffnagle, G. B. Distinct compartmentalization of CD4+ T-cell effector function versus proliferative capacity during pulmonary cryptococcosis. Am J Pathol 168, 847-55 (2006).
13. Rivera, A. et al. Innate immune activation and CD4+ T cell priming during respiratory fungal infection. Immunity 25, 665-75 (2006).
14. Harrington, L. E. et al. Interleukin 17-producing CD4+ effector T cells develop via a lineage distinct from the T helper type 1 and 2 lineages. Nat Immunol 6, 1123-32 (2005).
15. Langrish, C. L. et al. IL-23 drives a pathogenic T cell population that induces autoimmune inflammation. J Exp Med 201, 233-40 (2005).
16. Bozza, S. et al. Lack of Toll IL-1R8 exacerbates Th17 cell responses in fungal infection. J Immunol 180, 4022-31 (2008).

17. Zelante, T. et al. IL-23 and the Th17 pathway promote inflammation and impair antifungal immune resistance. Eur J Immunol 37, 2695-706 (2007).
18. Moore, K. W., de Waal Malefyt, R., Coffman, R. L. & O'Garra, A. Interleukin-10 and the interleukin-10 receptor. Annu Rev Immunol 19, 683-765 (2001).
19. Stampfli, M. R. et al. Interleukin-10 gene transfer to the airway regulates allergic mucosal sensitization in mice. Am J Respir Cell Mol Biol 21, 586-96 (1999).
20. Hawrylowicz, C. M. & O'Garra, A. Potential role of interleukin-10-secreting regulatory T cells in allergy and asthma. Nat Rev Immunol 5, 271-83 (2005).
21. Hernandez, Y. et al. Distinct roles for IL-4 and IL-10 in regulating T2 immunity during allergic bronchopulmonary mycosis. J Immunol 174, 1027-36 (2005).
22. Yang, X., Wang, S., Fan, Y. & Han, X. IL-10 deficiency prevents IL-5 overproduction and eosinophilic inflammation in a murine model of asthma-like reaction. Eur J Immunol 30, 382-91 (2000).
23. Laouini, D. et al. IL-10 is critical for Th2 responses in a murine model of allergic dermatitis. J Clin Invest 112, 1058-66 (2003).
24. Chan, S. Y. & Loscalzo, J. Pathogenic mechanisms of pulmonary arterial hypertension. J Mol Cell Cardiol 44, 14-30 (2008).
25. Dorfmuller, P., Perros, F., Balabanian, K. & Humbert, M. Inflammation in pulmonary arterial hypertension. Eur Respir J 22, 358-63 (2003).
26. Daley, E. et al. Pulmonary arterial remodeling induced by a Th2 immune response. J Exp Med 205, 361-72 (2008).

Appendix 1

Development and Validation of a Flow Cytometric Method for Leukocyte Differential Analysis

INTRODUCTION

The severity and character of airway inflammation is analyzed frequently by leukocyte differential analysis of cells recovered by bronchoalveolar lavage (BAL). Commonly, cells are affixed to glass sides by cytospin, treated with a cytological stain, and analyzed under a microscope. However, differentiation of monocytes from activated lymphocytes and eosinophils from neutrophils can be problematic, and variability between experimenters can introduce inconsistencies. In this study, we aimed to develop a simple, two-color flow cytometric leukocyte differential analysis for cells recovered from the airway by BAL. Our goal was to differentiate the four main leukocyte populations: macrophages, neutrophils, lymphocytes, and eosinophils. This method will allow for the consistent analysis of large numbers of cells to gauge the severity and character of airway inflammation.

RESULTS

A simple, two-color flow cytometric method for leukocyte differential analysis of cells recovered from the airway by BAL is described in this section. Several combinations of cell surface markers were tested in a series of experiments. Differential expression of CD11c and Gr1 (Ly6-G/C) in addition to differences in the forward-scatter (FSC) and side-scatter (SSC) profiles allowed for the resolution of the four main leukocyte subsets: macrophages, neutrophils, lymphocytes, and eosinophils.

Preliminary studies indicated that cells from all four main leukocyte subsets were found in the airway after several weekly exposures to *Aspergillus fumigatus*. Differential expression of CD11c and Gr1 resulted in the resolution of four distinct populations of airway cells (Figure A1-1). Staining with isotype control antibodies illustrated the range of autofluorescence exhibited by all the cells from the airway. The vast majority of the autofluorescent^{high} cells stained for the expression of CD11c. It is firmly established that autofluorescent^{high} cells recovered from the airway are macrophages[1]. A population of Gr1^{high} cells was separated from the remaining CD11c^{-} population. Gr1^{high} cells are predominantly neutrophils[2]. After the separation of the CD11c^{+} population and the Gr1^{high} population, two distinct populations remained: an autofluorescent^{low}, CD11c^{-}Gr1^{-} population, and an autofluorescent^{int}, CD11c^{-}Gr1$^{low\text{-}int}$ population. The latter two populations did overlap to a slight degree on the CD11c vs. Gr1 plot.

Definitive identification of the leukocyte subsets was guided by three consecutive flow cytometric cell sorting experiments. BAL cells from mice

exposed several times to *A. fumigatus* conidia were stained for CD11c and Gr1 and purified by FACS. Purified cells were affixed to glass slides by cytospin, stained with a modified Wright-Giemsa, and analyzed by standard cytological criteria. The results are summarized in the remainder of this section. $CD11c^{+}$ leukocytes were $FSC^{int\text{-}high}SSC^{int\text{-}high}$, and these cells were predominantly macrophages (Figure A1-2ii, iii, and iv). $Gr1^{high}$ leukocytes included three populations of cells ranging from $FSC^{low}SSC^{low\text{-}int}$ to $FSC^{int}SSC^{int}$. All three populations of $Gr1^{high}$ cells were predominantly neutrophils, and there were not obvious morphological differences between the three populations (Figure A1-2ii, vii, viii, xi, and xii). $CD11c^{-}Gr1^{-}$ leukocytes were $FSC^{low}SSC^{low}$, and these cells were predominantly lymphocytes (Figure A1-2ii, v, and ix). $CD11c^{low}Gr1^{low\text{-}int}$ leukocytes were $FSC^{low}SSC^{int\text{-}high}$, and these cells were predominantly eosinophils (Figure A1-2ii, vi, and x). Sorted cells were greater than 90% pure, indicating that this method was useful for performing a leukocyte differential analysis.

Based on the validating results of the cell sorting experiments, macrophages and neutrophils were routinely identified solely by the expression of CD11c and Gr1 (Figure A1-3). As mentioned above, lymphocytes and eosinophils overlapped slightly on the CD11c vs. Gr1 plot. However, lymphocytes and eosinophils were fully separated by FSC vs. SSC analysis, because lymphocytes were SSC^{low} and eosinophils were $SSC^{int\text{-}high}$. Therefore, lymphocytes and eosinophils were routinely identified by the combination of FSC vs. SSC profiles and CD11c vs. Gr1 expression (Figure A1-3).

Other cell surface markers, besides CD11c and Gr1, were employed to analyze the leukocyte populations. The following cell surface markers were chosen based on reports from other investigations: F4/80, CD11b, Siglec F, and CCR3. Low-level expression of F4/80 was detected in macrophage and eosinophil populations. Low-level expression of CD11b was detected on small percentages of cells in the macrophage and lymphocyte population. In contrast, neutrophils and eosinophils uniformly expressed a high level of CD11b. High-level expression of Siglec F was detected on eosinophils. Macrophage and neutrophil populations expressed Siglec F as well, but the fluorescent shift was not as great. The eosinophil population uniformly expressed CCR3, and minor expression of CCR3 was detected among the other subsets.

IL-5 is critical for the development and recruitment of eosinophils[3]. After several exposures to *A. fumigatus* conidia, BAL cells from C57BL/6 and IL-$5^{-/-}$ mice were analyzed by the flow cytometric leukocyte differential analysis method described in this section in order to verify the correct identification of the neutrophil and eosinophil granulocyte populations. Eosinophils and neutrophils were identified in C57BL/6 mice. In IL-$5^{-/-}$ mice, the neutrophils were present, but the eosinophil population was virtually absent.

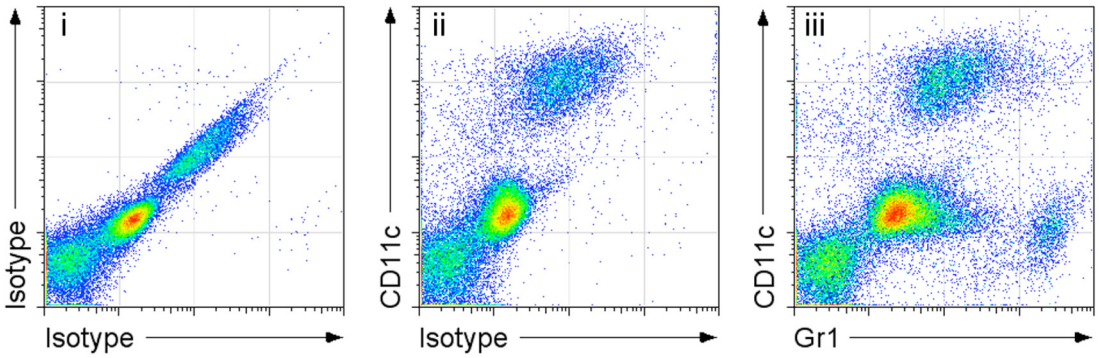

Figure A1-1. Staining of cells recovered from the airways with CD11c and Gr1 allows for the resolution of four discrete subsets.
As described in the methods, leukocytes were recovered from the airways by bronchoalveolar lavage after several weekly exposures to *A. fumigatus* and analyzed by flow cytometry. Cells were stained with isotype control antibodies, anti-CD11c, and anti-Gr1 as indicated on the axes labels for each plot.

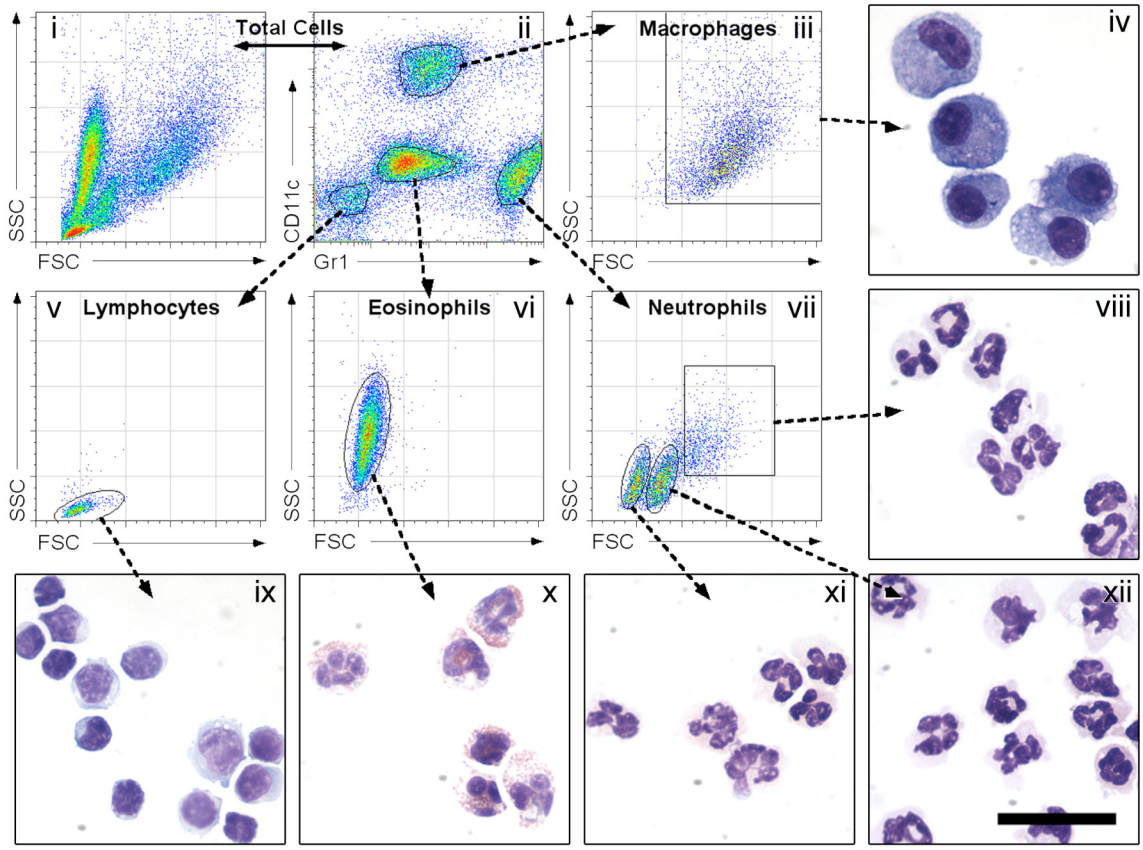

Figure A1-2. CD11c and Gr1 expression distinguishes the four major leukocyte subsets. Flow cytometric cell sorting was employed to validate a method for the leukocyte differential analysis of cells recovered from the airway. Cells were distinguished based on the expression of CD11c and Gr1and the forward- and side-scatter profile. The strategy for identifying each population was developed during three successive sorting experiments, and a representation of the final experiment is presented here. Based on data from preliminary studies, cells were pooled from mice exposed to *A. fumigatus* a variable number of times in order generate a population of total cells composed of relatively similar frequencies of each leukocyte subset. The forward- and side-scatter profile and the CD11c and Gr1 expression pattern of the total cells population is shown (i and ii). Cells were separated into four main populations based on the expression of CD11c and Gr1, and conservative gates were drawn around the central densities of each population (ii). The forward- and side-scatter profiles of each gated population was examined (follow dashed arrows from ii to iii, v, vi, and vii; compare to the total cells population in i). For three of the gated populations, the forward- and side-scatter profiles revealed essentially a single population of cells (iii, v, and vi). The forward- and side-scatter profile of the fourth population revealed three distinguishable populations (vii). Cells were sorted based on primary (ii) and secondary (iii, v, vi, and vii) gates as indicated by the dashed arrows. Sorted cells were later affixed to glass slides and stained with a modified Wright-Giemsa. Representative photomicrographs are shown (iv, viii-xii). All photomicrographs are shown at the same scale and the black bar is 20μm in length (xii). The purity of each sorted population was determined by evaluation of the cells under a microscope using standard morphological criteria. The purity of each population sorted by this strategy was greater than 90%. The population identities are labeled on the density plots of the primary gated cells (iii, v, vi, and vii). (Note: The three populations in vii were all determined to be neutrophils based on morphological analyses.)

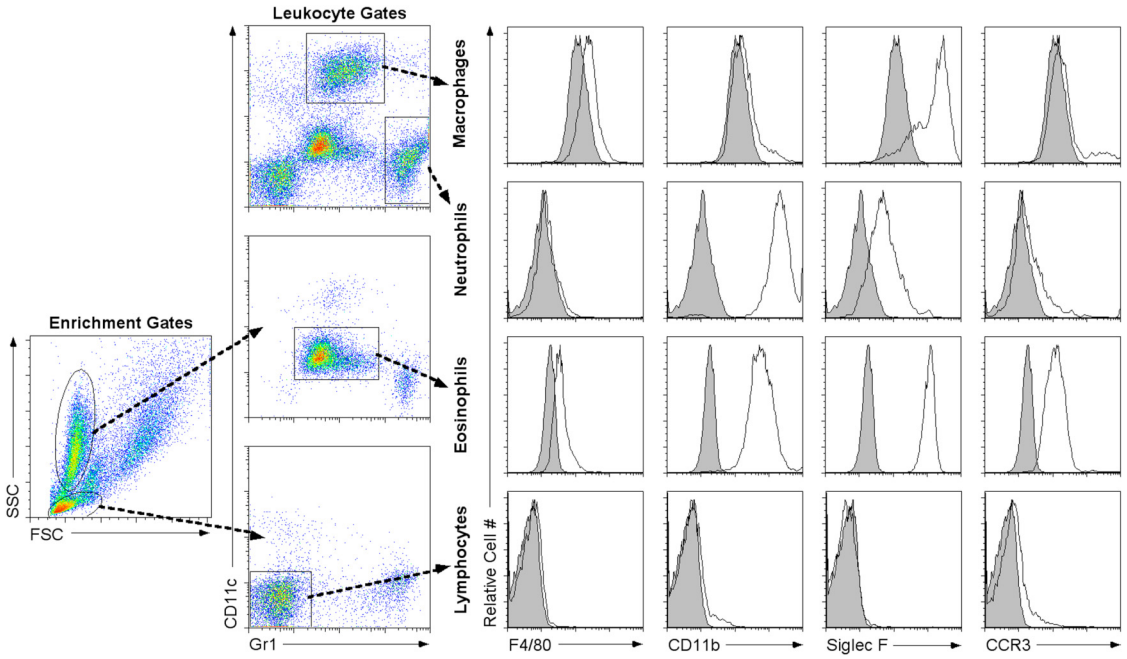

Figure A1-3. The examination of additional cell surface molecules confirms the utility of the CD11c/Gr1 combination for airway leukocyte differential analysis.

As previously described, a flow cytometric method was established for performing a leukocyte differential analysis on cells recovered from the airway. In practice, leukocyte subsets were identified as shown here. Macrophages and neutrophils were separated by their expression of CD11c and Gr1 (top density plot in "leukocyte gates" column; follow dashed arrows). Lymphocytes and eosinophils overlapped to a small extent based on their CD11c and Gr1 expression, but they do not overlap based on their forward- and side-scatter profiles. Therefore, lymphocytes and eosinophils were enriched independently with gates based on forward- and side-scatter ("enrichment gates" density plot; follow dashed arrows), and then identified from within the enriched population based on their expression of CD11c and Gr1 (middle and bottom density plots in "leukocyte gates" column; follow dashed arrows). Each leukocyte population was evaluated further for their expression of certain surface markers of interest in a third fluorescent channel. The leukocyte subset is labeled to the left of each row of histograms, and the surface marker is labeled on the x-axes for each column of histograms. Background staining with isotype control antibodies is shown on each plot by the shaded histogram. Data from one of two representative experiments is shown.

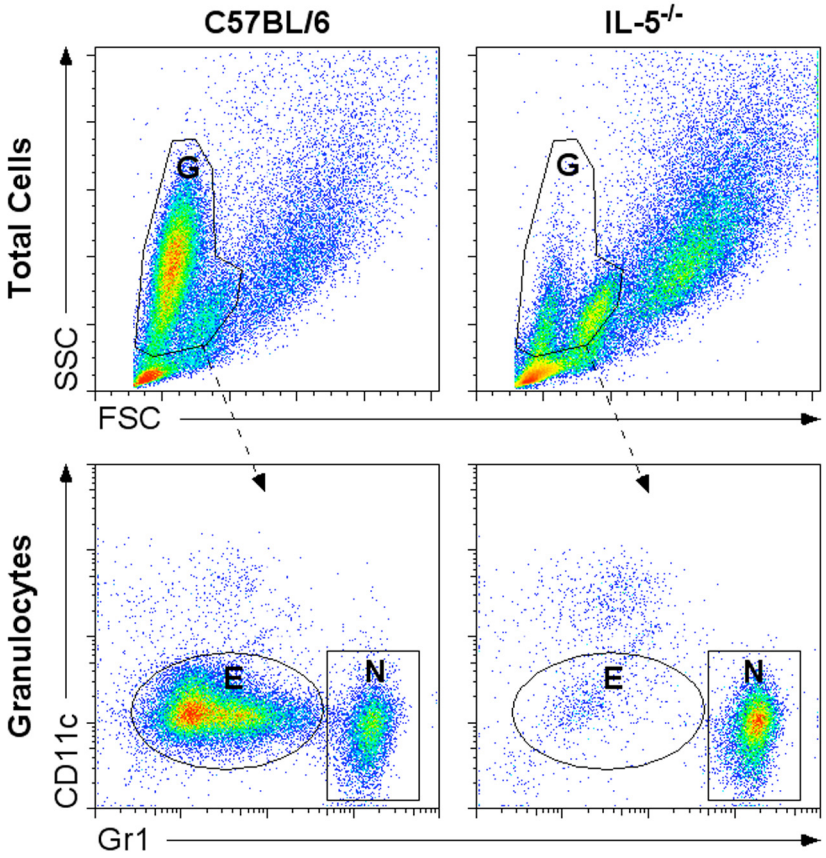

Figure A1-4. The flow cytometric method for leukocyte differential analysis correctly discriminates between the granulocyte populations.
IL-5-deficient mice were employed to verify further the correct identification of granulocytes using the flow cytometric method for leukocyte differential analysis previously described. Mice were exposed to *A. fumigatus* several times to induce the characteristic allergic airways disease. A granulocyte gate was roughly drawn to include neutrophils and eosinophils and exclude macrophages and lymphocytes (G, plots in "total cells" row). Gated granulocytes were separated into neutrophils and eosinophils based on their expression of CD11c and Gr1 according to the established method (N and E, plots in "granulocytes" row).

DISCUSSION

The severity and character of airway inflammation is evaluated commonly by leukocyte differential analysis of cells recovered by bronchoalveolar lavage (BAL). In this study, we aimed to develop a simple, two-color flow cytometric scheme for differentiating the four main leukocyte subsets from within the total population of cells recovered from the airway by BAL. Differential expression of CD11c and Gr1 (Ly6-G/C) in addition to differences in the FSC and SSC profiles allowed for the resolution of macrophages, neutrophils, lymphocytes, and eosinophils. We also analyzed the cell surface expression of other markers commonly employed for leukocyte subset identification, including F4/80, CD11b, Siglec F, and CCR3, and decided that CD11c vs. Gr1 was the preferred combination for our aims. This method allowed us to analyze large numbers of cells in order to accurately characterize airway inflammation in a relatively investigator independent manner, and the data collected is well suited for convincing presentation.

A primary goal of this study was to overcome the difficulty in differentiating neutrophils and eosinophils. In general, eosinophils have a ring-shaped nucleus and eosinophilic granules, while neutrophils have a polymorphonucleus and lack cytoplasmic granules. However, there is considerable overlap in nuclear morphology, neutrophils may contain granules, and eosinophils may degranulate. CCR3 is the receptor for eotaxin, and CCR3 is expressed by murine eosinophils[4]. In another study with similar aims to the present one, CCR3 was selected as the identifying marker for eosinophils[5]. In our study, eosinophils

uniformly expressed CCR3. However, the level of expression of CCR3 by eosinophils was relatively low, and expression of CCR3 by eosinophils overlapped with that of neutophils. This was potentially problematic because neutrophils and eosinophils also overlapped for CD11c, FSC, and SSC. Siglec F was reported as a useful marker to identify eosinophils[6]. In the present study, eosinophils uniformly expressed high levels of Siglec F, while neutrophils expressed moderate levels of Siglec F. Lymphocytes did not express Siglec F, but nonetheless the lymphocytes did overlap with the neutrophil population for Siglec F expression. This was potentially problematic because lymphocytes and neutrophils also overlapped for CD11c, FSC, and SSC. So, neutrophils could not be distinguished from lymphocytes or eosinophils based on FSC vs. SSC profile, but neutrophils could be distinguished from lymphocytes and eosinophils based on Gr1 expression. In addition, lymphocytes and eosinophils did not exhibit overlapping SSC profiles, so a unique identifying marker for eosinophils was not necessary.

It is difficult to differentiate activated lymphocytes from monocytes due to similarities in size and appearance. Generally speaking, monocytes are blood-borne cells that rapidly differentiate into macrophages or dendritic cells when the migrate into peripheral tissues[7]. Macrophages exhibit impressive tissue-specific heterogeneity[8]. The cell surface molecules CD11b and F4/80 are commonly used as macrophage-specific markers. However, in the alveolar compartment macrophages were $CD11b^{low}F4/80^{low}CD11c^{high}autofluorescent^{high}$[9]. Macrophages in the present study had a similar appearance. In contrast,

lymphocytes were $CD11c^{-}Gr1^{-}autofluorescent^{low}SSC^{low}FSC^{low\text{-}int}$, and thus, lymphocytes were easily distinguished from monocytes/macrophages. $CD4^{+}$ and $CD8\alpha^{+}$ T cells and $CD19^{+}$ B cells were contained entirely within the lymphcyte gated population (data not shown). $NK1.1^{+}$ cells, NK cells and NKT cells, constituted less than 1% of the total cell population (data not shown).

In most tissues, CD11c is a unique indentifier of dendritic cells. In the alveolar compartment macrophages and dendritic cells cannot be distinguished by CD11c expression. However, macrophages are $autofluorescent^{high}$ and dendritic cells are $autofluorescent^{low9}$. Furthermore, dendritic cells generally express higher levels of MHCII and co-stimulatory receptors. We evaluated dendritic cells and macrophages in the BAL samples obtained from mice exposed several times to *A. fumigatus* (data not shown). In agreement with Osterholzer et al., we determined that dendritic cells are optimally identified by utilizing three fluorescent channels for CD11c, MHCII, and autofluorescence. Dendritic cells were present in the airway, but consitituted less than 5% of the total cells. The majority of the $CD11c^{+}MHCII^{+}$ dendritic cells were also $Gr1^{-}$, and therefore, they were not included in the macrophage gated population (data not shown). $Gr1^{+}CD11c^{+}MHCII^{+}$ dendritic cells that may be included in the macrophage gate represented a negligible percentage of the macrophage population (data not shown). That does not mean that the activity of these cells was negligible in the airway inflammatory response, just that the presence of these cells did not alter the determination of macrophage numbers in a meaningful way.

As in the present study, a previous report demonstrated that sorted $Gr1^{high}$ cells were predominantly neutrophils[10]. We detected three discernable populations on the FSC vs. SSC plot that was contained within the homogeneous $Gr1^{high}CD11c^{low}$ neutrophil gate. There were no obvious disparities in the cytological appearances of the three populations. For instance, immature neutrophil band cells were not confined to one population. Also, granulated neutrophils were not observed in any sorted neutrophil population. Recently, three distinct neutrophil subsets with separate functional characteristics were identified in the context of infection with methicillin-resistant *Staphylococcus aureus*[11]. In response to *A. fumigatus* conidia, the three populations of neutrophils were invariably present regardless of the number of exposures to conidia or of the deficiency for critical cytokines. Thus, it was not apparent that the three populations of neutrophils in this study represented functionally distinct populations.

$Gr1^{+}$ blood monocytes migrate into tissues under inflammatory conditions, and quickly differentiate[12]. Blood monocytes also express CD11b and F4/80 in mice. In the present study, monocyte/macrophage gated cells expressed little to no CD11b and F4/80. On the otherhand, splenic macrophages expressed both CD11b and F4/80 (data not shown). So, these data imply that $Gr1^{+}$ inflammatory monocytes recruited to the airway during the inflammatory response to *A. fumigatus* conidia likely differentiate rapidly into $Gr1^{-}CD11c^{+}$ cells, and $Gr1^{+}CD11c^{-}$ or $Gr1^{+}CD11c^{+}$ monocyte/macrophages are likely a very small population at any given time.

Eosinophil degranulation would affect the cytological appearance of the cells, but it remains controversial as to whether murine eosinophils regularly degranulate in allergic airway disease[13, 14]. The high SSC profile of eosinophils is related to the presence of intracellular granules, so degranualtion may also be expected to reduce SSC height. In the present study, the eosinophil population was a distinct population of $FSC^{low}SSC^{int\text{-}high}$ cells with a single central density apparent on density plots. There was no evidence of a second population density that might represent degranulated eosinophils. The sorted eosinophil population was 99% pure. The few eosinophils that were sorted with the lymphocyte population at a lower SSC height had a level of granularity similar to the eosinophil-gated cells . Nonetheless, under cytological evaluation heterogeneity in the extent of eosinophil granularity was appreciated. So, degranulation may have been involved in the allergic response, but degranulation did not affect the flow cytometric identification of eosinophils.

In this study, we developed a simple, two-color flow cytometric scheme for differentiating the four main leukocyte subsets from within the total population of BAL cells recovered from the allergic airway. Differential expression of CD11c and Gr1 (Ly6-G/C) in addition to differences in the FSC and SSC profiles allowed for the resolution of macrophages, neutrophils, lymphocytes, and eosinophils. This method is well suited for the reliable evaluation of large numbers of cells, and the data collected is well suited for visual presentation.

References

1. Hallden, G., Skold, C. M., Eklund, A., Forslid, J. & Hed, J. Quenching of intracellular autofluorescence in alveolar macrophages permits analysis of fluorochrome labelled surface antigens by flow cytofluorometry. J Immunol Methods 142, 207-14 (1991).
2. Hestdal, K. et al. Characterization and regulation of RB6-8C5 antigen expression on murine bone marrow cells. J Immunol 147, 22-8 (1991).
3. Foster, P. S., Hogan, S. P., Ramsay, A. J., Matthaei, K. I. & Young, I. G. Interleukin 5 deficiency abolishes eosinophilia, airways hyperreactivity, and lung damage in a mouse asthma model. J Exp Med 183, 195-201 (1996).
4. Grimaldi, J. C. et al. Depletion of eosinophils in mice through the use of antibodies specific for C-C chemokine receptor 3 (CCR3). J Leukoc Biol 65, 846-53 (1999).
5. van Rijt, L. S. et al. A rapid flow cytometric method for determining the cellular composition of bronchoalveolar lavage fluid cells in mouse models of asthma. J Immunol Methods 288, 111-21 (2004).
6. Voehringer, D., van Rooijen, N. & Locksley, R. M. Eosinophils develop in distinct stages and are recruited to peripheral sites by alternatively activated macrophages. J Leukoc Biol 81, 1434-44 (2007).
7. Tacke, F. & Randolph, G. J. Migratory fate and differentiation of blood monocyte subsets. Immunobiology 211, 609-18 (2006).
8. Gordon, S. & Taylor, P. R. Monocyte and macrophage heterogeneity. Nat Rev Immunol 5, 953-64 (2005).
9. Vermaelen, K. & Pauwels, R. Accurate and simple discrimination of mouse pulmonary dendritic cell and macrophage populations by flow cytometry: methodology and new insights. Cytometry A 61, 170-77 (2004).
10. Ramalingam, T., Rajan, B., Lee, J. & Rajan, T. V. Kinetics of cellular responses to intraperitoneal Brugia pahangi infections in normal and immunodeficient mice. Infect Immun 71, 4361-7 (2003).
11. Tsuda, Y. et al. Three different neutrophil subsets exhibited in mice with different susceptibilities to infection by methicillin-resistant Staphylococcus aureus. Immunity 21, 215-26 (2004).
12. Geissmann, F., Jung, S. & Littman, D. R. Blood monocytes consist of two principal subsets with distinct migratory properties. Immunity 19, 71-82 (2003).
13. Malm-Erjefalt, M., Persson, C. G. & Erjefalt, J. S. Degranulation status of airway tissue eosinophils in mouse models of allergic airway inflammation. Am J Respir Cell Mol Biol 24, 352-9 (2001).
14. Shinkai, K., Mohrs, M. & Locksley, R. M. Helper T cells regulate type-2 innate immunity in vivo. Nature 420, 825-9 (2002).

Appendix 2

Additional Data

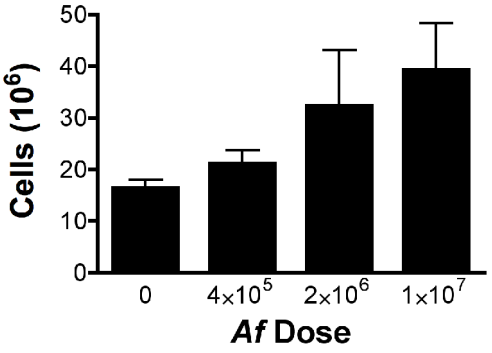

Figure A2-1. Dose response to inhaled *A. fumigatus* conidia
Cells were recovered from the airway by bronchoalveolar lavage and enumerated under a light microscope with a hemacytometer.

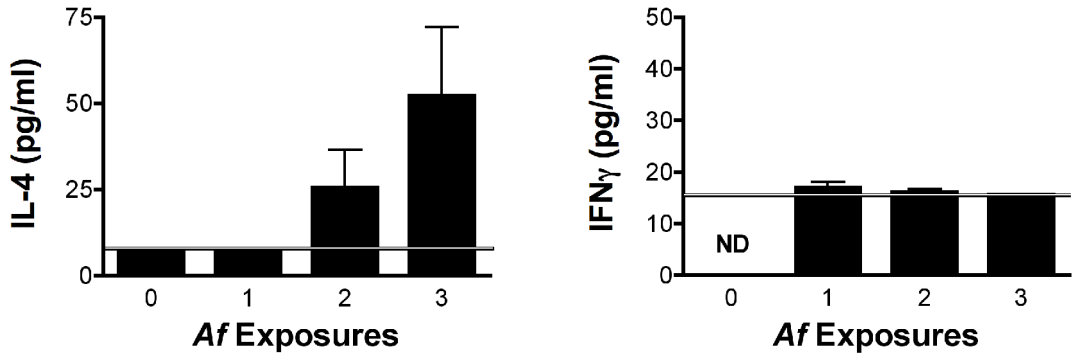

Figure A2-2. Peak levels of T_H2 cytokines coincide with the pattern of leukocyte recruitment.
Cytokines present in the cell-free bronchoalveolar lavage fluid were quantified by ELISA. The limit of detection for each assay is indicated with a horizontal line.

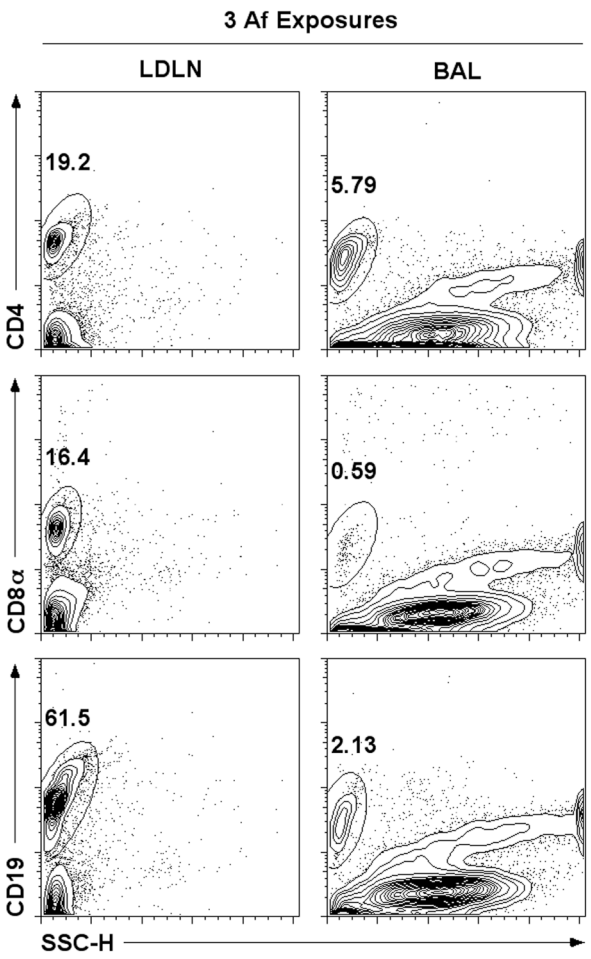

Figure A2-3. The responding T cell population has a low CD8/CD4 T cell ratio.
After three exposures to conidia, cells recovered from the lung-draining lymph node and airway were analyzed for expression of CD4, CD8α, and CD19 on lymphocytes as described in the materials and methods. The percentage of total cells within each gate is included on each plot.

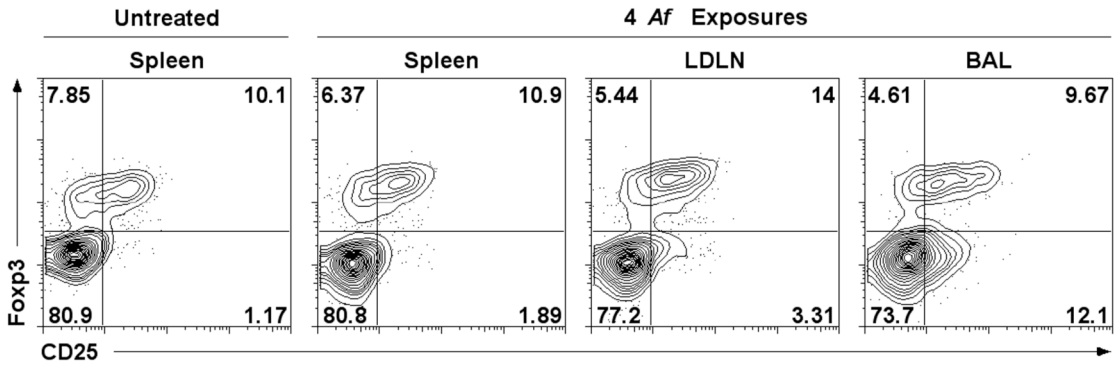

Figure A2-4. $CD4^+$ T_{Reg} cells are recruited to the airway.
As described in the materials and methods, cells were collected from various tissues (including spleen, lung draining-lymph nodes (LDLN), and airway (BAL)) from untreated mice and mice exposed to *A. fumigatus* four times (n=3 per group) as indicated above the figure. Cells were pooled for analysis. Gated $CD4^+$ lymphocytes were analyzed for expression of the CD25 and Foxp3 by flow cytometry (see axes labels for contour plots). Quadrants were set with isotype control-stained $CD4^+$ lymphocytes (not shown) and the percentage of $CD4^+$ lymphocytes in each quadrant is included on each plot.

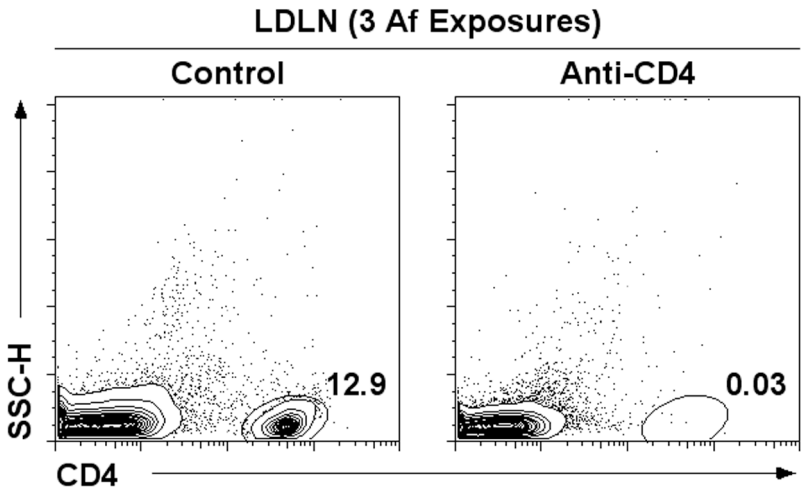

Figure A2-5. Anti-CD4 treatment depletes $CD4^+$ T cells
Depletion of $CD4^+$ T cells after anti-CD4 treatment was confirmed by flow cytometry using a different anti-CD4 antibody as described in the materials and methods. Depletion was >99% in the lung-draining lymph nodes (shown above) and in the spleen and airway (data not shown).

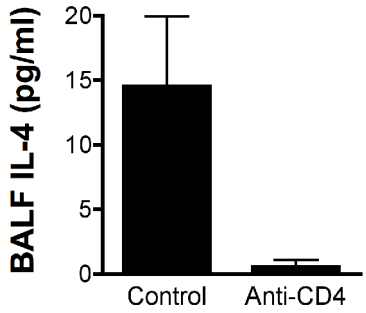

Figure A2-6. $CD4^+$ T cells are necessary for the production of a T_H2 cytokine.
Mice in both groups were exposed to *A. fumigatus* three times, and not treated or treated with anti-CD4. IL-4 present in the cell-free BALF was quantified by ELISA.

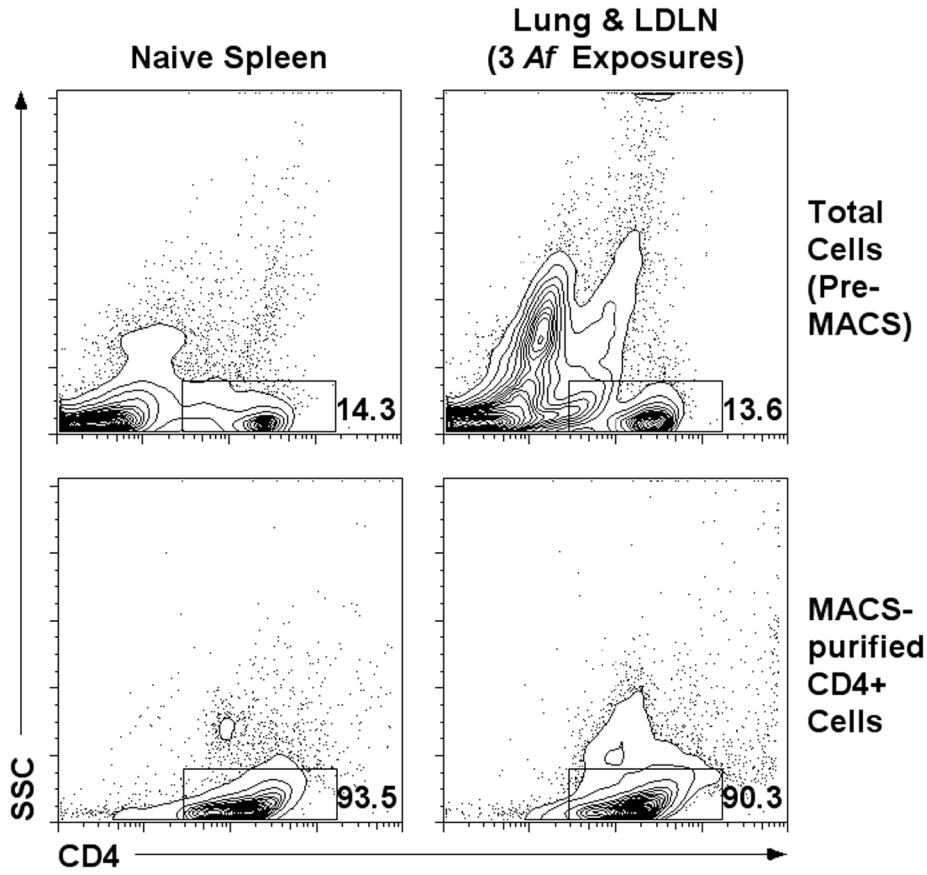

Figure A2-7. Magnetic isolation enriched for $CD4^+$ T Cells
As described in the methods, naïve $CD4^+$ T cells were purified from the spleens of naïve animals, and *Af*-primed $CD4^+$ T cells were purified from a pool of lung leukocytes and lung-draining lymph node cells harvested from mice exposed to conidia three times. The graph depicts the cell populations before and after magnetic cell isolation, and the $CD4^+$ lymphocyte percentage of the total cell population is included on the plots.

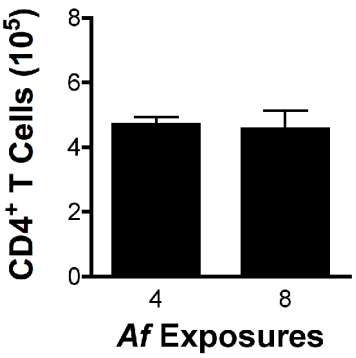

Figure A2-8. $CD4^+$ T cells in the airway are maintained with chronic exposure to conidia.
Cells were recovered from the airway by bronchoalveolar lavage and the expression of CD4 was analyzed by flow cytometry as described in the materials and methods.

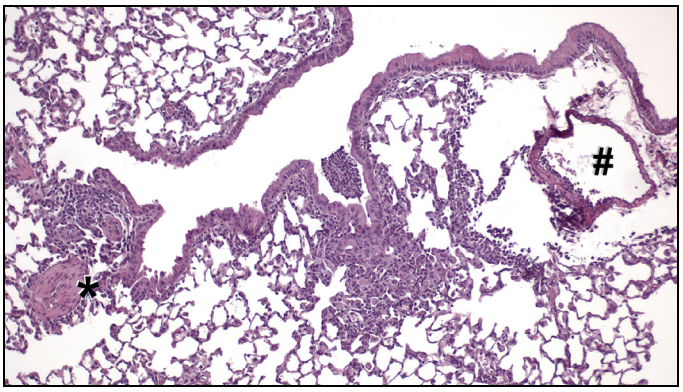

Figure A2-9. Remodeling causes lumen narrowing and occlusion of small- to medium-sized, but not large-sized, muscular pulmonary arteries after long-term, repeated exposure.
Histological sections of lung tissues were stained with H&E. This representative photomicrograph includes a medium-sized muscular artery (asterisk) and a large-sized muscular artery (pound) adjacent to conducting airways. Images depict the extent of arterial remodeling present 24h after the eighth weekly exposure.

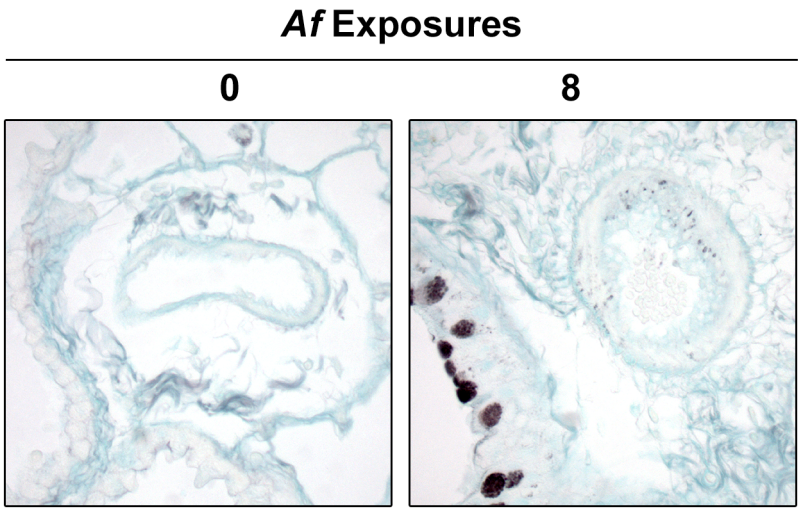

Figure A2-10. Hyphal invasion is not present in remodeled arteries. Histological sections of lung tissues were stained with GMS. Representative photomicrographs include medium-sized muscular arteries adjacent to conducting airways.

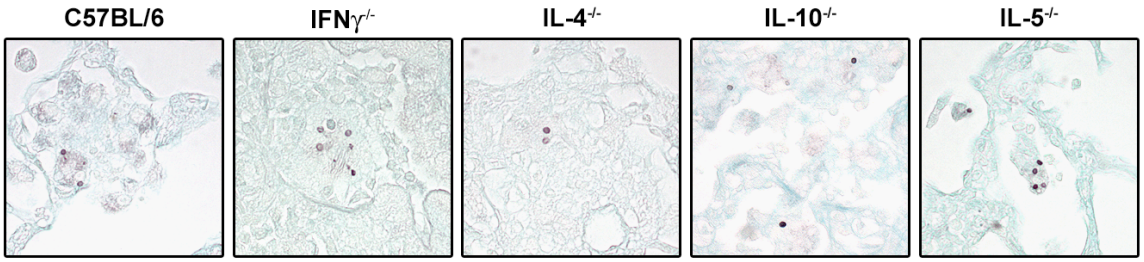

Figure A2-11. Cytokine-deficient mice prevent *A. fumigatus* colonization in the lung.
Mice were exposed to *A. fumigatus* once a week for eight total exposures. Histological sections of lung tissues were stained with GMS. Representative photomicrographs depict isolated conidia, stained black.

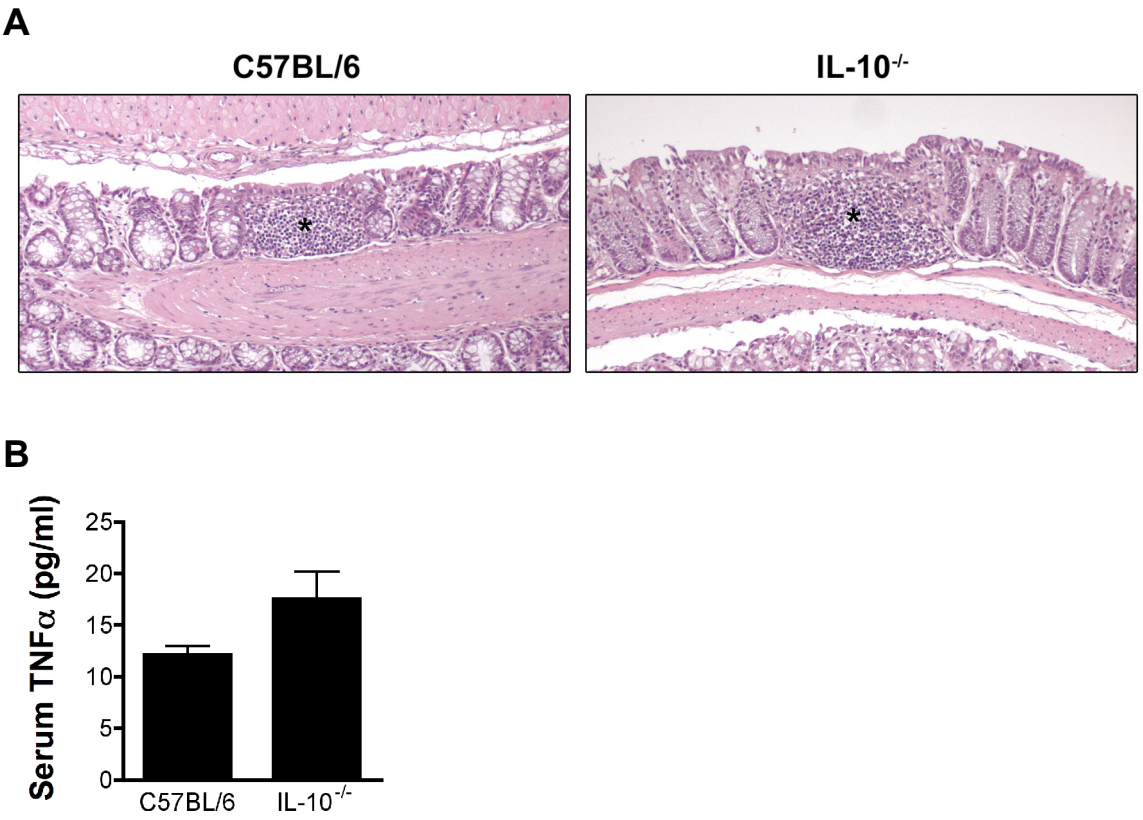

Figure A2-12. Absence of a T_H2 response in IL-$10^{-/-}$ is not likely due to colitis.
A) Sections are large colon tissue was stained with H&E and representative images are shown. Isolated lymphocyte aggregates (asterisks) present in C57BL/6 and IL-$10^{-/-}$ mice represent normal gut-associated lymphoid tissue with intact overlying epithelium. B) The level of TNFα in the serum was analyzed by ELISA.

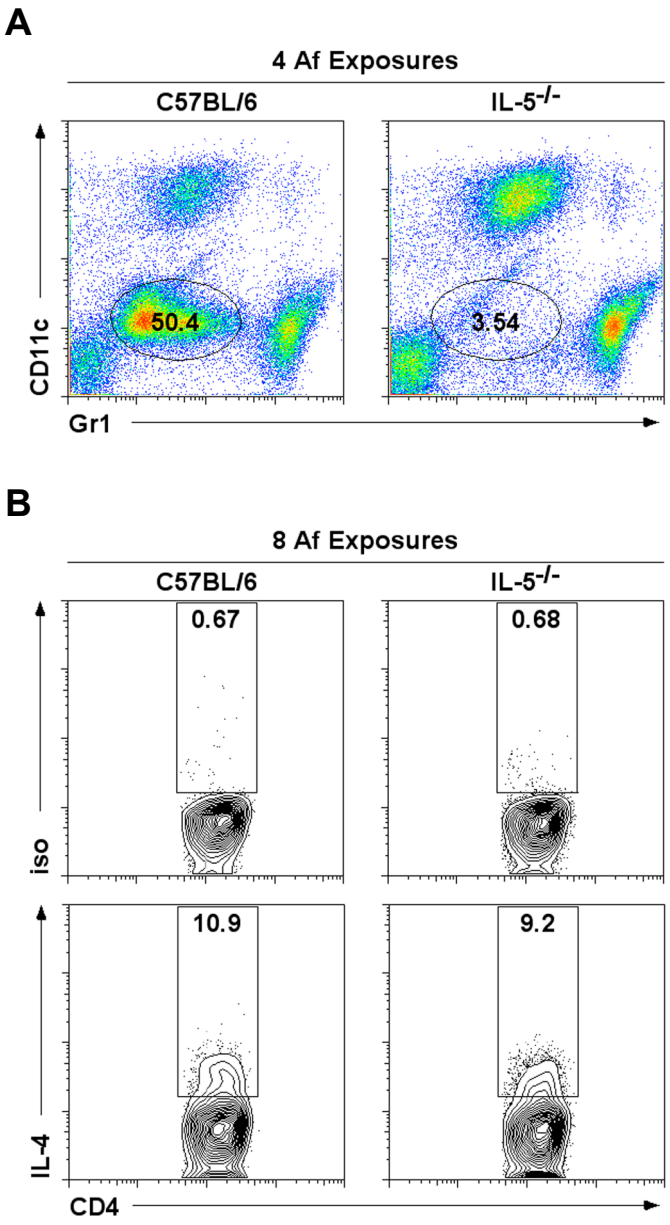

Figure A2-13. IL-5$^{-/-}$ do not exhibit airway eosinophilia but do develop CD4^{+} T_H2 cells.
A) During the peak of allergic inflammation, airway eosinophils (gate with percentage of total cells) were identified by flow cytometry. B) During chronic inflammation, airway CD4^{+} T cell production of IL-4 (gate with percentage of gated CD4^{+} T cells) was analyzed by intracellular flow cytometry. See axis labels on plots.

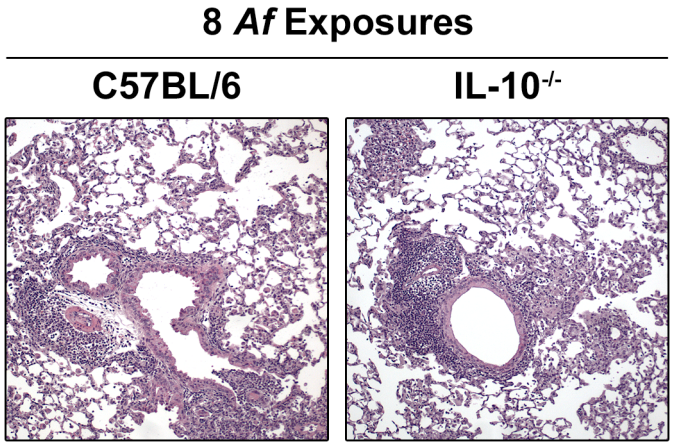

Figure A2-14. Like C57BL/6, IL-10$^{-/-}$ develop severe pulmonary inflammation with chronic exposure to conidia.
Mice were exposed to conidia eight times on a weekly basis. Representative H&E micrographs depict the severity of pulmonary inflammation.

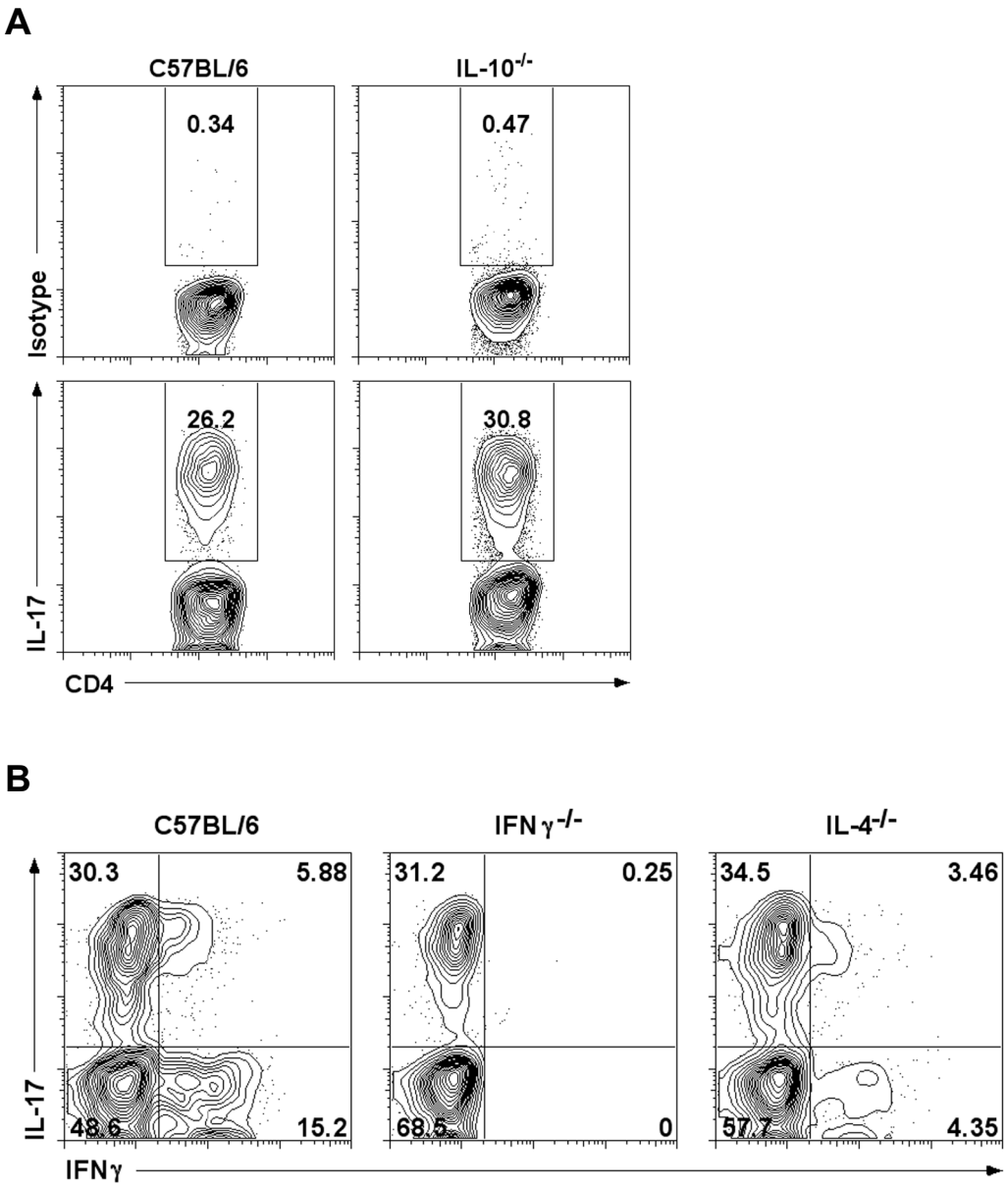

Figure A2-15. Strains that do and do not develop pulmonary arterial remodeling contain airway $CD4^+$ T_H17 cells.
A and B) Airway cells were collected after various strains of mice (see labels above plots) were exposed to conidia 8 times on a weekly basis. Production of IL-17 (and IFNγ in B) by CD4+ T cells (see gates for percentage of gated $CD4^+$ T cells expressing cytokine) was analyzed by intracellular flow cytometry.